博士論文

# Application of remote sensing and resource assessment techniques for the single-tree management system of high-value hardwood species in northern Japan

(高価値広葉樹の単木管理システムにおけるリモートセンシングと資源評価技術の応用)

KYAW THU MOE

チョー・トゥー・モー

# Application of remote sensing and resource assessment techniques for the single-tree management system of high-value hardwood species in northern Japan

(高価値広葉樹の単木管理システムにおけるリモートセンシングと資源評価技術の応用)

KYAW THU MOE

Department of Forest Science

Graduate School of Agricultural and Life Sciences

The University of Tokyo

Dissertation submitted in partial fulfilment of the requirements for the degree of

Doctor of Philosophy (Ph.D.)

**Dissertation Committee**

Dr. Toshiaki OWARI (Chief)

Dr. Norihiko SHIRAISHI

Dr. Satoshi TSUYUKI

Dr. Satoshi TATSUHARA

Dr. Takuya HIROSHIMA

September, 2020

**Table of Content**

Table of Content ..... i

Acknowledgements ..... iv

Summary ..... vi

Chapter 1: Introduction ..... 1

1.1 Background ..... 1
1.1.1 High-value timber species ..... 1
1.1.2 Single-tree management for high-value timber species ..... 3
1.1.3 Remote sensing for single-tree management ..... 5
1.1.4 Resource assessment methods for single-tree management ..... 6

1.2 Objectives of the study ..... 8

1.3 Organization of the thesis ..... 10

Chapter 2: The applicability of UAV-DAP for tree height estimation: comparison with airborne LiDAR and field survey ..... 12

2.1 Introduction ..... 12

2.2 Materials and methods ..... 13
2.2.1 Study area ..... 13
2.2.2 Data ..... 15
2.2.2.1. Field Data ..... 15
2.2.2.2 LiDAR Data ..... 15
2.2.2.3 UAV Data ..... 16
2.2.3 Data processing and canopy height model (CHM) generation ..... 16
2.2.3.1 LiDAR data processing and LiDAR-CHM generation ..... 16
2.2.3.2 UAV data processing and UAV-DAP-CHM generation ..... 17
2.2.4 Individual tree height measurement using RS data ..... 17
2.2.5 Data analysis ..... 18
2.2.5.1 Individual tree height comparison ..... 18
2.2.5.2 Height-Diameter relationships ..... 19

2.3 Results ..... 19
2.3.1 Correlation between observed tree heights ..... 19
2.3.2 Height differences between three height measurement methods ..... 21
2.3.3. Relation between tree height and DBH ..... 22
2.3.3.1 Height-Diameter relationships ..... 22
2.3.3.2 H-D models ..... 23

2.4 Discussion ..... 25

2.5 Conclusions ..... 27
Chapter 3: Estimation of spatial positions and DBH of high-value timber species ..... 29
3.1 Introduction ..... 29
3.2 Materials and methods ..... 30
3.2.1 Study area and field survey ..... 30
3.2.2 Remote sensing data ..... 31
3.2.3 Classification of forest canopy into species level ..... 31
3.2.3.1 Image segmentation ..... 31
3.2.3.2 Variable extraction ..... 32
3.2.3.3 Variable selection, classification and accuracy assessment ..... 33
3.2.4 Estimation of DBH ..... 34
3.3 Results ..... 35
3.3.1 Multiresolution segmentation of forest canopy ..... 35
3.3.2 Variable selection, classification of forest canopy and accuracy assessment ..... 37
3.4 Discussion ..... 42
3.4.1 Segmentation of forest canopy ..... 42
3.4.2 Classification of forest canopy ..... 43
3.4.3 Estimation of individual tree DBH ..... 44
3.5 Conclusions ..... 45
Chapter 4: Resource assessment of high-value timber species ..... 46
4.1 Introduction ..... 46
4.2 Materials and methods ..... 48
4.2.1 Study site and data ..... 48
4.2.2 Measures of sustainability ..... 49
4.2.3 Data analysis ..... 50
4.3 Results ..... 50
4.3.1 Changes in stocking of high-value timber species ..... 50
4.3.2 Changes in the demographic characteristics of high-value timber species ..... 53
4.3.3 Changes in species proportion of high-value timber species ..... 55
4.3.4 Selection harvest ..... 56
4.4 Discussion ..... 57
4.5 Conclusions ..... 61
Chapter 5: Predicting individual tree growth of high-value timber species ..... 62
5.1 Introduction ..... 62
5.2 Materials and Methods ..... 63
5.2.1 Study are and data ..... 63
5.2.2 Data preparation ..... 63
5.2.3 Individual tree BAI model ..... 64

5.2.4 Mixed-effects modeling....65
5.2.5 Data analysis....66
5.3 Results....67
5.3.1 Observed basal area increment (BAI)....67
5.3.2 Model fitting, parameter estimation and goodness of fit....68
5.3.3 Model prediction for BAI and years to reach target DBH....69
5.4. Discussion....71
5.4 Conclusion....73
Chapter 6: General discussion and conclusion....74
6.1 General discussion....74
6.1.1 General consideration of RS and resource assessment techniques for the single-tree management of high-value timber species....74
6.1.1.1 RS technique....74
6.1.1.2 Resource assessment technique....76
6.2 Conclusion....77
6.2.1 Summary of the results....77
6.2.2 Main Conclusion....78
6.3 Limitations and future direction....79
References....81

**Acknowledgements**

Many people have helped me during the three years of my study in Japan. First of all, I would like to express my profound gratitude to my supervisor, Associate Professor Dr. Toshiaki Owari, for providing me the opportunity to study in Japan. His continuous support, guidance, valuable advices and suggestions throughout this study helped me a lot in writing this dissertation. I would like to extend my deepest gratitude to the members of the evaluation committee of this study - Dr. Norihiko Shiraishi, Dr. Satoshi Tsuyuki, Dr. Satoshi Tatsuhara, and Dr. Takuya Hiroshima - for their comments and suggestions to improve this dissertation.

This thesis would not have been accomplished without the support of technical staff members of the University of Tokyo Hokkaido Forest. I would like to express my sincere appreciation to Kazunobu Iguchi, Shinya Inukai, Yoshikazu Takashima, Takashi Inoue, Yoshinori Eguchi, Masaki Tokuni, Satoshi Fukuoka, Haruki Sato, Hitomi Ogawa, Hisatomi Kasahara, and other technical staff members of the University of Tokyo Hokkaido Forest for their significant contribution in the field and UAV-data collection. I am deeply indebted to Dr. Naoyuki Furuya, Hokkaido Research Center, Forestry and Forest Products Research Institute and Associate Professor Junko Morimoto, Hokkaido University for their support, valuable comments and suggestions for this study. I also would like to thank Dr. Sadeepa Jayathunga for sharing her knowledge related to LiDAR and UAV data processing.

I would also like express my heartfelt thanks to Associate Professor Dr. Susumu Goto, Assistant Professor Dr. Naoko Miura and staff members of Education and Research Center of the University of Tokyo Forests for their supporting me throughout my study period.

My study in Japan would have been impossible without the financial support of Ministry of Education, Culture, Sports, Science and Technology of Japan (MEXT - Monbukagakusho Scholarship), for which I am very much indebted. This study was also supported by JSPS KAKENHI grant numbers 16H0494 and 17H01516, and JSPS Core-to-Core Program grant number JPJSCCB20190007.

I would like to extend my sincere thanks to Ministry of Natural Resources and Environmental Conservation of Myanmar and University of Forestry and Environmental Science (UFES) for giving me a permission to pursue my study in Japan. I am also grateful to Retired Rector of the UFES, Dr. Myint Oo, for his encouragement to continue doctoral study and apply for the MEXT Scholarship. My seniors, teachers, and colleagues of the UFES, particularly Mr. Zaw Win Myint, helped me a lot during my stay in Japan. My thanks also go

to all of them. Even though the names were not mentioned here specifically, I would like to sincerely thank to those who supported me in one way or another during my study in Japan.

Last, but not least, I owe a special debt of gratitude to my beloved family for their moral support and encouragement though out this study.

KYAW THU MOE

September, 2020

**Summary**

High-value timber species play a significant economic role in forest management. In uneven-aged mixed conifer-broadleaf forests in northern Japan, monarch birch (*Betula maximowicziana*), castor aralia (*Kalopanax septemlobus*), and Japanese oak (*Quercus crispula*) are important producers of high commercial value timber. The supply of high-value timber from these species is exclusively dependent on selective harvesting of large-size trees within mixed forests. Single-tree management system has been applied for the management of high-value timber species. Single-tree management is a forest management approach that aims at enhancing selected trees of high timber quality and value in a forest stand. Under single-tree management system, identification and registration of target trees, measurement of their size and assessment of timber quality, and periodic monitoring of selected trees are three most important tasks. To accomplish these important steps, forest managers mostly rely on the extensive field survey. Recently developed remote sensing (RS) technology, such as airborne laser scanning (ALS), unmanned aerial vehicle digital aerial photogrammetry (UAV-DAP) have great potential for acquiring individual tree information of high-value timber species for the purpose of single tree management. The major aim of this study is to examine the potential use of UAV-DAP in combination with long-term forest measurement dataset for single-tree management of high-value timber species. To fulfill the major aim, four specific research questions will need to be addressed: (1) Is UAV-DAP applicable in practical forest measurement of high-value timber species, e.g., tree height? (2) If it is applicable, how do UAV-DAP could be used in single tree identification and estimation the single tree positions and their tree size? (3) How to assess the resource sustainability of target high-value timber species? and (4) How to estimate the time for a selected tree to reach a desired size?

To apply the RS and resource assessment techniques for practical purposes, the first research question is whether these techniques could be used reliably. The Chapter 2 of the thesis deals with the assessment of accuracy of RS data in practical field application. Since height information can be directly derived from RS data, individual tree height derived from field survey, LiDAR data, and UAV-DAP data were compared. In addition, the accurate measurement of individual tree height is necessary for both practical management and scientific reasons such as estimation of stem volume. The spatial position, tree height, and diameter at breast height (DBH) of 178 field measured trees of monarch birch, castor aralia and Japanese oak were used for the purpose of comparison. Field measured trees were manually digitized with the aid of field recorded tree spatial position and high resolution

orthophotographs, and tree height were extracted for these tree crowns. Tree heights from three different sources were cross-compared statistically through paired t-tests, correlation coefficients, and height-diameter models. The results indicated that UAV-DAP derived tree heights were highly correlated with LiDAR tree height and field measured tree height. The performance of individual tree height measurement using traditional field survey is likely to be influenced by individual species. Overall mean height difference between LiDAR and UAV-DAP derived tree height indicates that UAV-DAP could underestimate individual tree height for target high-value timber species. The results of Chapter 2 confirmed the applicability of UAV-DAP for the tree height measurement of large-size high-value timber species.

The Chapter 3 deals with the second research question of how UAV-DAP could be used for the retrieval of individual tree spatial positions and individual tree DBH. High-resolution spectral information of UAV-DAP and LiDAR were applied in this Chapter. Multi-resolution segmentation was employed on UAV-DAP orthophotographs to derived individual tree crown objects. Object-based image analysis with random forest classification was used to classify forest canopy into five categories of three high-value timber species, other broadleaf species, and conifer. UAV-DAP can produce overall accuracy of 73% and 63% for classifying forest canopy into five categories in sub-compartment 36B and 59A, respectively. These results were used to identify the individual tree spatial position of high-value timber species. When estimating DBH, UAV-DAP can produce high-prediction accuracy comparable to field and LiDAR data. The results of Chapter 3 are useful for forest managers for searching of high-value timber trees with their estimated tree size in large area of mixed-wood forests.

Assessment of sustainability was employed in Chapter 4 focusing on the third research question. The sustainability of three high-value timber species were investigated using nearly 50 years of census data in long-term permanent plots. Commonly used variables in forest inventory, such as stocking, demographic parameters, and species proportions of these species were used as measures of sustainability. Results showed that the tree density and basal area of the three high-value timber species increased during the study period. Moreover, the basal area increment (BAI) of these species showed an increasing trend across census periods. However, while no significant differences in the tree mortality of these species were observed, the numbers of in-growth fluctuated across census periods. Increasing trends in species proportions of monarch birch and Japanese oak were observed. Even though there were some fluctuations across census periods, especially in smaller diameter classes, diameter distribution curves of high-value timber species followed a reversed J-shaped pattern. The results revealed that the

sustainability measures of high-value timber species can be achieved in forest stands managed under single-tree selection system.

Understanding individual tree growth of these species is important for the simulation and development of forest management options as well as for the purpose of periodic monitoring. In the Chapter 5, individual tree growth models of three high-value timber species were developed using long-term plot measurement data. Linear mixed-effects modelling approach was used to predict the individual tree basal area growth as a function of initial tree size, stand structure, and forest management. Model prediction followed by leave-one-out cross validation revealed a correlation between predicted and observed basal area increments with correlation coefficients of 0.62, 0.73 and 0.70 and root mean square errors values of 10.44, 7.91, and 11.62 $cm^2$/year for monarch birch, castor aralia, and Japanese oak, respectively. The results of model prediction were used to estimate the time for a certain diameter tree to reach a target diameter using compound interest formula. The results indicated that a 30 cm DBH tree will take 29, 28 and 48 years to reach 50 cm DBH and 48, 46, and 80 years to reach 70 cm DBH for monarch birch, castor aralia, and Japanese oak, respectively.

Overall, the results of this thesis indicated that the use of RS data and resource assessment techniques could facilitate the retrieval of individual tree information of high-value timber species and could support single-tree management systems. The applicability of UAV-DAP data in practical forest measurement of high-value timber species was confirmed. In addition, the results can provide individual tree spatial positions and their tree size which can be used in the practical field survey. Resource assessment techniques could be used for adapting silvicultural practices and harvesting practices as well as for simulating various silvicultural and management options for managing high-value timber species in a sustainable manner. The development of tree growth model will provide valuable information to estimate the timing of management and for periodic monitoring of economically high-value timber species. The combined use of RS data and long-term forest measurement data in the single-tree management planning of high-value timber species should be analyzed further.

# Chapter 1

# Introduction

## 1.1 Background

### 1.1.1 High-value timber species

High-value timber species are those that produce high-quality wood, used especially in the veneer and furniture industries (Oosterbaan et al., 2009). Despite their spatial occurrence at very low densities (Schulze et al., 2008), high-value timber species play a significant economic role in forest management and are increasingly important elements of forest production (Hemery et al., 2008). Trees of high economic value are often large in size (Owari et al., 2016) contributing to heterogeneity in forest structure, dynamics, and functions within forest ecosystem (Vandekerkhovea et al. 2018). Because of their high commercial value, high-value timber species can be targeted for excessive and illegal harvesting in some parts of the world (Ding et al., 2017; Khai et al., 2016). Due to heavy logging of high-value timber species, their depletion is of growing concern, with some species included on the International Union for Conservation of Nature (IUCN) red list (Bourland et al., 2012). Therefore, some high-value timber species have been designated for special attention in conservation and forest management practices (Prates-Clark et al., 2008).

High-value timber species are distributed throughout the world. In Southeast Asia, high-value timber species include teak (*Tectona grandis*), rosewood (*Dalbergia* spp. and *Pterocarpus* spp.) (Khai et al., 2016; Winfield et al., 2016). Other high-value timber species include genera such as *Fraxinus*, *Acer*, *Prunus*, *Sorbus*, *Juglans*, *Tilia*, *Alnus*, and *Betula* in Europe (Hemery et al., 2010; Oosterbaan et al., 2009), big-leaf mahogany (*Swietenia macrophylla*), ipê (*Tabebuia serratifolia* and *Tabebuia impeti*ginosa), jatobá (*Hymenaea courbaril*), and freijó cinza (*Cordia goeldiana*) in Latin America (Schulze et al., 2008), *Calophyllum brasiliensis*, *Carapa guianensis* and *Virola surinamensis* in the Amazon Basin (Prates-Clark et al., 2008).

In uneven-aged mixed conifer-broadleaf forests in northern Japan, monarch birch (*Betula maximowicziana* Regel), castor aralia (*Kalopanax septemlobus* (Thunb.) Koidz), and Japanese oak (*Quercus crispula* Blume) are important producers of high commercial value timber (Owari et al., 2016). These high-value timber species are shown in Figure 1.1. Monarch birch is the most valuable timber species and the log price may reach up to 20,000 US dollar per cubic meter and its value increases after death due to the changes of wood colour preferred by customers (Owari et al., 2016). This species plays an important role in stability and

sustainability of forest ecosystems as a major pioneer and a long-lived tree species (Tsuda et al., 2010). Because of high-quality and high-value wood, its use as a commercial tree species from natural forests is being promoted (Tsuda and Ide, 2005). Castor aralia is the second most expensive timber with its prices reaching up to ca. 7,500 USD per cubic meter (Owari et al., 2016). This species can typically be found as one of the sparsely distributed tree species in cool-temperate forests of northern Japan. Japanese oak, also a valuable timber species producing high-quality wood for whisky barrel making (Miyamoto et al., 2010), and is also one of the representative broadleaf species in northern Japanese forests.


**Figure 1.1:** High-value timber species. (**a**) Monarch birch (*Betula maximowicziana*), (**b**) Castor aralia (*Kalopanax septemlobus*), and (**c**) Japanese oak (*Quercus crispula*).

This study focuses on these three high-value timber species growing in cool-temperate mixed forests in northern Japan. The supply of high-quality timber from high-value tree species is primarily dependent on the cutting of large trees within the mixed forests. Shibano et al. (1990) suggested that monarch birch trees should be harvested at DBH > 60 cm, when the heartwood ratio is expected to be greater than 60%. According to Owari et al. (2016), DBH threshold to register as superior tree has been set to 50 cm under single-tree management system. Other study by Miyamoto et al. (2010) proposed single-tree management of Japanese trees for whisky barrels and they classified trees with DBH > 40cm as large-sized trees for

single-tree management. With the right management, valuable timber trees may yield high quality timber within relatively short production time (Hemery et al., 2008).

### 1.1.2 Single-tree management for high-value timber species

Various silvicultural and forest management practices have been developed that can facilitate sustainable management of forest resources (Löf et al., 2016; O'Hara, 2016; O'Hara et al., 2007). Forest management practices generally fall into two categories – even-aged and uneven-aged management (Puettmann et al., 2015; Pukkala et al., 2011; Sharma et al., 2016). Under even-aged management, forest stands with trees of a single age-class are typically regenerated either naturally or artificially after a clear-cutting operation. Uneven-aged management is a forest management system which is implemented by maintaining multiple age-classes through different kinds of selection cuttings, creating continuous tree cover in a stand at all times (Sharma et al., 2016). Uneven-aged forest management is assumed to achieve greater sustainability in forest resource management in comparison with even-aged forest management (Dieler et al., 2017; O'Hara et al., 2007). Therefore, uneven-aged forest management system has gained growing interest in many parts of the world due to its stability in forest stand structure (Kuuluvainen et al., 2012; Laiho et al., 2011; Puettmann et al., 2015; Pukkala et al., 2011). However, uneven-aged forest management system is likely to be more stand-oriented management, and focus on the size and structure of the whole forest stand.

Forest management focusing on the high-value timber species should aims to produce high-quality timber from these species with a minimum number of silvicultural interventions (Hemery et al., 2008). However, uneven-aged forests with complex forest structure and composition restrict forest management to exclusively focus on certain species with high commercial value. Due to operational costs and labour constraints, forest management may not able to focus on certain species with high-commercial value that have potential to produce high quality timber. Therefore, the tree-oriented or single-tree management approach are recommended for the management of high-value timber trees (Abetz and Klädtke, 2002; Giuliarelli et al., 2016; Owari et al., 2016).

In general, single-tree management is a forest management approach that aims at enhancing selected trees in the forest stand by applying well-defined silvicultural practices such as frequent thinning, pruning, removing trees that compete the growth of selected target trees (Kerr, 1996; Manetti et al., 2016). Its main objective is obtaining high-quality timber in a

short rotation period with minimum operational costs (Oosterbaan et al. 2009). By applying single-tree management system, it helps to determine which trees already reached a target diameter, what time a target trees will reach a target diameter, which trees need certain silvicultural operations to improve their growth (Abetz and Klädtke, 2002).

Previous studies reported that single-tree management of high-value timber species ensures their sustainable production while maintaining biodiversity of forest. Study by Löf et al. (2016) presented a combined management regime that may ensure the production of high-value oak timber and biodiversity conservation in Sweden. Owari et al. (2016) analyzed more than 2000 inventory plots to characterize the stand types in which superior trees of high-value timber species can be occurred, and found that superior trees generally grew in mature species-rich stand. They reported that single-tree management facilitates the sustainable use of high-value timber species by explicitly monitoring the numbers, attributes and locations of high-value trees, and contributes to stand structural heterogeneity. The silvicultural measures, that can be used at individual tree level, necessary to achieve the goals of improving high-value timber species were presented by Oosterbaan et al. (2009). By the application of adequate silvicultural measures, high quality timber of high-value timber species can be achieved.

The single-tree management system for high-value timber species has been practicing since 1965 in northern Japanese mixed conifer-hardwood forests (Yamamoto et al. 1989). The system has three main components: namely (1) single tree selection and registration, (2) measurement and assessment of selected target trees, and (3) periodic monitoring for optimal harvest (Owari et al., 2016; Yamamoto et al., 1989). However, no silvicultural operations, in general, under single-tree management system were carried. Under this system, large-sized trees, with high timber quality and value, are needed to be individually selected and registered, as superior trees, and monitored for their management (Miyamoto et al., 2010; Owari et al., 2016). The criteria for the selection of superior trees include both quantitative, such as DBH, crown length, bole height, and qualitative, such as straight trunk with few bending, twisting, knot, dormant bud, and decay (Oosterbaan et al., 2009; Owari et al., 2016). However, searching and locating of superior quality high-value timber trees within a large area of structurally complex forests remain a challenging task for forest managers. Forest inventory needs to provide information on tree size, tree vitality, and spatial position of superior high-value individuals to periodically monitor for harvest at optimal time for the reliable application of single-tree management system.

### 1.1.3 Remote sensing for single-tree management

Forest resource information plays an important role for forest management at global, regional and local scales (Kangas et al., 2019). Forest managers rely upon timely information on important forest attributes at the stand and landscape scales derived from forest inventory (Hoover et al., 2020). Therefore, forests are inventoried for strategic, tactical, and operational planning and forest management purposes (McRoberts et al., 2010; White et al., 2016), with the goal of providing accurate estimates of forest vegetation characteristics, including quantity, quality, extent, health, and composition within the area of interest (Reutebuch et al., 2005). However, forest information derived from ground-based survey have proven to be less effective in terms of time, labour, and cost (Wang et al., 2004; Xie et al., 2008), and limited to provide detailed spatial variations (Kane et al., 2010). Traditional forest inventory, in addition, may not be feasible to provide individual tree information which play a critical role in single-tree management.

From forest management viewpoint, particularly for single-tree management, species-specific information, such as tree species, tree height, DBH, and spatial position, of high-value timber species is necessary for individual tree selection, and periodic monitoring. Since field survey for searching of superior quality high-value trees is time consuming and required extensive resources, the use of remote sensing (RS) technology would provide promising information of individual trees for single-tree management system. RS technology is increasingly popular for acquiring forest information at large spatial scale (Kangas et al., 2018; Næsset, 2004; White et al., 2016; Wulder et al., 2012). However, the use of RS data for the purpose of single-tree management need to provide accurate estimate of individual tree information.

Even though there are different sources of RS data that are acquired using various kind of active and passive sensors, one of RS techniques that have potential to be used in single-tree management is airborne laser scanning (ALS) data due to its applicability in retrieval of individual tree information. ALS is an active remote sensing technique, that uses LiDAR sensors, providing a range of features related mainly to the trees, including discrete return and full-waveform features. In addition, LiDAR become the dominant RS technology during the last two decades as it can quickly provide highly accurate and spatially detailed information across an entire forest landscape (Lim et al., 2003; Silva et al., 2016; Wulder et al., 2014, 2012) and individual tree level, e.g. the estimation of individual tree height (Andersen et al., 2006; Mielcarek et al., 2018; Sibona et al., 2016; Y. Wang et al., 2019), and DBH (Yu et al., 2011)

that are important inventory parameters for single-tree management system. LiDAR intensity and waveform data may provide useful information for discriminating individual species (Alexander et al., 2015; Fassnacht et al., 2016; Hovi et al., 2016) which have potential to be used for the estimation of spatial position of high-value timber trees.

Another RS technique which has potential for single-tree management system is unmanned aerial vehicle digital aerial photogrammetry (UAV-DAP). UAV-DAP have become popular RS techniques for fine scale remote sensing due to its flexibility in planning image acquisition, low operational cost, high spatial and temporal resolution (Anderson and Gaston, 2013; Colomina and Molina, 2014). Software development, such as structure-from-motion (SfM) technique, enables the development of photogrammetric point cloud (PPC) and high resolution orthophotographs (Goodbody et al., 2019; Iglhaut et al., 2019; Lisein et al., 2013). Several previous studies evaluated the performance of UAV-DAP derived PPC in comparison with highly accurate LiDAR data (Lisein et al., 2013; Ota et al., 2015; Wallace et al., 2016; White et al., 2013) confirming the applicability of PPC in forest variable estimation.

RS techniques for single-tree management need to provide individual tree level species and structural information such as DBH and tree height. Even though UAV-DAP and LiDAR data were widely used in the estimation of forest resource information, their application in single-tree management was not yet been widely studied. Taking the advantages of spectral, red-green-blue (RGB), information derived from UAV-DAP in combination with LiDAR data, it has the potential to be applied in individual tree selection and measurement of high-value timber species for single-tree management system. With the availability of highly accurate LiDAR DTM, the repeated UAV flight missions will be of great potential for periodic monitoring of selected superior tree individuals.

### 1.1.4 Resource assessment methods for single-tree management

The achievement of sustainability from the use of various forest management practices is a central precept of forestry and is therefore central to all silvicultural systems (O'Hara et al., 2007). As discussed in Section 1.1.1, high-value timber species may be subject to overharvesting and illegal harvesting in many parts of the world. Even though such issues are currently negligible in Japan, it is worth to examine high-value timber resources under certain forest management regime, i.e., selection system. Understanding the resource conditions of high-value timber species could provide information for management decision on whether or

not a specific stand structure should be maintained which favour the growth of high-value timber species. In general, stocking, i.e., tree density and basal area is widely used forest inventory parameters. These forest inventory data were widely used for strategic level forest and environmental decisions (Fridman et al., 2014). Stand demographic parameters, i.e., growth, ingrowth or recruitment, and mortality are widely used to predict the forest dynamics. Repeated measurement of these variables, i.e., stocking and demographic parameters, could provide robust indicators for determining the sustainability of forest resources.

Single-tree management system is designed for an operational management of target high-value trees and the establishment of growth models play an important role under single-tree management (Abetz and Klädtke, 2002). From practical forest management perspective, individual tree growth model provides useful information for the estimation of time for a tree of certain size to reach a desired size (Cunha et al., 2016; Tenzin et al., 2017). This information plays an important role for the application of single-tree management system of high-value timber species. One of important tasks under single-tree management include the periodic monitoring of superior individual to estimate the optimum time for harvesting (Owari et al., 2016). Simple and practically applicable individual tree growth models for high-value timber species are required since it can be used for periodic monitoring and estimation of future resource conditions.

Modelling forest growth is intrinsic part of forestry research, as growth models are useful for inventory updating, harvest scheduling, silvicultural treatments evaluation, and management planning (Vanclay, 1994). The most flexible growth model in irregular and mixed forests is a set of individual tree models consisting of separate models for different species or species groups (Orellana et al., 2016). Individual tree growth models using individual tree as the basic unit in the growth modelling are therefore becoming widely used as they are capable of simulating various silvicultural and management options in stands with diverse structure, species composition and management history (Pokharel and Dech, 2012). In addition, information on individual tree growth is an important element in sustainable forest management which allows the selection of tree species for logging or protection, estimating the cutting cycles and simulating silvicultural treatments (Adame et al., 2008).

## 1.2 Objectives of the study

Although UAV-DAP and LiDAR data have great potential to be applied in single-tree management, many previous studies generally focused on the data-driven application of these data in the accuracy of forest resource estimation. The application of these data with well-defined practical forest management purposes needs to be examined. The application of UAV-DAP data in the single-tree management, which requires extensive resource for acquiring individual tree information of target species, will be of great benefit to forest managers. On the other hand, simple, easy to use, and practically applicable resource assessment techniques will help forestry practitioners in assessing forest management practices and allow to formulate future management scenarios. Therefore, this thesis aimed to apply the RS data combined with resource assessment techniques for single-tree management system of high-value timber species.

To apply the RS techniques for retrieval of individual tree information, the first question is whether RS techniques are reliable for operational forest measurement practices. Therefore, it is important to assess whether these techniques could be applied reliably in practical forest measurements. Therefore, the first objective of the study was to compare the accuracy of RS data, i.e., LiDAR data and UAV-DAP data, with field data for individual tree attribute estimation for high-value timber species. To compare the accuracy of RS data, I focused on the reliability of tree height derived from RS data and field data of individual tree. Previous studies have tested the applicability of UAV-DAP (Laurin et al., 2019; Panagiotidis et al., 2017; Surový et al., 2018) and LiDAR (Andersen et al. 2006; Sibona et al., 2016; Wang et al., 2019) data in comparison with field data for individual tree height information in different type of forests, mostly in the forest plantations or forest with simple structure in which tree top of individual tree can be easily detected. Broadleaf tree species were not generally focused in these previous studies. Particularly, high-value broadleaf species, e.g. target species in this study, produce extensive and highly heterogenous crown structure which may not be detected their tree tops easily. The applicability of UAV-DAP and LiDAR data in the tree height estimation of these tree species needs to be addressed. Further, a rigorous comparison of individual tree height estimation between LiDAR, UAV-DAP and field survey data is relatively rare. Therefore, my first objective tries to address these issues.

If the RS techniques, i.e. UAV-DAP and LiDAR, can be applied reliably in individual tree height measurement of high-value timber species, further research question is that how these techniques could be used in estimation of individual tree information, such as tree spatial

position and the stem size. This question was addressed in the second objective: to estimate the spatial distribution and stem size of superior trees individuals, which play a critical role under single-tree management, using RS data. The existing literature suggests that LiDAR data in combination with other type of RS data, i.e., multispectral or hyperspectral data, could provide species-specific information (Dalponte et al., 2019; Fassnacht et al., 2016; Singh et al., 2015). However, the use of UAV-DAP data for the purpose of individual tree attribute estimation, such as species identity, DBH, etc., is still sparse, particularly those for high-value timber species in mixed-wood forest. In addition, the application of the research results in the field is still limited. These issues were tried to address in the second research objectives.

Whether forest management practices ensured the sustainability of forest resources are critical question in forest management. Assessing the resource sustainability of a certain forest management regime, e.g. selection system, is important for reliable application of a forest management system. It is necessary to develop indicators that can be used for the purpose of sustainability assessment. However, forest trees may take several decades to assess their response to any changes in their surrounding environment. Therefore, it is relatively difficult to develop specific indicators to judge the sustainability of forest management. In this case, long-term forest measurement data are invaluable providing reliable data source for evidence-based policy making. The third objective of this thesis is to assess the resource conditions of high-value timber species under selection system.

Understanding individual tree growth of these species play an important role in forest management simulations and estimation of future forest resource conditions. One of the main questions in forestry is that when a tree will reach a certain target diameter. Generally, tree growth models were widely used in many different regions for this purpose (Cunha et al., 2016; Tenzin et al., 2017). In mixed conifer-broadleaf forest in northern Japan, Tatsumi et al., (2016) quantified the neighborhood competition on the diameter growth of 38 tree species, including high-value timber species, using two times DBH measurement data. Using the tree ring data of 76 large-sized monarch trees, Shibano et al. (1995) examined the diameter growth of monarch birch trees in mixed conifer-broadleaf forest in northern Japan. However, these studies required intensive data collection of individual tree spatial positions and tree ring data from a larger number of trees which may need extensive resources, time and efforts. A simple and practically applicable tree growth model of high-value timber species was not widely studied. Therefore, simple, easy-to-develop, and practically applicable individual tree growth models are necessary. The fourth objective of the thesis is, therefore, to develop a simple and practically

applicable individual tree growth model that can be used to predict the time required for the management of selected high-value timber individuals.

### 1.3 Organization of the thesis

This thesis consists of 6 chapters. The first chapter is the Introduction. Chapter 2 to Chapter 5 deal with each research objectives mentioned in section 1.2. The applicability of UAV-DAP data compared to field measured and LiDAR data, focusing on tree height measurement was assessed Chapter 2. Estimation of individual tree spatial position and stem size for high-value timber species was examined in Chapter 3. In Chapter 4, I assessed the resource assessment techniques for high-value timber species, using commonly used stand parameters and demographic parameters. Individual tree growth model for three high-value timber species were developed using long-term forest measurement data of permanent plots in Chapter 5. I estimated the time required for a certain diameter trees to reach a desirable target diameter using the developed growth models. Chapter 6 discussed the potential application of RS data and individual tree growth model for single-tree management system of high-value timber species. In addition, I discussed management implications, the major findings, limitations and future directions of the thesis as a whole in Chapter 6. The flow chart of the study is shown in Figure 1.2

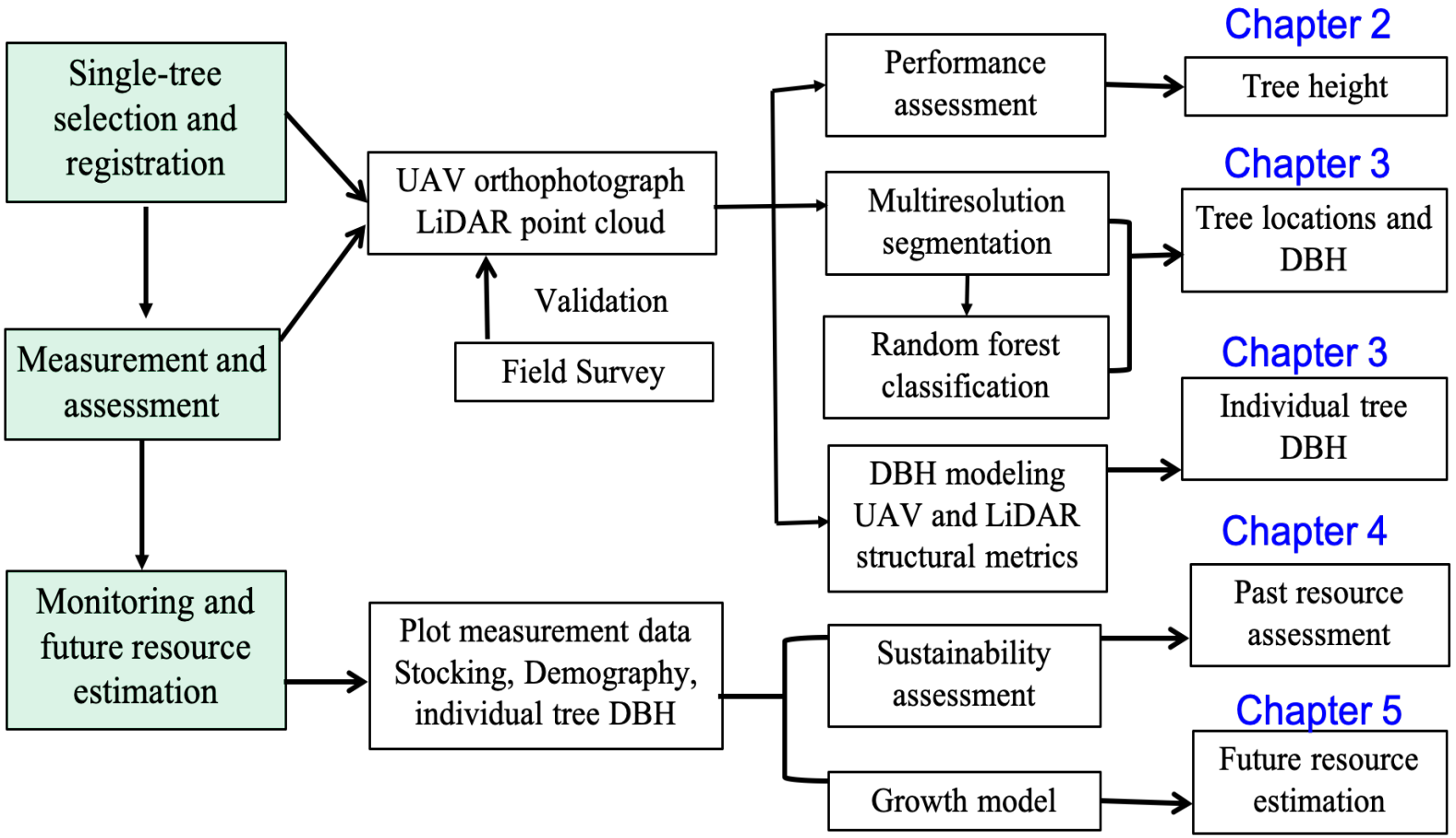


**Figure 1.2:** Flow chart of the study

# Chapter 2

# The applicability of UAV-DAP for tree height estimation: comparison with airborne LiDAR and field survey

## 2.1 Introduction

For the purpose of single-tree management, the forest inventory needs to provide accurate information of high-value individuals such as tree height and diameter at breast height (DBH). The individual tree DBH can be measured accurately by traditional field measurements, but tree height is relatively difficult to measure accurately (Laurin et al., 2019). Further, the results of tree height measurements are greatly influenced by many factors including biophysical and topographic factors, instrument errors, and human errors (Hunter et al., 2013; Kitahara et al., 2010; Larjavaara and Muller-Landau, 2013; Stereńczak et al., 2019). Although errors are likely to be presented in the field measurements of tree height than other parameters, such as DBH (Hunter et al., 2013; Luoma et al., 2017), field-measured tree heights have been widely understood to be the most reliable source of tree height information (Bragg, 2014).

With the advancement of RS technology such as ALS and UAV-DAP, the use of RS technology may overcome difficulty in accurate tree height measurement in the field. ALS is an active remote sensing technique that uses a light detection and ranging (LiDAR) sensor, which enables us to measure the three-dimensional (3D) distribution of vegetation canopy components as well as sub-canopy topography, resulting in an accurate estimation of vegetation height and ground elevation (Lim et al., 2003; Wulder et al., 2014). Previous studies have demonstrated the ability of LiDAR data in the estimation of forest information over large areas of forests with high accuracy (Hyyppä et al., 2012; Kaartinen et al., 2012; Takagi et al., 2015). Further, a LiDAR 3D forest structure can provide accurate individual tree height information (Ganz et al., 2019; Hirata, 2004; Imai et al., 2004; Sibona et al., 2016; Y. Wang et al., 2019). However, the major limitation of LiDAR data is the high acquisition cost, which limits its application in forest management directives (Goodbody et al., 2019; Iglhaut et al., 2019).

Recently UAV-DAP has become a popular RS technique for fine-scale remote sensing due to its flexibility in data acquisition, low operational cost, and high spatial and temporal resolution (Colomina and Molina, 2014). Software developments, such as Structure-from-

Motion (SfM), offer the efficient processing of digital aerial photographs (DAPs) acquired from low-cost UAV platforms, providing an cost-effective alternative to generate the 3D forest information, i.e., photogrammetric point cloud (PPC) (Nex and Remondino, 2014; Torresan et al., 2018; Verhoeven et al., 2012). Although PPC fails to provide ground information especially in dense vegetation cover, it can provide an upper canopy surface (Vastaranta et al., 2013; White et al., 2013). Thus, the accurate DTM is a prerequisite for the accurate characterization of forest information using PPC. Where highly accurate DTM exists, PPC has been proven to provide a cost-effective estimation of forest information with high accuracy comparable to LiDAR data (Bohlin et al., 2012; Cao et al., 2019; Jayathunga et al., 2018a; Noordermeer et al., 2019; Ota et al., 2015; Puliti et al., 2015; Wallace et al., 2016). Moreover, recent studies suggested that UAV-DAP could provide highly accurate individual tree height information (Huang et al., 2019; Panagiotidis et al., 2017; Surový et al., 2018; Zarco-Tejada et al., 2014). However, most of these studies have been employed in forests with simple structural complexity such as plantations or even-aged forests.

Applications of UAV-DAP for individual tree height measurement, particularly for large-size broadleaved trees, have not been widely studied, especially in structurally complex mixed forests. Moreover, a rigorous comparison of individual tree height estimation between LiDAR, UAV-DAP and field survey data is rare. Therefore, I tried to address these issues in this study.

The aim of this Chapter is, therefore, to examine whether UAV-DAP could be used to derive the height of large-size high-value trees. First, I compared individual tree height derived from field survey, LiDAR, and UAV-DAP data. Since tree height can be predicted from the individual tree DBH (Feldpausch et al., 2011; Hulshof et al., 2015; Mehtätalo et al., 2015), secondly, I assessed the relationship between individual tree DBH and the tree height derived from field survey, LiDAR, and UAV-DAP through height-diameter models to examine how three height sources can be explained by tree diameter.

## 2.2 Materials and methods

### 2.2.1 Study area

The study area is the University of Tokyo Hokkaido Forest (UTHF) (Figure 2.1). UTHF is located in Furano City, central Hokkaido Island in northern Japan (43°10–20′ N, 142°18–40′ E, 190–1459 m asl). UTHF is a pan-mixed forest, where uneven-aged mixed forests with

coniferous and broad-leaved tree species are the main vegetation cover. The mean annual temperature was 6.4 °C and precipitation was 1297 mm at the arboretum of the UTHF (230 m asl) during 2001–2010, and snow usually covers the ground from late November to early April with a maximum depth of approximately 1 m. The predominant tree species included Sakhalin fir (*Abies sachalinensis*), Yezo spruce (*Picea jezoensis*), Japanese linden (*Tilia japonica*), and painted maple (*Acer pictum* var. *mono*) (Owari et al., 2011). Other common conifer tree species include *Taxus cuspidata*, *Picea glehnii*. *B. maximowicziana*, *K. septemlobus*, *Q. crispula*, and *Ulmus laciniata*, which are among the common deciduous broadleaved species. The forest floor is often occupied by evergreen dwarf bamboo (*Sasa senanensis* and *Sasa kurilensis*).

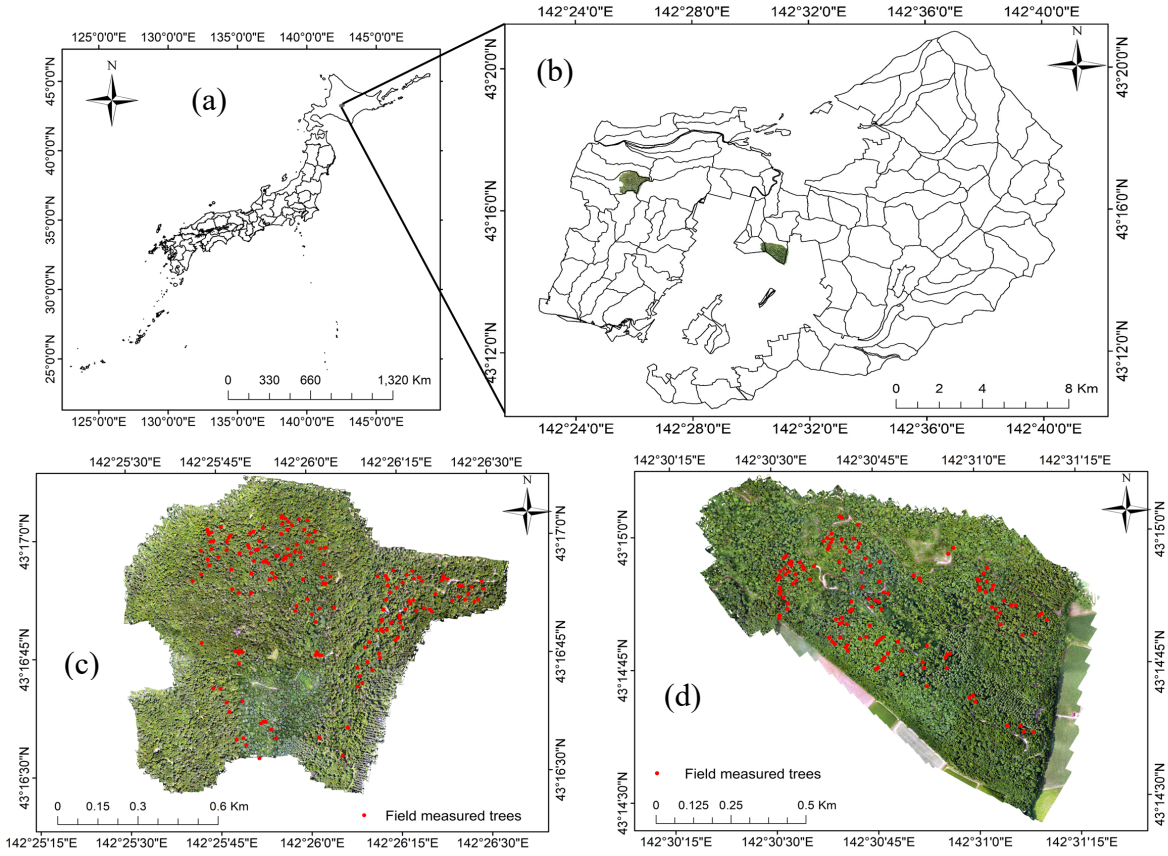


**Figure 2.1:** Location of the study area. (a) The University of Tokyo Hokkaido Forest, (b) Sub-compartment 36B and 59A, and permanent plots (c) Field measured trees at sub-compartment 36B, (d) Field measured trees at sub-compartment 59A.

### 2.2.2 Data

#### 2.2.2.1. Field Data

I used field measured trees of 178 high-value timber species. Measurements were carried out during July and August of 2019. Measurement parameters included the DBH, tree height, and spatial positions of individual trees. A summary of field measurement is given in Table 2.1. DBH was measured using diameter tape. The tree heights were measured using a Vertex III hypsometer and transponder (Haglöf Sweden AB, Långsele, Sweden). Tree height measurements were carried out three times, and average height values were assumed as the corresponding tree height. Individual tree spatial positions were recorded using global navigation satellite system (GNSS). An R2 integrated GNSS system (Trimble Inc., Sunnyvale, CA, USA) was used to record individual tree spatial positions with an accuracy of less than 1 m.

**Table 2.1:** Summary statistics of field measured trees (standard deviation in parenthesis).

| | DBH (cm) | | |
|---|---|---|---|
| | **Mean** | **Minimum** | **Maximum** |
| Monarch birch (n = 62) | 60.07 (10.13) | 41.80 | 90.60 |
| Castor aralia (n = 64) | 59.34 (12.92) | 44.00 | 94.40 |
| Japanese oak (n = 52) | 74.38 (14.09) | 44.20 | 111.20 |

#### 2.2.2.2 LiDAR Data

LiDAR data were acquired in September 2018 using an Optech Airborne Laser Terrain Mapper (ALTM) Orion M300 sensor (Teledyne Technologies, Waterloo, ON, Canada) mounted on a helicopter. The detail specifications of LiDAR data are summarized in Table 2.2. The acquired data included first, second, third and last return and waveform data. The classification of LiDAR data into ground and non-ground points was initially processed by the data provider (Hokkaido Aero Asahi, Hokkaido, Japan), and data were delivered in LAS format. In this study, we used first and last return data only.

**Table 2.2:** LiDAR flight parameters.

| Parameters | Description |
|---|---|
| Flying speed (km/h) | 140.4 |
| Flying height (m) | 600 |
| Course overlap (%) | 50 |
| Beam divergence (mrad) | 0.16 |
| Pulse rate (kHz) | 100 |
| Scan angle (°) | ±30 |
| Point density (points/$m^2$) | 16.07 |

#### 2.2.2.3 UAV Data

UAV imagery was acquired on 8 and 10 July 2019 for sub-compartment 36B and 11 and 30 July 2019 for sub-compartment 59A. We used an Inspire-2 platform mounted with a Zenmuse X5S RGB camera (DJI, Shenzhen, China) for image acquisition. Eight separate flights for sub-compartment 36B and 10 separate flights for sub-compartment 59A were employed. In both sub-compartments, the flying altitudes were set to 120 m, but the actual flying height may have varied because of the terrain conditions. The average ground sampling distances were 2.3 cm/pixel. Image overlaps were 80% for both longitudinal and lateral overlaps. Before flight missions, ground control points (GCPs), take-off and landing points were set in available open areas. The locations of GCPs were recorded using the Trimble R2 GNSS. 10 GCPs in sub-compartment 36B and 9 GCPs in sub-compartment 59A were collected. There were total of 3292 images for compartment 36B and 2231 images for compartment 59A. All imagery had a photo resolution of 5280 × 3956 pixels.

### 2.2.3 Data processing and canopy height model (CHM) generation

#### 2.2.3.1 LiDAR data processing and LiDAR-CHM generation

For this study, LiDAR data processing was performed using US Forest Service FUSION/LDV 3.8.0 software (McGaughey, 2018). LiDAR digital terrain models (LiDAR-DTM) of 0.5 m spatial resolution were generated using GroundFilter and GridSurfaceCreate functions. LiDAR point clouds were normalized to the height above ground by the subtraction of the LiDAR-DTM elevation from LiDAR digital surface models (LiDAR-DSM) to generate the LiDAR canopy height model (LiDAR-CHM). I used the CanopyModel function in FUSION/LDV software to generate a LiDAR-CHM with a 0.5 m spatial resolution.

#### 2.2.3.2 UAV data processing and UAV-DAP-CHM generation

I used the 3D modelling software Agisoft Metashape Professional Edition 1.5.3 (Agisoft, St. Petersburg, Russia) for UAV photogrammetric processing. Metashape offers a user-friendly workflow that combines proprietary algorithms based on computer vision SfM and stereo-matching for image alignment and reconstruction of the 3D image (Verhoeven et al., 2012). The workflow included four stages: image alignment, building a dense point cloud, building a digital elevation model (DEM) and building an orthomosaic. During the image alignment stage, the stage at which camera location, orientation and other internal parameters are optimized (Agisoft., 2018), I used high accuracy for image matching. Using the SfM techniques, this stage extract features within the images and match those features to pair the images. This stage produced a sparse 3D point cloud. After initial alignment, I deleted abnormal points based on gradual selection procedures in Metashape (Agisoft., 2018) to optimize the camera locations. I then added GCPs in each corresponding image for a more accurate optimization of camera locations and orientation as well as other internal camera parameters. In the building dense point cloud stage, the stage that generates a dense point clouds, I used medium quality to reduce the image processing time and mild depth filtering to remove the outliers. I followed the Metashape default setting for the DEM building stage and orthomosaic building stage. Dense point clouds were exported in LASer (.las) format with average point density of 547.01 points/$m^2$ and orthophotographs with a 3 cm pixel resolution were exported in GeoTiff format.

Previous studies (Jayathunga et al., 2018a; Ota et al., 2015; White et al., 2013) highlighted the need for accurate DTM for the normalization of UAV-DAP point clouds. To generate UAV-DAP-CHM, I used LiDAR-DTM for normalization of PPC. I used the same procedure as the LiDAR-CHM generation in the FUSION software package, and the resulting UAV-DAP-CHM was exported with a 0.5 m spatial resolution.

### 2.2.4 Individual tree height measurement using RS data

In order to evaluate the reliability of individual tree height measurement using different data sources—i.e., field, LiDAR and UAV-DAP—exact individual trees need to be identified in all three data sources. Further, methods of measuring tree height need to be carried out separately to ensure independent measurements from the statistical point of view. An individual tree crown detection algorithm may impose errors in detecting individual trees and previous studies reported poor results in tree detection under a complex forest structure

(Kaartinen et al., 2012; Wang et al., 2016). Therefore, field measured individual tree positions were used to identify the exact trees on both CHMs with the help of UAV-DAP orthophotographs. The manual delineation of an individual tree crown was carried out using high resolution orthophotographs. These crown polygons were used as reference crowns and for extracting individual tree heights from both LiDAR-CHM and UAV-DAP-CHM.

In forestry, tree height can be defined as the vertical distance between the ground level and tip of the tree (Husch et al., 2003). I also used this definition in measuring tree height in the field. According to this definition, the difference between maximum point within a crown and the ground is the tree height. Therefore, the maximum value within a manually delineated crown polygon was considered to be the corresponding tree height. Height measurements were carried out separately for LiDAR-CHM and UAV-DAP-CHM.

It should be noted that there is a temporal discrepancy of 10 to 11 months between the LiDAR data acquisition and UAV imagery acquisition. Field measurements were carried out at the same time as UAV imagery acquisition. Previous studies suggested that trees typically invest heavily in height growth when young, rapidly approaching their maximum height, but then continue to grow in diameter throughout their lives (King, 2005). In my data, only large diameter trees (DBH > 40 cm) were included (Table 2.1). Therefore, I assumed that there are no large increments in the tree heights of large size trees.

### 2.2.5 Data analysis

#### 2.2.5.1 Individual tree height comparison

The individual tree height comparison was carried out in pairs; i.e., Field height vs LiDAR height, Field height vs UAV-DAP height, and LiDAR height vs UAV-DAP height. To access the degree of association between pairs, I calculated the Pearson correlation coefficient (r). Further, I calculated the root mean square difference (RMSD). The RMSD indicates the average height difference between measurement methods and clarifies the magnitude of the differences between measurement methods. Further, I calculated the mean difference (MD) to indicate whether tree heights derived from one measurement technique were generally greater or smaller than those derived from another measurement technique.

#### 2.2.5.2 Height-Diameter relationships

Tree height-diameter (H-D) models are widely used to predict individual tree heights (Hulshof et al., 2015; Imani et al., 2017; Mehtätalo et al., 2015). Tree height data predicted from DBH using these models can be used as an input variable in various forest models such as growth and yield models, and biomass models (Hunter et al., 2013; Takagi et al., 2015). Most of the previously published studies used one tree height measurement technique, i.e., field survey, in H-D models. As UAV-DAP and LiDAR data could provide accurate tree height information, it is worth to examine how different tree height data sources perform in H-D models. To assess the performance of different tree height measuring techniques in the H-D model, I tested a simple non-linear function (Equation 2.1) which was widely used in the height-diameter allometric models:

$$\text{Height} = 1.3 + a \times \text{DBH}^b \qquad \text{Equation (2.1)}$$

where, a and b are parameters to be estimated. The value of 1.3 is included in all models to account for the fact that DBH is measured at 1.3 m above the ground. It was excluded when height values from LiDAR and UAV-DAP were used in model development. I tested species-specific non-linear models to examine the relationships between DBH and tree height derived from field, LiDAR and UAV-DAP data. RMSE and coefficient of determination ($R^2$) values were used for model evaluation. All statistical analyses were performed in R software (R Core Team, 2019).

## 2.3 Results

### 2.3.1 Correlation between observed tree heights

Observed tree heights are listed in Table 2.3. The comparison of field, LiDAR and UAV-DAP tree height for the three species is summarized in Table 2.4 and Figure 2.2. The RMSD and r values showed good agreement and consistency between the field, LiDAR and UAV-DAP tree height measurement. Among the three pairs for the individual tree height comparison of all species, the LiDAR vs UAV-DAP pair has the highest *r* values and lowest RMSD values, while the lowest r values and highest RMSD values occurred in Field vs UAV-DAP pair. The same results were also found for species specific comparison. The correlation coefficients in Table 2.4 also indicate that tree height measurement accuracy could differ between species.

**Table 2.3:** Observed tree height from field, LiDAR and UAV-DAP (standard deviation in parenthesis).

| Species | Field Height (m) | | | LiDAR Height (m) | | | UAV-DAP Height (m) | | |
|---|---|---|---|---|---|---|---|---|---|
| | Mean | Min | Max | Mean | Min | Max | Mean | Min | Max |
| Monarch birch (n = 62) | 25.35 (2.65) | 20.87 | 32.83 | 25.39 (1.66) | 22.13 | 30.64 | 25.21 (2.01) | 21.43 | 30.73 |
| Castor aralia (n = 64) | 23.40 (3.10) | 14.10 | 29.73 | 23.70 (2.51) | 16.58 | 30.27 | 23.52 (2.75) | 15.92 | 30.50 |
| Japanese oak (n = 52) | 24.67 (2.64) | 20.43 | 30.13 | 24.56 (1.79) | 20.81 | 28.80 | 24.24 (2.03) | 20.21 | 29.48 |

**Table 2.4:** Correlation of tree height derived from field, LiDAR and UAV-DAP data for three high-value timber species.

| Species | Field vs LiDAR | | | Field vs UAV-DAP | | | LiDAR vs UAV-DAP | | |
|---|---|---|---|---|---|---|---|---|---|
| | r | RMSD | Bias | r | RMSD | Bias | r | RMSD | Bias |
| Monarch birch (n = 62) | 0.69 | 1.91 | −0.05 | 0.61 | 2.12 | 0.14 | 0.77 | 1.29 | 0.19 |
| Castor aralia (n = 64) | 0.76 | 2.04 | −0.30 | 0.74 | 2.14 | −0.12 | 0.92 | 1.07 | 0.18 |
| Japanese oak (n = 52) | 0.63 | 2.05 | 0.11 | 0.55 | 2.31 | 0.43 | 0.91 | 0.91 | 0.31 |
| All (n = 178) | 0.73 | 2.00 | −0.93 | 0.68 | 2.18 | 0.13 | 0.89 | 1.11 | 0.22 |

Note: all values of r were statistically significant at $p < 0.001$. Paired sample t-tests were not statistically significant for all pairs of comparison at 0.05 significant levels.

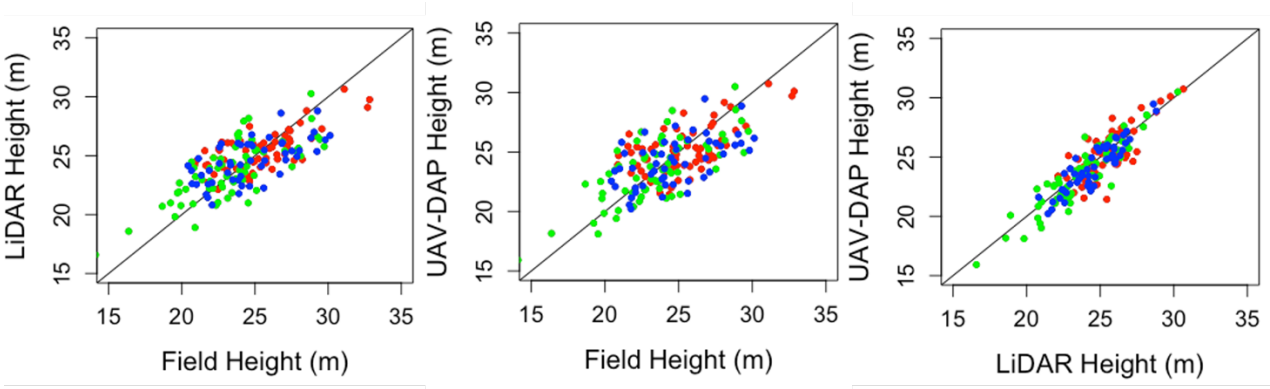


**Figure 2.2:** Correlation between tree heights derived from field survey, LiDAR, and UAV-DAP data. Red, green, and blue dots represent individual monarch birch, castor aralia, and Japanese oak tree heights, respectively.

### 2.3.2 Height differences between three height measurement methods

Height differences between Field vs LiDAR, Field vs UAV-DAP and LiDAR vs UAV-DAP are shown in Table 2.5 and Figure 2.3. As shown in Figure 2.3 (a), the height differences between field and LiDAR tree height increase as the field measured tree heights increase. A similar trend was observed in the height differences of field-measured and UAV-DAP tree height (Figure 2.3 (b)). However, tree height differences between LiDAR and UAV-DAP decreased with increasing UAV-DAP tree height as shown in Figure 2.3 (c).

**Table 2.5:** Height differences between field measured and RS tree height (standard deviation in parenthesis).

| Species | Field vs LiDAR (m) | | | Field vs UAV-DAP (m) | | | LiDAR vs UAV-DAP (m) | | |
|---|---|---|---|---|---|---|---|---|---|
| | Mean | Min | Max | Mean | Min | Max | Mean | Min | Max |
| Monarch birch | −0.05 (1.9) | −3.85 | 3.60 | 0.14 (2.13) | −4.88 | 3.10 | 0.19 (1.29) | −2.47 | 4.00 |
| Castor aralia | −0.30 (2.0) | −3.80 | 3.95 | −0.12 (2.15) | −4.27 | 4.47 | 0.18 (1.07) | −2.70 | 3.19 |
| Japanese oak | 0.11 (2.1) | −3.72 | 3.87 | 0.43 (2.29) | −4.68 | 4.66 | 0.31 (0.86) | −1.56 | 2.20 |
| All | −0.09 (2.0) | −3.85 | 3.95 | 0.13 (2.19) | −4.88 | 4.66 | 0.22 (1.09) | −2.74 | 4.00 |

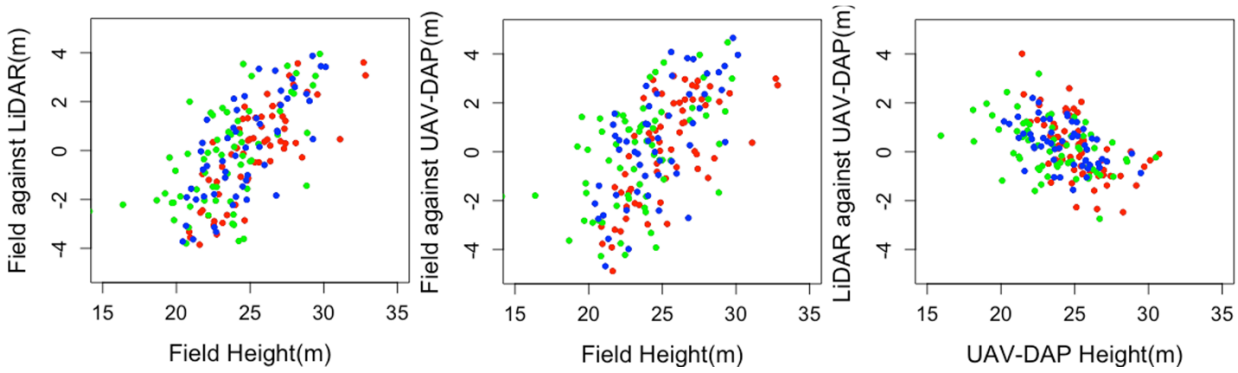


**Figure 2.3:** Height differences between measurement methods. (a) Difference between field height and LiDAR height, (b) Difference between field height and UAV-DAP height, and (c) Difference between LiDAR height and UAV-DAP height. Red, green, and blue dots represent individual monarch birch, castor aralia, and Japanese oak tree height respectively.

According to Figures 2.3 (a) and (b), field tree height measurements were likely to produce lower tree height values for lower height trees and higher tree height values for higher trees when compared with RS data. Figure 2.3 (c) indicates that UAV-DAP could produce higher tree height values of higher trees and lower tree height values for lower trees when compared with LiDAR data. However, the mean difference in Table 2.5 indicates that UAV-

DAP underestimates the individual tree height in comparison with LiDAR data. The lowest and highest individual tree height differences between LiDAR data and UAV-DAP were −2.74 m and 4.00 m, respectively, with mean tree height differences for all species of less than 1 m.

### 2.3.3. Relation between tree height and DBH

#### 2.3.3.1 Height-Diameter relationships

Correlations between individual tree DBH and tree height derived from the field survey, LiDAR, and UAV-DAP are summarized in Table 2.6 and Figure 2.4. The tree height derived from LiDAR data showed a stronger correlation with DBH than field-measured and UAV-DAP tree height. A better correlation between tree height and DBH was observed for castor aralia than the other two species, while Japanese oak exhibited a significant but relatively poor correlation among the three species.

**Table 2.6:** Pearson's correlation coefficient between tree height and DBH.

| Species | Field Height | LiDAR Height | UAV-DAP Height |
|---|---|---|---|
| Monarch birch | 0.41 * | 0.58 *** | 0.47 *** |
| Castor aralia | 0.56 *** | 0.67 *** | 0.65 *** |
| Japanese oak | 0.34 * | 0.35 * | 0.25 |
| All | 0.41 *** | 0.46 *** | 0.40 *** |

Significance: *** $p < 0.001$, * $p < 0.05$.

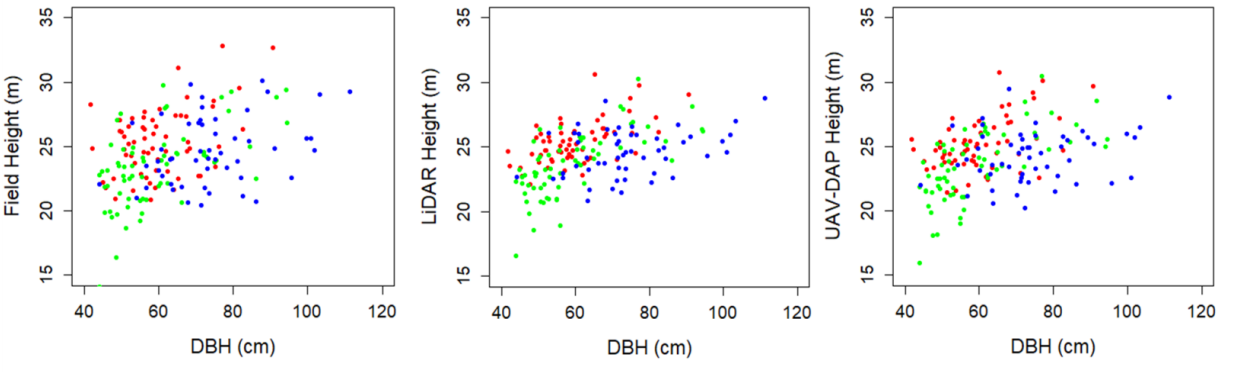


**Figure 2.4:** Correlation between individual tree DBH and tree height derived from Field, LiDAR, and UAV-DAP. Red, green, and blue dots represent individual monarch birch, castor aralia, and Japanese oak tree respectively.

#### 2.3.3.2 H-D models

The results of the non-linear H-D models are summarized in Table 2.7. In comparison with the field measured tree height, the UAV-DAP tree height showed better prediction power in terms of RMSE for all species (Table 2.7). H-D model using LiDAR derived tree height exhibited lower RMSE values and higher $R^2$ values for all target species. Figure 2.5 indicates the distribution of prediction errors across DBH and tree height which also shows the lower variation for LiDAR derived tree height estimation. It also shows that UAV-DAP derived tree height can be predicted from tree DBH with comparable level of prediction errors to field and LiDAR derived tree height. Figure 2.5 also reveals the smaller prediction errors for LiDAR derived tree height and UAV-DAP derived tree height. The mean prediction errors across height classes were shown in Figure 2.6. According to Figure 2.6, highest negative mean prediction errors were observed for field measured tree height in the lower high classes and larger positive mean prediction errors were observed in higher height classes for all species. Lower positive and negative mean prediction errors were found for LiDAR and UAV-DAP derived tree height. In Figure 2.7, I showed the similarity of LiDAR and UAV-DAP tree height predicted from tree DBH to the field measured tree height for height diameter curve.

**Table 2.7:** H-D models using tree height derived from field survey, LiDAR and UAV-DAP data.

| | **Field Height** | | | | **LiDAR Height** | | | | **UAV-DAP Height** | | | |
|---|---|---|---|---|---|---|---|---|---|---|---|---|
| | **a** | **b** | **RMSE** | **$R^2$** | **a** | **b** | **RMSE** | **$R^2$** | **a** | **b** | **RMSE** | **$R^2$** |
| Monarch birch | 9.22 ** | 0.25 ** | 2.42 | 0.18 | 9.95 *** | 0.23 *** | 1.35 | 0.50 | 10.10 *** | 0.22 *** | 1.77 | 0.27 |
| Castor aralia | 5.35 *** | 0.36 *** | 2.53 | 0.47 | 5.74 *** | 0.35 *** | 1.81 | 0.88 | 5.20 *** | 0.37 *** | 2.04 | 0.77 |
| Japanese oak | 10.69 ** | 0.19 ** | 2.46 | 0.13 | 13.96 *** | 0.13 * | 1.67 | 0.13 | 15.49 *** | 0.10 | 1.96 | 0.10 |

a and b are the parameters of Equation (2.1). Significance: *** $p < 0.001$, ** $p < 0.01$, * $p < 0.05$.

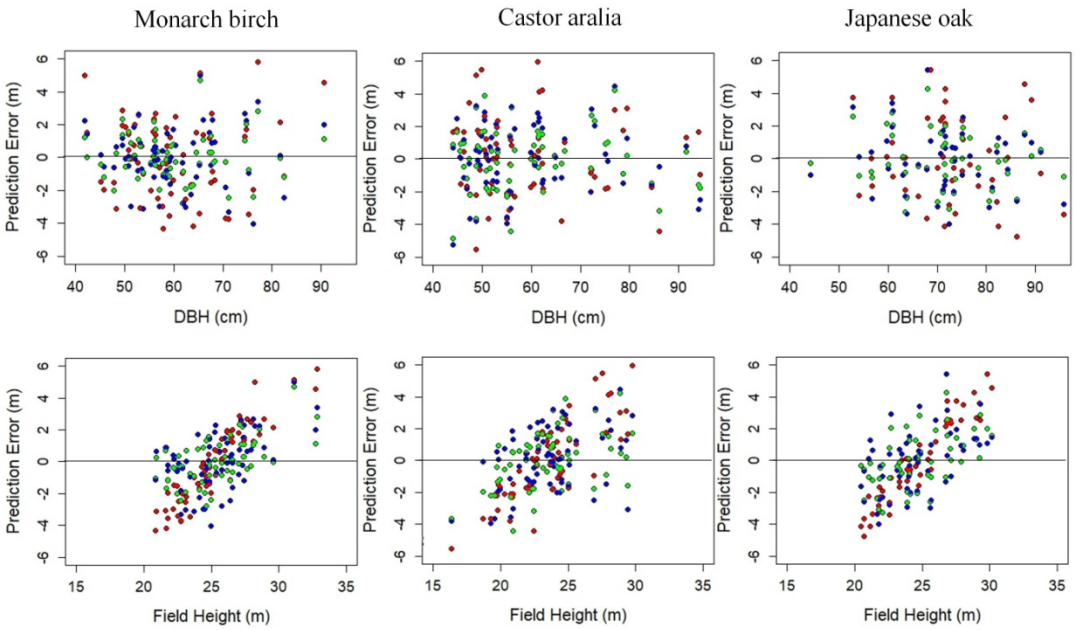


**Figure 2.5:** Distribution of prediction error across DBH and height. Red, green, and blue dots represent prediction errors for field height, LiDAR height, and UAV-DAP height, respectively.

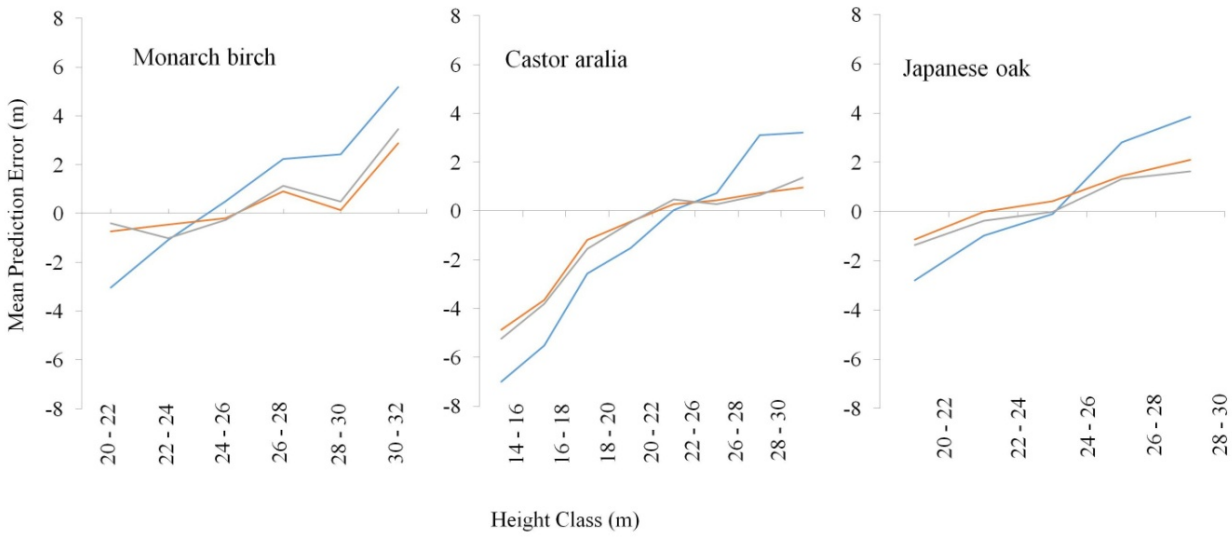


**Figure 2.6:** Mean prediction errors and height classes (field measured height). Blue, red, and gray lines represent mean prediction errors for field height, LiDAR height, and UAV-DAP height, respectively.

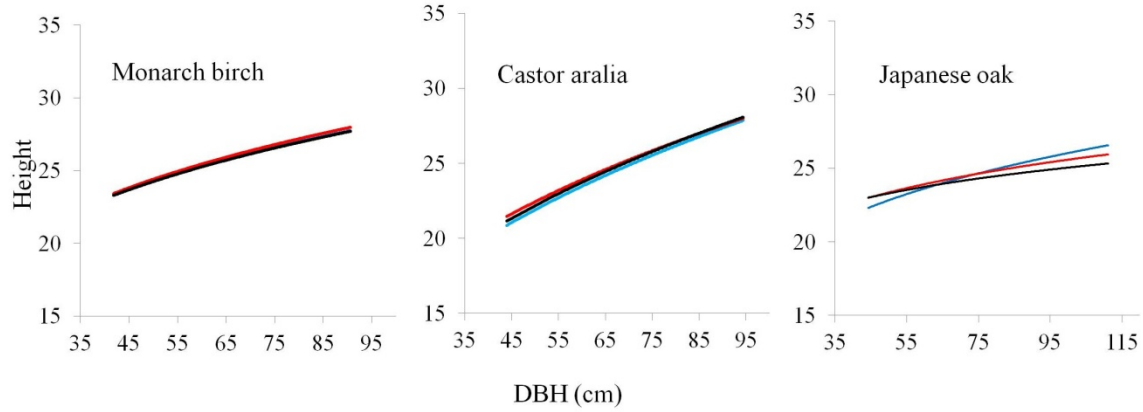


**Figure 2.7:** Height-Diameter curves. Blue, red, and black lines represent field measured height, predicted LiDAR height, and predicted UAV-DAP height, respectively.

## 2.4 Discussion

In this Chapter, I demonstrated the ability of UAV-DAP to perform the individual tree height estimation of high-value timber individuals in mixed conifer-broadleaf forests in northern Japan. The results showed that UAV-DAP enabled individual tree height estimation with comparable accuracy to airborne laser scanning or LiDAR data and field-measured data.

According to Table 2.4, stronger correlation coefficients were observed in LiDAR and UAV-DAP tree height comparison among three pairs of comparison. LiDAR derived tree height showed better correlation with field measure tree height than UAV-DAP derived tree height. This result is consistent with a previous study (Wallace et al., 2016). They also reported a stronger correlation between Field vs LiDAR than Field vs UAV-DAP. However, the correlation between LiDAR and field measured tree height in this study was lower than other studies (Ganz et al., 2019; Hirata, 2004; Sibona et al., 2016; Y. Wang et al., 2019). This lower correlation could be related to the species, the tree height itself and measurement errors in the field. In addition, the accuracy of tree heights derived from RS data might also be influenced by many factors such as structural complexity of the forest canopy which could affect photogrammetric reconstruction (Jayathunga et al., 2018b; Lisein et al., 2013; Wallace et al., 2016). Moreover, LiDAR data also have limitations such as tree height estimation errors due to different canopy height model generation methods (Mielcarek et al., 2018), susceptibility to influence of slope and crown shape on canopy height (Khosravipour et al., 2015).

One of the key questions when using field-measured tree height as reference data for the evaluation of LiDAR or UAV-DAP is the accuracy of field measurement. A previous study

(Sibona et al., 2016) assessed the accuracy of LiDAR tree height using actual tree height derived from 100 felled trees. They found that tree height derived from LiDAR data was closer to actual height than field measurement. Since target species in my study are large-size high-value broadleaved trees, some error in field measurement could be expected because of the tree height itself and tree crowns which limit the visibility to the tree tops. This was also highlighted by Hunter et al. (2013) and Stereńczak et al. (2019). These studies reported that small measurement errors were found in conifer species and larger trees were subjected more to height measurement errors in the field. Further, the number of leaves present in my study species may impact the accuracy of field tree height measurement. Huang et al. (2019) also highlighted that the effect of number of leaves in the canopy may affect the tree height estimation for deciduous trees.

For all three high-value broadleaved species, the highest correlation and consistency was observed between UAV-DAP tree height and LiDAR tree height. Using the area-based approach, previous studies comparing the performance of UAV-DAP and LiDAR data also reported the high correlation and accuracy in forest attribute estimation such as mean height, and dominant height (Bohlin et al., 2012; Cao et al., 2019; Jayathunga et al., 2018b; Noordermeer et al., 2019).

Among the three broadleaved species, castor aralia showed a higher correlation than the other two species in all three pairs of comparison. The crown of castor aralia is somewhat rounded and regular in shape, which makes it easier for the surveyor to detect the tree tops from the ground during the field measurement than other two species. The size and shape of monarch birch crown are highly irregular. Moreover, the maximum size of field measured trees of Japanese oak was 110 cm in DBH with an average DBH larger than other two species. The older and larger oak tree crowns may produce extensive crowns, causing difficulty in determining the position of the highest point of the oak trees. This could contribute to some errors in estimating tree height using height measuring instruments. Larjavaara and Muller-Landau (2013) also reported that, under typical forest conditions with limited visibility to the tree tops, tree height measurement instruments cannot produce manufacturer-reported accuracies.

Positive height differences were observed for higher trees and negative height differences were found for lower height trees between field and RS-derived tree height (Figure 2.3), meaning field measured tree height overestimated the tree height of higher trees and underestimated the height of lower trees. This result is consistent with previous studies. For

example, a previous study in the Brazilian Amazon (Hunter et al., 2013) reported that ground-based measurements of tree heights of emergent crowns exceeded LiDAR-measured tree heights by an average of 1.4 m. Moreover Laurin et al. (2019) and Wang et al. (2019) reported that traditional field measurement techniques may overestimate the tree height of tall trees. Imai et al. (2014) also concluded in their study in Japan that LiDAR data tend to estimate the tree height as lower than the actual height.

In terms of LiDAR and UAV-DAP tree height differences; there was a positive height difference in lower trees and negative height difference in higher trees. Tree height differences between LiDAR and UAV-DAP varied with species. The largest height difference was found for monarch birch (-2.74 m and 4.00 m). A previous study in a mixed conifer-broadleaf forest in northern Japan (Jayathunga et al., 2018b) reported that the mean differences between LiDAR-CHM and UAV-DAP-CHM in terms of the maximum tree heights of the sample plots were 2.96 m and 1.05 m in two study compartments. However, higher mean height differences were found in UAV-DAP data (Jayathunga et al., 2018b).

The consistency of three tree height sources were also accessed by H-D model. UAV-DAP derived tree height can be explained by tree diameter with high accuracy compare to LiDAR and field measured tree height (Table 2.7, Figures 2.5 – 2.7). Mean prediction errors of the tested height-diameter models also revealed the lowest errors for LiDAR and UAV-DAP derived tree height in all height class. In Figure 2.5, highest negative mean prediction errors were found for castor aralia which may be due to the unequal high distribution of field measured tree of castor aralia trees with minimum height values of 14.1 m which could affect the model performance. For all species, higher prediction errors were observed for field measure tree height (Figure 2.6). This can also be confirmed by the larger RMSE values of field measured tree height. Therefore, this study confirmed the applicability of the UAV-DAP for tree height estimation of large-size high-value trees and its potential for estimating tree diameter. The use of UAV-DAP could facilitate the periodic monitoring and assessment of high-value timber species.

## 2.5 Conclusions

This Chapter demonstrates the applicability of UAV-DAP for individual tree height estimation of large-size high-value timber species in mixed conifer-broadleaf forests in northern Japan. I compared the tree heights derived from field survey, LiDAR data and UAV-

DAP data through statistical analysis and height-diameter models. The results revealed the high similarity between three different height sources. Lower tree height values for higher trees and higher values for lower trees may occur in UAV-DAP derived tree height in comparison with field-based measurement. Although overall mean tree height difference between LiDAR and UAV-DAP data indicates that UAV-DAP could underestimate the tree height, it is likely to observe higher tree height values for higher trees and lower tree height values for lower trees in UAV-DAP derived tree height when comparing with LiDAR derived tree height for the study species. In addition, the height-diameter models revealed that tree height derived from UAV-DAP can be used reliably as an alternative data sources to field and LiDAR data for tree height information of high-value timber species. Smaller mean prediction errors across RS-derived tree height classes were observed in comparison with field measured tree height confirming the high accuracy of UAV-DAP which can facilitate tree height estimation of high-value timber species.

Main focus in this Chapter only includes high-value broadleaf species. As this Chapter demonstrated the applicability of UAV-DAP for tree height estimation, it would be better to further examine other species so that it can use in the periodic monitoring of permanent sample plots in the study area. I focused on how UAV-DAP in combination with LiDAR data would be useful for species-specific or single-tree management planning by accurately locating the spatial position and stem size of high-value tree individuals in the next chapter.

# Chapter 3

# Estimation of spatial positions and DBH of high-value timber species

## 3.1 Introduction

To identify the individual tree spatial positions of high-value timber species using RS data for the purpose of single-tree management, the first task is to discriminate the forest canopy into species level. Previous studies demonstrated the applicability of multispectral or hyperspectral data in forest species detection (Dalponte et al., 2019, 2012b; Franklin and Ahmed, 2018). LiDAR intensity or waveform data were also used for classifying forest canopy into species level (Cao et al., 2016; Marselis et al., 2018; Yao et al., 2012). Studies suggested that the accuracy of tree species detection using multispectral or hyperspectral data could improve when it combines with LiDAR data (Dalponte et al., 2012a; Matsuki et al., 2015; Shi et al., 2020). In addition, multi-spectral or hyperspectral data have many constraints in their acquisition and need complex data processing (Nguyen et al., 2019). In this case, spectral information included in very high-resolution UAV-DAP data may be an alternative source to multispectral or hyperspectral data and LiDAR data. Therefore, I examined the use of UAV-DAP for the estimation of individual tree spatial positions of high-value timber species in this Chapter.

The use of LiDAR and UAV-DAP for forest attribute estimation generally followed two common approaches: area-based approach (ABA) and individual tree detection (ITD) approach (Dalponte et al., 2017; Goodbody et al., 2019; Guerra-Hernández et al., 2018; Hyyppä et al., 2012; Jayathunga et al., 2018a). In the ABA, plot- and stand-level forest structural attributes were estimated from vegetation metrics derived from LiDAR and UAV-DAP canopy height models (CHM). In the ITD approach, the CHMs or normalized point clouds were segmented into tree crown, and variables such as tree height, crown area, and structural metrics within the segmented tree crown were extracted. However, the accuracy of tree crown detection largely depends on the forest conditions, i.e., tree density, forest types, and tree species (Kaartinen et al., 2012; Vauhkonen et al., 2012). Even though satisfactory results were obtained for conifer trees and plantation (González-Ferreiro et al., 2013; Guerra-Hernández et al., 2018; Kukunda et al., 2018), studies suggest that individual tree detection (ITD) algorithms may not produce highly accurate results when target species are broadleaf (Kaartinen et al., 2012; Vauhkonen et al., 2012; Wang et al., 2016). Estimation of individual

tree size information for large size high-value timber trees with highly heterogeneous tree crowns remains a challenging task. In this Chapter, I examined this issue.

This Chapter deals with the second objective of estimation of individual tree spatial position of high-value timber species and their tree sizes that can be used for the single-tree management of high-value timber species. RGB information derived from UAV-DAP data together with LiDAR data were used to estimate the tree spatial positions. Individual tree DBH was estimated from LiDAR and UAV-DAP structural metrics.

## 3.2 Materials and methods

### 3.2.1 Study area and field survey

The study area and field survey used in this Chapter are same as the Chapter 2. Please refer to Section 2.2.1.

Field measured data of 213 sample trees of target high-value timber species, i.e., monarch birch, castor aralia, and Japanese oak, and 77 sample trees of other common broadleaf trees, i.e., *A. pictum* var. *mono*, *T. japonica*, *Ulmus* spp., and *Fraxinus mandshurica* were used in this Chapter. In addition to field measured trees, surrounding large trees near field measured trees that can be easily identified on the UAV-DAP orthophotographs were also recorded. Therefore, there were 132 trees of high-value timber species and 62 trees of other broadleaf species in sub-compartment 36B (194 broadleaf trees), and 88 trees of high-value timber species and 33 trees of other broadleaf species in sub-compartment 59A (121 broadleaf trees) were obtained. These datasets were used for the purpose of classifying forest canopy. Individual tree crowns of all these trees were manually digitized using the field measured crown information and visual interpretation of UAV-DAP orthophotographs. These manually digitized tree crown polygons were used as reference tree crowns for classification of forest canopy into species level described in sub-section 3.2.3. For individual tree DBH estimation of high-value timber species described in sub-section 3.2.4, I used 213 field measured sample trees and their field measured crown information and manually digitized tree crown area. A summary of field measurement data for high-value timber species is given in Table 3.1.

**Table 3.1:** Summary statistics of field measured trees

| | DBH (cm) | | Height (m) | | Crown area ($m^2$) | |
|---|---|---|---|---|---|---|
| | **Mean (SD)** | **Min - Max** | **Mean (SD)** | **Min - Max** | **Mean (SD)** | **Min - Max** |
| Monarch birch (n = 77) | 60.1 (10.1) | 41.8 - 90.6 | 25.4 (2.7) | 20.9 - 32.8 | 182.8 (63.1) | 69.5 - 366.1 |
| Castor aralia (n = 73) | 59.3 (12.9) | 44.0 - 94.4 | 23.4 (3.1) | 14.1 - 29.7 | 101.9 (44.3) | 37.4 - 251.0 |
| Japanese oak (n = 63) | 74.4 (14.1) | 44.2 - 111.2 | 24.7 (2.6) | 20.4 - 30.1 | 158.6 (55.1) | 72.7 - 305.3 |

Note: SD, Min and Max stand for standard deviation, minimum and maximum, respectively.

### 3.2.2 Remote sensing data

The LiDAR data and UAV-DAP data used in this Chapter are same as the Chapter 2. Please refer to Chapter 2 (Sub-section 2.2.2.2 and 2.2.2.3 for LiDAR data and UAV-DAP data, respectively). LiDAR and UAV-DAP data processing methods are described in the sub-section 2.2.3.

### 3.2.3 Classification of forest canopy into species level

Classification of forest canopy into species level was performed through the following steps: image segmentation, variable extraction, and variable selection, classification and accuracy assessment.

#### 3.2.3.1 Image segmentation

RGB information embedded in UAV-DAP data would provide more successful delineation for large and highly heterogenous broadleaf tree crown. The object-based-image-analysis (OBIA) method was used to delineate forest canopy into individual tree crown (Apostol et al., 2020; Baena et al., 2017; Blaschke, 2010). OBIA is based on a segmentation procedure that starts from individual pixels that are merged to most similar adjacent regions. This method is particularly suitable in the case of high spatial resolution imagery in which pixels are significantly smaller than the objects of interest (Blaschke, 2010).The information from three image spectral bands (i.e., red, green and blue) of UAV-DAP orthophotographs together with LiDAR CHM, were used together for image segmentation using a multiresolution segmentation algorithm in eCognition Developer (Trimble Inc., Sunnyvale, CA, USA). This algorithm chooses the importance (weight) of data layer, i.e., RGB layers and CHM layer, used

for image segmentation. The importance of CHM layer was set at three times higher than the RGB layers (Apostol et al., 2020).

#### 3.2.3.2 Variable extraction

After the segmentation of each tree crown, various spectral and texture variables (Alonzo et al., 2018; Lisein et al., 2015; Michez et al., 2016) and structural variables (Alonzo et al., 2018; Dalponte et al., 2009) were extracted from each individual tree crown. Since the target species were broadleaf trees with high heterogeneity within an individual tree crown, the exact overlap of algorithm-derived tree crowns and manually digitized tree crowns were not achieved. The same problem was also reported in previous studies (Apostol et al., 2020; Ma et al., 2015; Michez et al., 2016; Singh et al., 2015). Therefore, segmented objects (tree crown in this case) with high percentage of overlap were selected for variable extraction. In this study, I selected largest tree crown objects within the manually digitized tree polygon for variable extraction. In the case of Ma et al. (2015), they selected 60% overlap objects for variable extraction to classify land cover classes. Apostol et al. (2020) used enclosed parts of algorithm-derived tree crowns on the target tree crown for variable extraction. Other studies (Heinzel et al., 2008; Immitzer et al., 2012) used sunlit parts of the tree crown objects for variable extraction for species classification purposes. The variables extracted from individual tree crowns were listed in Table 3.2.

**Table 3.2:** Spectral, textural, and structural variables extracted from each tree crown polygon

| Variables names | Formula (for spectral variables) |
|---|---|
| Spectral variables | |
| Mean value of R, G and B | $\overline{R}$ , $\overline{G}$ , $\overline{B}$ |
| Sum of mean R, G and B | $\overline{R} + \overline{G} + \overline{B}$ |
| Normalized R | $= \overline{R} / (\overline{R} + \overline{G} + \overline{B})$ |
| Normalized G | $= \overline{G} / (\overline{R} + \overline{G} + \overline{B})$ |
| Normalized B | $= \overline{B} / (\overline{R} + \overline{G} + \overline{B})$ |
| Mean brightness | $= (\overline{R} + \overline{G} + \overline{B})/3$ |
| Normalized Green-Red Vegetation Index (NGRVI) | $= (\overline{G} - \overline{R}) / (\overline{G} + \overline{R})$ |
| Normalized Red-Blue Vegetation Index (NRBVI) | $= (\overline{R} - \overline{B}) / (\overline{R} + \overline{B})$ |
| Normalized Green-Blue Vegetation Index (NGBVI) | $= (\overline{G} - \overline{B}) / (\overline{G} + \overline{B})$ |
| Textural variables (Grey Level Co-occurrence Matrix (GLCM)) | |
| Homogeneity, standard deviation, mean, variance, contrast, dissimilarity, entropy | |
| Structural variables | |
| Maximum height (H-max), mean H, percentile height of 5%, 10-90% (H05, H10 – H99), intensity at different height fraction of 5%, 10-90% (Int05, Int10 – Int99), crown area | |

Note: R, G and B represent red, green, and blue respectively.

### 3.2.3.3 Variable selection, classification and accuracy assessment

Various variable selection and classification algorithm were applied in remote sensing image classification. Non-parametric methods are widely popular for this purpose as they can be used with arbitrary data distributions (Immitzer et al., 2012). Among non-parametric methods, random forest (RF) is one of the most used classification methods in the field of image classification as it is simple and does not require sophisticated parameter tuning (Immitzer et al., 2012; Rodriguez-Galiano et al., 2012). RF can handle high data dimensionality (i.e., small number of observations with high number of independent variables) (Belgiu and

Drăgu, 2016). Using the object information described in Table 3.2, image objects derived from multiresolution segmentation were classified into five classes: monarch birch, castor aralia, Japanese oak, other broadleaf, and conifer. Other broadleaf includes major canopy species of *A. pictum* var. *mono*, *T. japonica*, *Ulmus* spp., and *F. mandshurica*. Conifer trees were not measured in the field. I, therefore, used visual interpretation of orthophotographs for digitizing conifer tree crowns. I used 50 conifer tree crowns in each sub-compartment to extract variables described in Table 3.2. The data were divided into training and validation data at a ratio of 70:30. I used randomForest package (RColorBrewer and Liaw, 2018) implemented in R statistical software package (R Core Team, 2019) for the classification. The accuracy assessment was carried out by generating a standard confusion matrix, as applied in previous studies. The resulting image objects were assumed as the individual tree locations of high-value timber species.

### 3.2.4 Estimation of DBH

Although largest tree crown objects within manually digitized tree crown were selected for variable selection, these tree crowns may not be useful for the estimation of tree DBH. In previous studies, segmented tree crowns with one-to-one relationship with manually digitized polygons or manually digitized crown variables were selected for individual tree parameter estimation (e.g., (Chen et al., 2007; Dalponte et al., 2011; Iizuka et al., 2018; Yu et al., 2011)). In this study, I used manually delineated tree crown to extract structural metrics from LiDAR and UAV-DAP CHM. A total of 30 crown, height, and structural variables (Table 3.2) were derived for each tree crown and these variables were used for the estimation of individual tree DBH. For the purpose of comparison, I also predicted the DBH values using field measured tree heights and crown areas. I used a linear mixed effects model, considering the sub-compartments as a random effect. For LiDAR- and UAV-DAP derived metrics, stepwise variable selection was carried and the final models were selected based on Akaike's information criterion (AIC) (Akaike, 1973). However, the variables with a variance inflation factor (VIF) larger than five were neglected in the final model in order to avoid multicollinearity (Kock and Lynn, 2012). The accuracy of the selected models was validated using leave-one-out-cross validation. The coefficient of determination for fixed effect parameters (marginal $R^2$), root-mean-square-error (RMSE) and Pearson's correlation coefficient (r) were determined for each species to assess the goodness of fit of the selected model.

## 3.3 Results

### 3.3.1 Multiresolution segmentation of forest canopy

Comparison of crown areas (CAs) were carried out in three pairs (i.e., field-measured CAs versus manually digitized CAs, field-measured CAs versus multiresolution segmented CAs, and manually digitized CAs versus multiresolution segmented CAs. The results of the comparison were shown in Figure 3.1. The results indicated the lower correlation between field-measured and multiresolution segmented crown areas for all species. A slightly better correlation was observed between manually digitized crown areas and multiresolution segmented crown areas. Among the three pairs of comparison, field-measured crown area and manually digitized crown area exhibited the highest correlation coefficients. Since the target tree species were large in size and their crown areas were highly heterogenous, tree crown area underestimation was observed in all species (Figure 3.1). Figure 3.2 shows the visual comparison between manually digitized tree crowns and multiresolution segmentation-derived tree crowns.

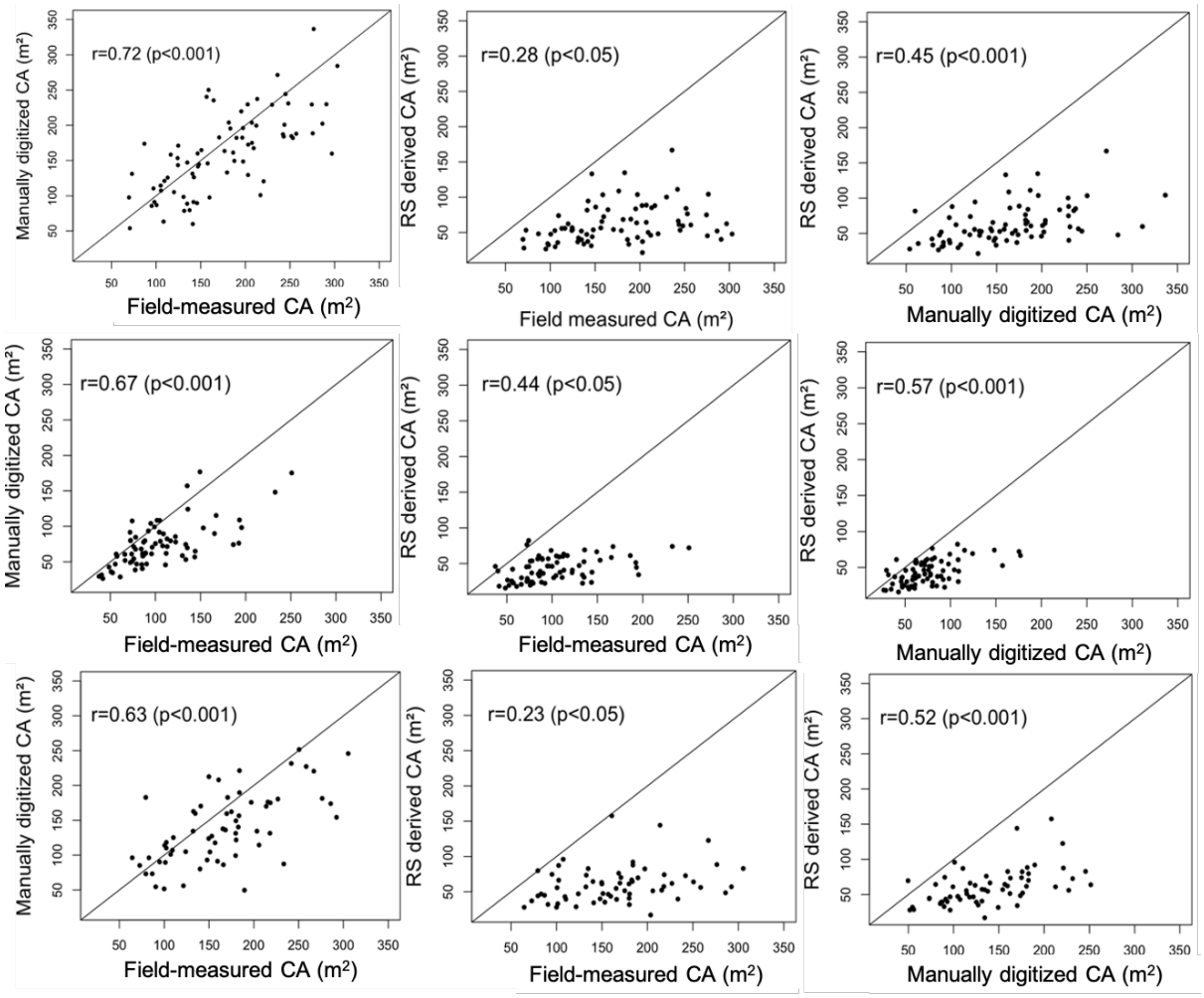


**Figure 3.1:** Correlation between crown areas derived from field measurement, manual delineation, and multiresolution segmentation of UAV orthophotograph. CA represent crown area. First, second, and third row represent monarch birch, castor aralia and Japanese oak, respectively. RS derived CA represents CA derived from multi-resolution segmentation.

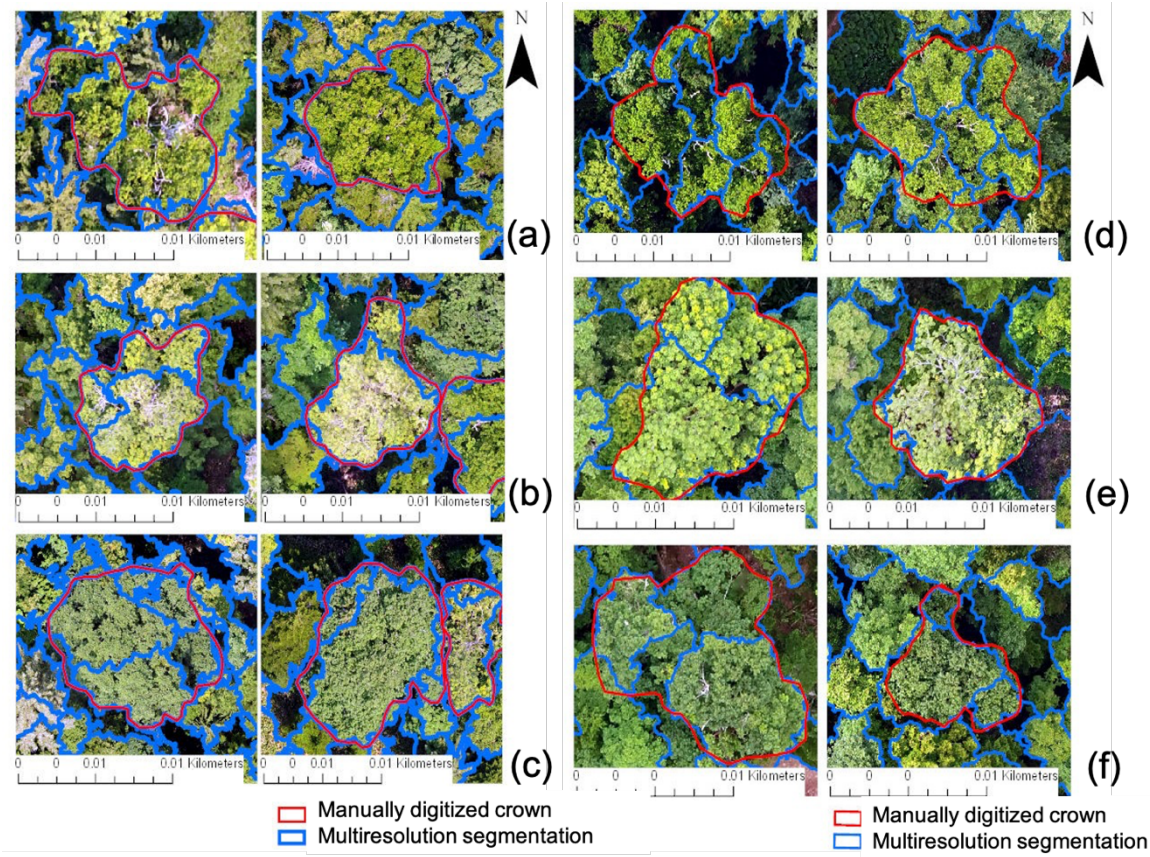


**Figure 3.2:** Individual tree crown derived from multiresolution segmentation for three high-value timber species. (a) Monarch birch, (b) castor aralia, and (c) Japanese oak in sub-compartment 36B and (d), (e), and (f) are the monarch birch, castor aralia and Japanese oak in sub-compartment 59A respectively.

### 3.3.2 Variable selection, classification of forest canopy and accuracy assessment

The results of the RF classification of the forest canopy into three high-value timber species, other broadleaf species, and conifer species are shown in Tables 5 and 6. Based on 75 validation crowns consisting of 11 monarch birch, 18 castor aralia, 12 Japanese oak, 21 other broadleaf, and 13 conifer trees, an overall accuracy classification value of 73% was obtained with a kappa coefficient of 0.66 in sub-compartment 36B (Table 3.3). Table 3.4 shows the results of the classification for sub-compartment 59A. The overall accuracy of 63% was obtained with a kappa coefficient of 0.53 based on the validation data (58 crowns) for 12 monarch birch, 9 castor aralia, 6 Japanese oak, 12 other broadleaf, and 19 conifer trees. Figures 3.3 and 3.4 show the important variables for the classification of the forest canopy in sub-compartments 36B and 59A, respectively.

The spatial positions of individual trees can be extracted from the classification results. Figure 3.5 shows monarch birch, castor aralia, Japanese oak, other broadleaf, and conifer tree crowns. These individual tree crowns indicate the tree locations of high-value timber species.

**Table 3.3:** Confusion matrix for RF classification forest canopy into high-value timber, other broadleaf and conifer classes based on 75 validation crowns from known tree positions in sub-compartment 36B.

| **Classified crowns** | **Reference crowns** | | | | | **UA/PA %** |
|---|---|---|---|---|---|---|
| | **Monarch Birch** | **Castor aralia** | **Japanese oak** | **Other broadleaf** | **Conifer** | |
| Monarch birch | 8 | 2 | 1 | 2 | 1 | 57/73 |
| Castor aralia | 0 | 14 | 0 | 2 | 1 | 82/78 |
| Japanese oak | 1 | 0 | 10 | 3 | 0 | 71/83 |
| Other broadleaf | 1 | 1 | 1 | 13 | 1 | 76/62 |
| Conifer | 1 | 1 | 0 | 1 | 10 | 77/77 |
| Overall accuracy | **73% (kappa = 0.66)** | | | | | |

UA and PA stand for user's accuracy and producer's accuracy, respectively.

**Table 3.4:** Confusion matrix for RF classification of forest canopy into high-value timber species, other broadleaf and conifer classes based on 58 validation crowns from known tree positions in sub-compartment 59A.

| **Classified crowns** | **Reference crowns** | | | | | **UA/PA %** |
|---|---|---|---|---|---|---|
| | **Monarch Birch** | **Castor aralia** | **Japanese oak** | **Other broadleaf** | **Conifer** | |
| Monarch birch | 7 | 0 | 0 | 0 | 1 | 87/58 |
| Castor aralia | 0 | 6 | 0 | 2 | 1 | 67/67 |
| Japanese oak | 0 | 0 | 5 | 6 | 0 | 45/83 |
| Other broadleaf | 1 | 2 | 0 | 3 | 1 | 43/25 |
| Conifer | 4 | 1 | 1 | 1 | 16 | 70/32 |
| Overall accuracy | **63 % (kappa = 0.53)** | | | | | |

UA and PA stand for user's accuracy and producer's accuracy, respectively.

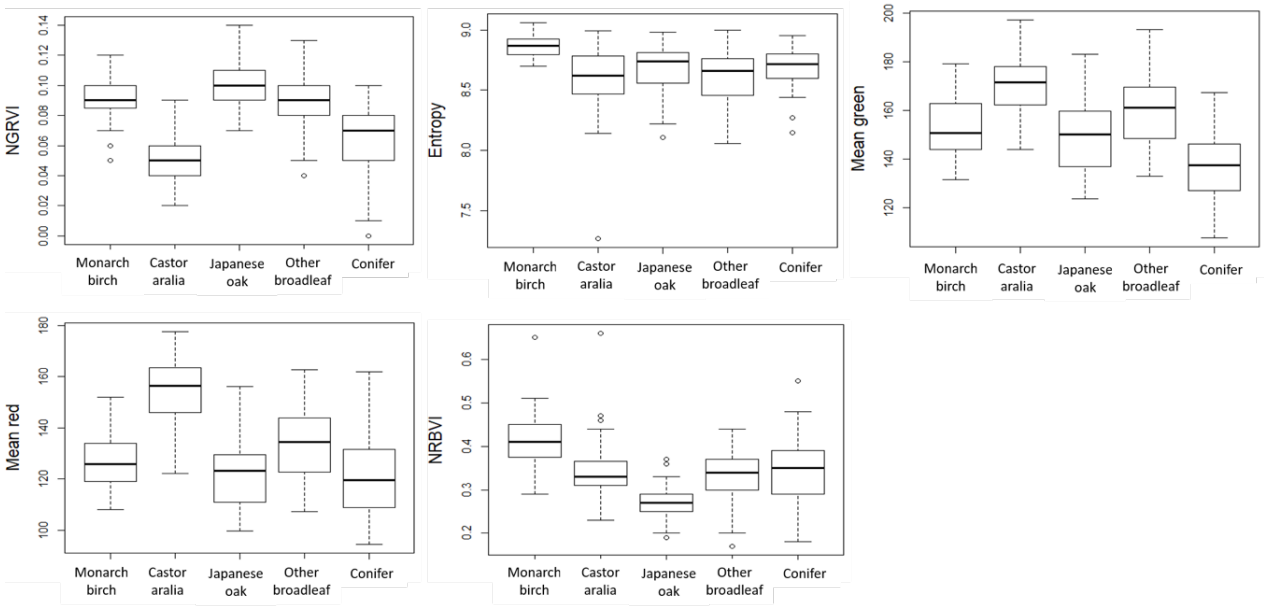


**Figure 3.3:** Species separability boxplots for classification of the forest canopy in sub-compartment 36B.

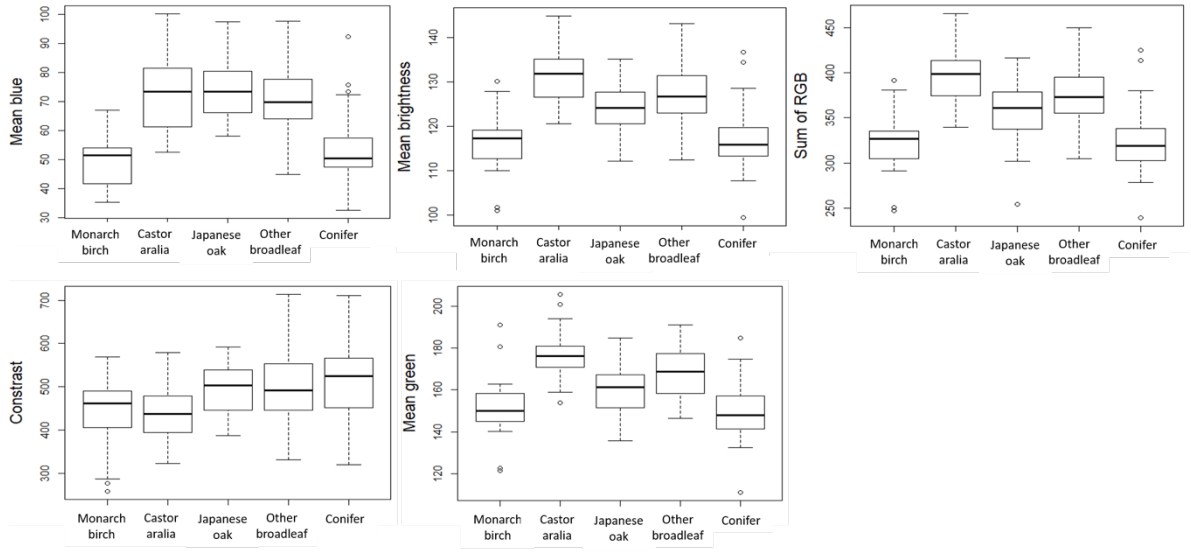


**Figure 3.4:** Species separability boxplots for classification of the forest canopy in sub-compartment 59A.

.

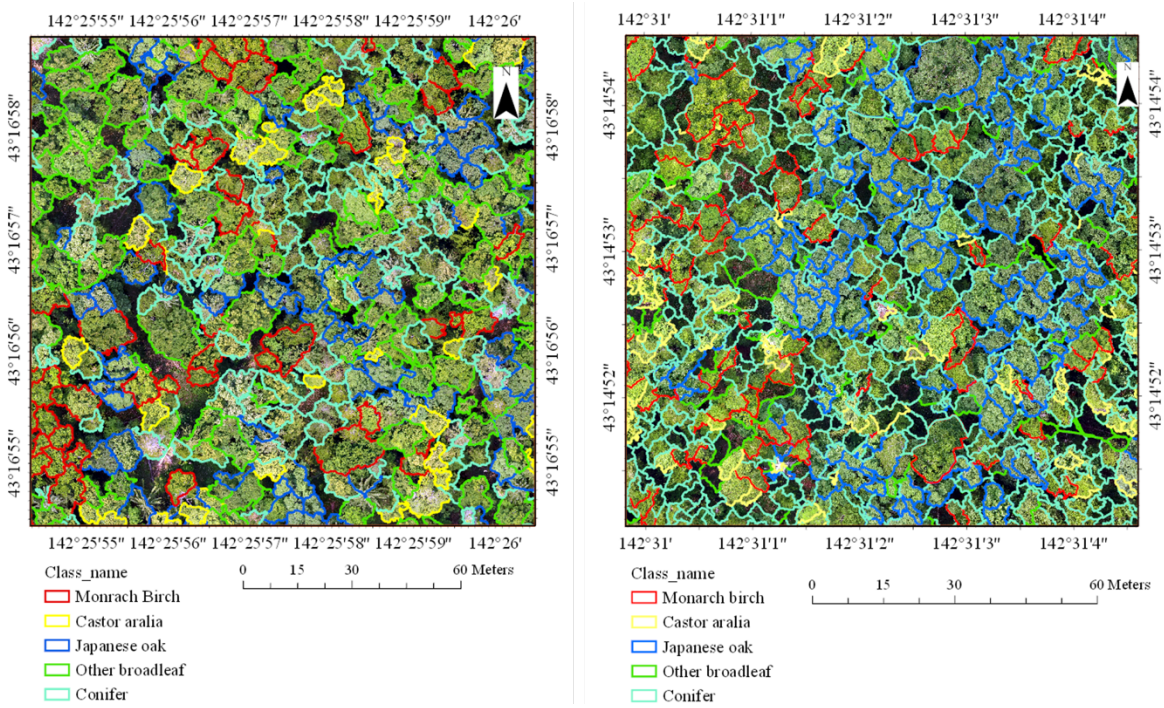


**Figure 3.5:** Individual tree crowns derived from the RF classification, where each tree crown also indicates the individual tree's spatial position: (a) sub-compartment 36B and (b) sub-compartment 59A.

### 3.3.3 DBH estimation

The selected models for DBH estimation using field, LiDAR and UAV-DAP data were shown in Table 3.5. Figure 3.7 showed the correlation between observed DBH and predicated DBH for three high-value timber species. The results indicated that models based on LiDAR data obtained higher correlation coefficients and lower RMSE values. Models based on UAV-DAP revealed a comparable prediction power to LiDAR based models and field survey-based models. Among the three data sources, models using field measured data exhibited the highest RMSE values and lower correlation values for all species. In general, the results showed the higher correlation for castor aralia while lower correlation values were observed for Japanese oak (Table 3.6 and Figure 3.7).

**Table 3.5.** DBH estimation models.

| Species | Model | Parameter estimates | $R^2$ (marginal) | RMSE (cm) |
|---|---|---|---|---|
| **Field** | | | | |
| Monarch birch | Intercept | 33.38*** | | |
| | $CA_f$ | 0.08*** | 0.32 | 8.90 |
| | Field Height | 0.45 | | |
| Castor aralia | Intercept | 16.03* | | |
| | $CA_f$ | 0.13*** | 0.47 | 10.57 |
| | Field Height | 1.29*** | | |
| Japanese oak | Intercept | 34.01** | | |
| | $CA_f$ | 0.12*** | 0.32 | 14.01 |
| | Field Height | 0.92 | | |
| **LiDAR** | | | | |
| Monarch birch | Intercept | 8.75 | | |
| | CAD | 0.10*** | 0.59 | 7.05 |
| | H-max | 1.29*** | | |
| Castor aralia | Intercept | -11.83 | | |
| | CAD | 0.23*** | 0.70 | 7.39 |
| | H99 | 2.34*** | | |
| Japanese oak | Intercept | 22.43 | | |
| | CAD | 0.17*** | 0.54 | 11.87 |
| | H99 | 3.18*** | | |
| | H30 | -3.06*** | | |
| **UAV-DAP** | | | | |
| Monarch birch | Intercept | 16.97* | | |
| | CAD | 0.11*** | 0.56 | 7.30 |
| | H99 | 0.97*** | | |
| Castor aralia | Intercept | 0.89 | | |
| | CAD | 0.22*** | 0.60 | 8.51 |
| | H99 | 1.81*** | | |
| Japanese oak | Intercept | 24.51 | | |
| | CAD | 0.20*** | 0.40 | 13.29 |
| | H99 | 1.07 | | |

Note: $CA_f$ represents field-measured crown area and CAD represents manually digitized crown area, respectively, for UAV orthophotographs. Significance code: *** $p < 0.001$, ** $p < 0.01$, * $p < 0.05$.

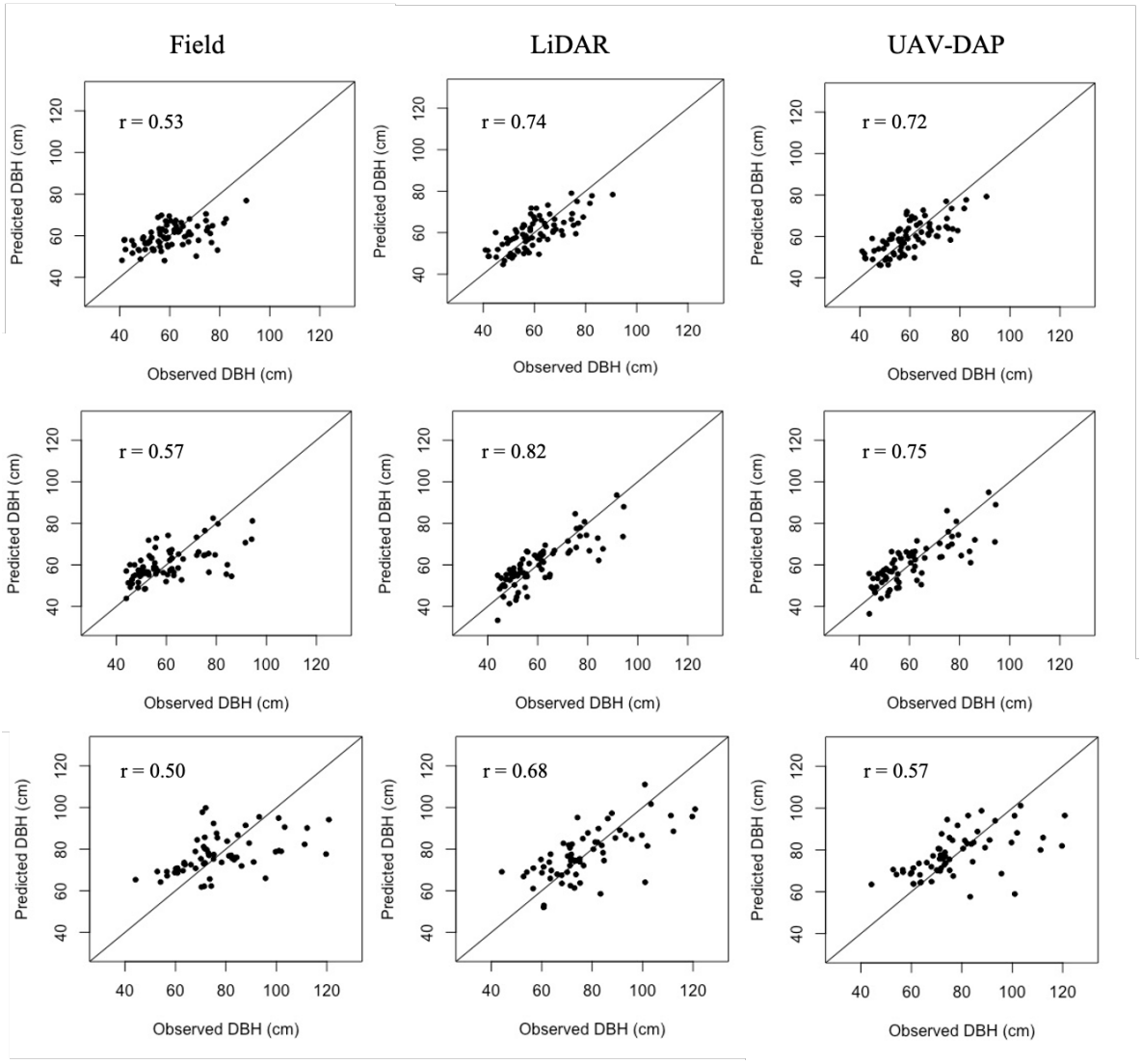


**Figure 3.6:** Observed and predicted DBH for monarch birch (first row), castor aralia (middle row), and Japanese oak (third row).

## 3.4 Discussion

### 3.4.1 Segmentation of forest canopy

In this Chapter, tree crown segmentation was conducted using the multiresolution segmentation method, which showed low segmentation accuracy (Figure 3.1) for all target high-value timber species. As shown in Figure 3.2, the crowns of target high-value timber species are largely heterogeneous, which could produce a lower segmentation accuracy. For all target species, underestimation of individual tree crown areas was observed. Deciduous species have a relatively flat outer canopy envelope and therefore, generally have more complex crown structures compared to coniferous species (Nuijten et al., 2019). In addition, the branching pattern of large size deciduous trees may lead tree detection algorithm to detect

a heterogenous individual tree crown as different tree crowns. In this Chapter, I used spectral band (i.e., R, G and B) derived from UAV-DAP together with LiDAR CHM for delineation purposes. The within crown heterogeneity of large size high-value timber species produced different tree crown objects for manually delineated tree crowns (Figure 3.2). Spectral variation due to shadow within an heterogenous individual tree crown could lead to segmentation of individual tree crown into several crowns (Figure 3.2).

Higher tree crown detection accuracies were reported for conifer species and planation in previous studies (González-Ferreiro et al., 2013; Guerra-Hernández et al., 2018). The results in this Chapter were consistent with other previous studies using different tree crown detection algorithms. Previous studies also reported that the results of individual tree crown detection algorithms could not produce highly accurate results especially when the target species were broadleaf (Kaartinen et al., 2012; Vauhkonen et al., 2012; Wang et al., 2016). Using the UAV-DAP derived canopy height models, Nuijiten et al. (2019) accessed the seasonal variation in the result of individual tree crown delineation using marker-controlled watershed segmentation algorithm in mixed deciduous forest stands. They reported the accuracy of 55% in the summer and 77% in the fall season. Dalponte et al. (2019) used hyperspectral data for the segmentation of the forest canopy, reporting that on average, 34% of the area of the delineated by tree crown detection algorithm overlapped the area of the manually delineated tree crown.

### 3.4.2 Classification of forest canopy

I classified forest canopy into three high-value timber species, other broadleaf, and conifer classes (Table 3.3 and Table 3.4). Even though the classification of forest canopy into two categories of broadleaf and conifer produce high accuracy as indicated in previous studies (Alonzo et al., 2017; Jayathunga et al., 2020), classification of forest canopy into several classes could be challenging since our data consisted of R, G, and B bands only. I obtained overall classification accuracy of 73% and 63% in sub-compartment 36B and 59A, respectively (Table 3.3, Table 3.4 and Figure 3.5). The important variables (Figure 3.3 and 3.4) for classification of forest canopy were different for the two sub-compartments. In sub-compartment 36B, NGRVI appeared to be the best spectral variable for classification, while the mean value of B was the best variable in sub-compartment 59A. This could be due to the timing of UAV flight missions between two sub-compartments. In addition, the weather condition during the flight missions may have influenced the spectral response of forest canopy, affecting the classification accuracy.

Lower classification accuracy was observed in sub-compartment 59A. The lower classification accuracy result in the current study could be due to the confusion of spectral signatures of each species. This issue was also highlighted in the previous studies (Franklin and Ahmed, 2018; Singh et al., 2015). The accuracy in the current study was relatively lower than other previous studies that used more spectral information, such as multispectral or hyper-spectral information. For example, Franklin et al. (2018) used multispectral data derived from UAV-DAP to classify forest canopy into five categories. They reported the overall classification of 78% for 23 validation tree crowns. A study by Lisein et al. (2015) tested the multitemporal UAV flights with multispectral camera to determine the best time window for classifying forest species. Using the random forest classification approach, they reported a lower error of 16% in discriminating 5 different categories of tree species. The use of hyperspectral data and LiDAR data for tree species classification were examined by Matsuki et al. (2015) and Dalponte et al. (2019). They reported the maximum classification accuracy values of 82% for 16 classes of tree species (Matsuki et al., 2015) and 88.1% for 9 classes (Dalponte et al., 2019).

### 3.4.3 Estimation of individual tree DBH

In addition to species classification, this Chapter demonstrated the applicability of RS data for the estimation of DBH, which is one of the important variables for single-tree management purpose. I compared the accuracy of field, LiDAR and UAV-DAP data for DBH estimation for three high-value timber species. In the DBH estimation models of RS data, significant variables used for prediction are tree-height-related variables (Table 3.5). The RS variables related to point density did not play important role in individual tree DBH estimation. This result is consistent with the previous studies (Chen et al., 2007; Yu et al., 2011). Yu et al. (2011) examined the use of LiDAR height and intensity metrics for the estimation of tree basal area and stem volume in Finland. They found that the best model for estimation individual tree DBH were models that included tree crown and height metrics. In addition, a study by Chen et al. (2007) also reported that models that included LiDAR height and crown metrics rather than intensity metrics seemed to be the best model for individual tree stem volume and basal area. However, all returns (i.e., first, second, third, and last return) were used to derived intensity metrics. The intensity metrics derived separately for each return within specific tree crown area could relate more to individual tree DBH.

The results of DBH estimation models also revealed that manually delineated tree crown area values, together with tree height values, could better estimate the individual tree DBH than field-measured crown area. The correlation between observed and predicted DBH was higher in DBH models that used manually delineated crown area. Among the tree species, the accuracy of DBH estimation for castor aralia seemed to be higher than for the other two species. Visually, castor aralia was relatively easier to distinguish in most case. Therefore, manual tree crown delineation may likely to be more accurate than other two species. In the literature, field measured tree crown and tree height were used for developing the tree diameter estimation models (Hulshof et al., 2015; Jucker et al., 2017; Verma et al., 2014). RS data could improve the accuracy of these diameter estimation models.

### 3.5 Conclusions

In this Chapter, I demonstrated the applicability of UAV-DAP and LiDAR data for the estimation of individual tree spatial positions and DBH values. I performed multiresolution segmentation of UAV-DAP orthophotographs, together with rasterized LiDAR CHM, in order to segment the forest canopy into individual tree crowns. I applied object-based image analysis and random forest classification techniques to classify the forest canopy into three high-value timber species, other broadleaf species, and conifer. The results indicated overall accuracy values of 73% and 63% in sub-compartment 36B and 59A, respectively. The DBH estimation results showed high prediction accuracy when using manually digitized tree crown area and LiDAR- and UAV-DAP derived tree height values. The UAV-DAP data had comparable prediction accuracy to field-measured data and LiDAR data. The results of this Chapter could be useful for forest managers when searching of high-value timber trees and estimating tree size in large area of mixed-wood forests.

# Chapter 4

# Resource assessment of high-value timber species

## 4.1 Introduction

The achievement of sustainability from the use of various forest management practices is a central precept of forestry and is therefore central to all silvicultural systems (O'Hara et al., 2007). Uneven-aged forest management or selection system has gained growing interest in many parts of the world due to its stability in forest stand structures (Kuuluvainen et al., 2012; Laiho et al., 2011; Puettmann et al., 2015; Pukkala et al., 2011), and there has been increasing criticism for even-aged forestry, wherein the whole forest area is clear-cut and regenerated artificially. Furthermore, sustainable forest management (SFM) has been encouraged as a guiding principle in forest management (MacDicken et al., 2015) and uneven-aged forest management is assumed to achieve greater sustainability in forest resource management in comparison with even-aged forest management (Dieler et al., 2017; O'Hara et al., 2007). It is sometimes referred to as close-to-nature forest management (O'Hara, 2016; Schütz et al., 2016), which implies the achievement of a form of silviculture that emulates natural processes resulting in stand structures that are natural, and it promotes natural processes such as soil productivity maintenance, nutrient cycling, and biodiversity (O'Hara, 2016).

In uneven-aged mixed conifer–broadleaf forests in northern Japan, the selection system has been practiced as a common management system since the early twentieth century (Yasuda et al., 2013). In fact, the selection management system attempts to mimic natural disturbances through the use of various management practices. General expectations of the use of selection management are the increased growth, recruitment, and survival of remaining trees (Yoshida et al., 2006). Several research attempts have been made in different parts of the world to investigate the impacts of selection management on the remaining forest stand demographic parameters, i.e., growth, recruitment, and mortality (Amaral et al., 2019; Klopcic and Boncina, 2011; Laiho et al., 2011; Schuler, 2004), as well as species composition and stand structure (Dieler et al., 2017; Ediriweera et al., 2020; Poudyal et al., 2019; Young et al., 2017). Many previous studies in mixed conifer–broadleaf forests in northern Japan have also assessed the impact of selection management on the growth, recruitment, and mortality of the remaining forest stand (Miya et al., 2009; Noguchi and Yoshida, 2009; Tatsumi et al., 2014; Yoshida et al., 2006; Yoshida and Noguchi, 2010). However, few studies have examined the sustainability

of forest stands, especially high-value timber species. Information on the sustainability of high-value timber species within mixed forests is important for forestry practitioners, especially when the goal of forest management is to manage certain species. Moreover, understanding the sustainability of uneven-aged mixed forests is useful for forest management decision (Müller et al., 2000) because it helps to determine whether or not a specific stand structure should be maintained (Kuuluvainen, 2002; Schall et al., 2018).

The assessment of sustainability in uneven-aged mixed forest is relatively difficult because forests are slow growing and it may take several decades to examine the long-term impacts of any given forest management activities. It requires criteria and indicators that can be measured during stand development (O'Hara et al., 2007) after forest management activities. The availability of long term forest measurement data, therefore, is an important source of information (Pretzsch et al., 2019), not only for providing information of forest stand dynamics but also to assess the sustainability of forest stands subjected to various natural and anthropogenic disturbances.

The parameters derived from long-term forest measurement data would be useful for assessing the sustainability of a forest management system. O'Hara et al. (O'Hara et al., 2007) compared forest stand parameters such as stocking (tree density and basal area), species diversity, stand structure, and increment between even-aged forest and a selection system in Central Europe as measures of sustainability using over 90 years of forest measurement data. In addition, Schuler (Schuler, 2004) examined the species composition, diversity, and growth of tree species in mixed mesophytic forest in the USA after 50 years of partial harvesting. In mixed conifer–broadleaf forest in northern Japan, Yoshida et al. (Yoshida et al., 2006) assessed the dynamics of a forest stand after 20 years of selection harvest. However, these studies examined long term changes in the stocking and demographic parameters of major tree species or stand level stocking, species diversity, and stand structure. The sustainability of high-value timber species after selection harvest has not been widely studied. Understanding the sustainability of high-value timber species will be useful for the reliable application of a selection system and species-specific forest management or a single-tree management system, which was recommended in previous studies (Lindenmayer et al., 2013; Owari et al., 2016).

The aim of this Chapter is, therefore, to assess the sustainability of high-value timber species in mixed forests managed under selection systems. Using 48 years of measurement data, I derived the stocking, demographic parameters, and species proportion of high-value timber species as measures of sustainability. To reach the objective, firstly, I assessed the

changes in stocking and demographic characteristics of high-value timber species over time. Secondly, the changes in the species proportion of high-value timber species were assessed. In addition, I also showed how the forest stand structure was changing by assessing the sustainability measures of all conifer and broadleaf species.

## 4.2 Materials and methods

### 4.2.1 Study site and data

The study area was located in UTHF. Figure 4.1 shows the location of study area. The information of the study area is described in Chapter 2 (sub-section – 2.2.1). Permanent plots were established throughout the UTHF to record long-term growth and stand development for the management of uneven-aged mixed forests (Owari, 2013). A stratified purposive sampling scheme was employed for the plot establishment to represent the major stand types, soil, and terrain conditions (Ishibashi and Hirokawa, 1986). Harvesting and management of forest stands were monitored using permanent plot data by assessing temporal dynamics of stand structure and fluctuation of forest resources. Within these plots, diameter at breast height (DBH) measurements of all trees with DBH ≥ 5 cm are performed by UTHF staff at regular, in most cases, 5-years interval with 0.1 cm precision. All trees were tagged with identification numbers (IDs) on metal plates nailed to steel rods to ensure that DBH measurements were repeated on the same trees. Plot data included species, DBH, survival status, and harvest of all trees with DBH ≥ 5.0 cm. For growth model development, I used tree census data from 31 permanent sample plots (plot sizes range from 0.22 to 1.00 ha) in the UTHF (Figure 4.1) where the selection system has been implemented. I used the tree census data of the plots measured between 1968 and 2016. Measurement intervals ranged from 3 to 12 years, and the number of measurements in the plots ranged from 8 to 11. The plots were subjected to selection harvest 3 to 5 times during the observation period.

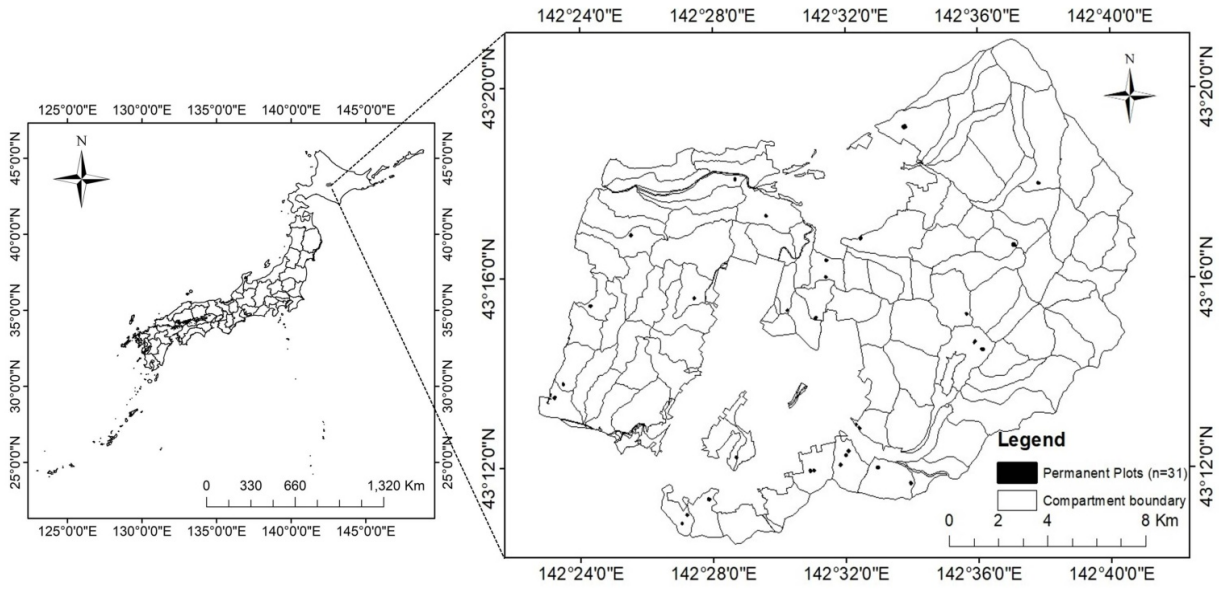


**Figure 4.1:** Locations of the permanent plots.

### 4.2.2 Measures of sustainability

In order to assess the sustainability of high-value timber species, I considered the stocking and demographic characteristics, and species proportion, as suggested by O'Hara et al. (O'Hara et al., 2007). Stocking included the tree density (number of trees per hectare - N, tree $ha^{-1}$) and basal area per hectare (BA, $m^2$ $ha^{-1}$). Demographic characteristics included basal area increment (BAI, $m^2$ $ha^{-1}$ $yr^{-1}$); number of recruitment or in-growth (N-rec, tree $ha^{-1}$), and number of tree mortality (N-mor, tree $ha^{-1}$). BAI was calculated based on two consecutive measurements of DBH. I excluded negative BAI values in the analysis, as these were assumed to be measurement errors. I also excluded dead trees in the second measurement of two consecutive measurements in BAI calculations. N-rec was calculated as the number of trees that were entered into the minimum 5.0 cm DBH in the second measurement of two consecutive measurements. I considered the dead trees in the second measurement of two consecutive measurements as N-mor, and I counted the number of dead trees between two measurements. In addition, I compared the changes in N, BA, and BAI to understand the general temporal trend of the study forest stand. Changes in the species proportions of high-value timber species as well as the proportion of conifer and broadleaf trees were also analyzed. I also assessed the selection harvest of conifer and broadleaf trees across the census periods.

### 4.2.3 Data analysis

For simplicity in the comparison of sustainability measures, I divided the measurement records into 5 census periods; I (1968–1978), II (1978–1988), III (1988–1998), IV (1998–2008), and V (2008–2016). The year of measurement was used to determine the census periods, i.e., all censuses that were measured in the years between 1968 and 1978 were assumed as period I. Friedman test was used to test stand level changes in stocking, demographic characteristics, and proportion of high-value timber species. For significant Friedman test results ($p < 0.05$), a post-hoc test was applied to detect which census periods showed significant increase or decrease in stocking, demographic characteristics, or species proportion. A linear mixed effect model was used to quantify whether the stocking, demographic characteristics, and species proportion increased or decreased over time. The model form can be described as the following equation:

$$Y_{ij} = a_0 + a_1 X_{ij} + plot_j + \varepsilon_{ij}. \qquad \text{Equation (4.1)}$$

where $Y_{ij}$ represents the sustainability measures mentioned in Section 4.2.2 for census year *i* in plot *j*, and $X_{ij}$ is census year *i* in plot *j*. $a_o$ and $a_1$ are fixed effect parameters, and $plot_j$ is the random effect parameter for plot *j*. The symbol $\varepsilon_{ij}$ stands for residuals. The significant slope coefficient ($p < 0.05$) was used as an indicator of either positive or negative trends of the forest characteristics mentioned in Section 4.2.2 over time (O'Hara et al., 2007). All statistical analysis were carried out in R software version 3.6.1 (R Core Team, 2019).

## 4.3 Results

### 4.3.1 Changes in stocking of high-value timber species

Changes in N and BA are shown in Table 4.1. Diameter distribution of high-value timber species are shown in Figure 4.2. During the 48-year period, the N of monarch birch significantly increased (Friedman test, $p < 0.05$) in the study permanent plots with the mean N of the last census period (2008–2016) being significantly higher than in the first two census periods (Table 4.1). The BA of monarch birch also increased, reaching the highest in the last period. Monarch birch BA in the last two periods was significantly higher than in the previous three periods. The N of castor aralia did not increase or decrease significantly ($p = 0.75$) in any period. However, the BA of castor aralia increased significantly ($p < 0.001$). The N of Japanese oak did not significantly increase in the first three periods, but it significantly increased in the last two periods. Similar to other two species, the highest BA of Japanese oak occurred in the

last period. According to the mixed effect model, the slope coefficients for N and BA for all species showed significant positive trends over time (Table 4.2).

**Table 4.1:** Stocking of high-value timber species (mean (standard deviation)).

| Census Periods | Monarch Birch | | Castor Aralia | | Japanese Oak | |
|---|---|---|---|---|---|---|
| | Density (N/ha) | Basal area ($m^2$/ha) | Density (N/ha) | Basal area ($m^2$/ha) | Density (N/ha) | Basal area ($m^2$/ha) |
| I | 3.83 (5.80) [a] | 0.13 (0.20) [a] | 19.26 (14.51) [a] | 0.30 (0.34) [a] | 11.03 (15.92) [a] | 0.55 (0.99) [a] |
| II | 3.59 (4.77) [a] | 0.16 (0.22) [a] | 21.18 (16.85) [a] | 0.40 (0.37) [ab] | 11.64 (15.39) [a] | 0.53 (0.85) [b] |
| III | 5.49 (7.58) [ab] | 0.17 (0.25) [a] | 21.79 (14.77) [a] | 0.43 (0.39) [b] | 12.54 (15.25) [a] | 0.48 (0.84) [b] |
| IV | 11.37 (18.5) [ab] | 0.20 (0.26) [b] | 24.39 (17.25) [a] | 0.48 (0.41) [c] | 16.26 (16.17) [b] | 0.62 (0.95) [c] |
| V | 11.24 (20.61) [b] | 0.26 (0.33) [c] | 23.39 (17.43) [a] | 0.56 (0.40) [d] | 15.05 (16.48) [b] | 0.68 (1.08) [d] |

Note: Census periods with different letters show significant differences ($p < 0.05$).

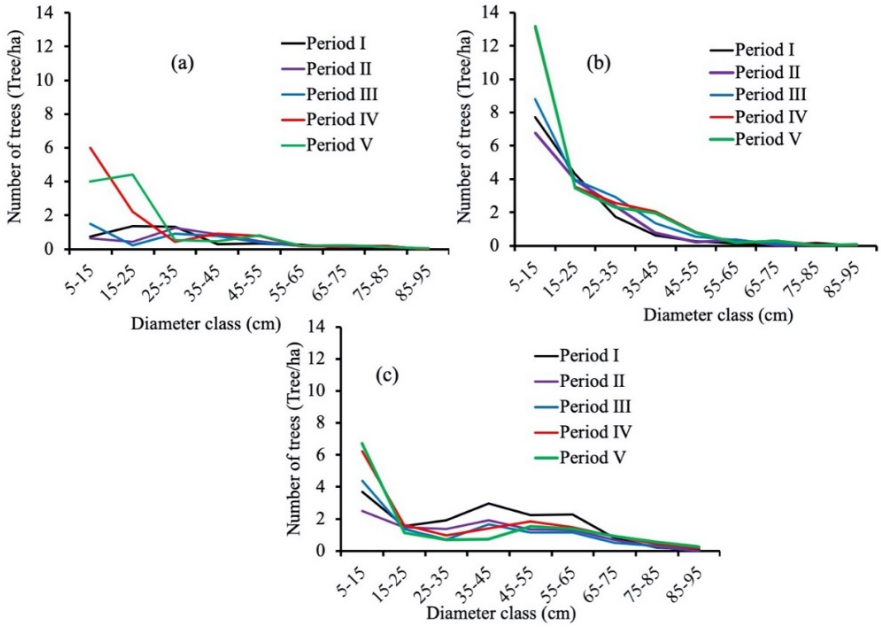


**Figure 4.2:** Diameter distribution of high-value timber species across census periods. (a) Monarch birch, (b) Castor aralia, and (c) Japanese oak. Number of trees indicate the mean values.

**Table 4.2:** The results of linear mixed-effect models showing the general temporal trend of stocking, demography and diversity indices for high-value timber species.

| Variable | Monarch Birch | | Castor Aralia | | Japanese Oak | |
|---|---|---|---|---|---|---|
| | $a_0$ | $a_1$ | $a_0$ | $a_1$ | $a_0$ | $a_1$ |
| Tree density (N/ha) | −477.64*** | 0.24*** | −207.00* | 0.11* | −359.84*** | 0.19*** |
| Basal area ($m^2$/ha) | −6.13*** | 0.003*** | −0.11*** | 0.006*** | −0.11*** | 0.006*** |
| Basal area increment ($m^2$/ha/year) | −0.27*** | 0.0001*** | −0.21*** | 0.0001* | −0.19*** | 0.0001** |
| Mortality (N/ha) | −32.57** | 0.02** | $-10.04^{ns}$ | $0.01^{ns}$ | −24.77* | 0.012* |
| In-growth (N /ha) | $-45.43^{ns}$ | $0.02^{ns}$ | $27.52^{ns}$ | $-0.01^{ns}$ | $-34.63^{ns}$ | $0.02^{ns}$ |
| Species proportion (%) | −45.87*** | 0.02*** | $-5.29^{ns}$ | $0.004^{ns}$ | −27.78*** | 0.015*** |

Significant code: * $p < 0.05$, ** $p < 0.01$, *** $p < 0.001$. ns stands for non-significant. $a_0$ and $a_1$ are fixed-effect parameters of equation (4.1).

For the purpose of comparison, Figure 4.3 shows changes in the N and BA of forest stand, conifer, and broadleaf across census periods. The Friedman test showed significant differences in both N and BA over time ($p < 0.05$). In addition, Figure 4.3 also shows the changes in the N and BA of conifer and broadleaf species during the 48-year period. The figure shows increasing trends in broadleaf N and BA, while decreasing trends can be observed for conifer N and BA. Friedman test also showed significant differences ($p < 0.05$). The results of the mixed effect model also confirmed the significant and positive trends in N and BA over time. However, significant and negative trends were observed for conifer N and BA, while a positive trend was observed for broadleaf species (Table 4.3).

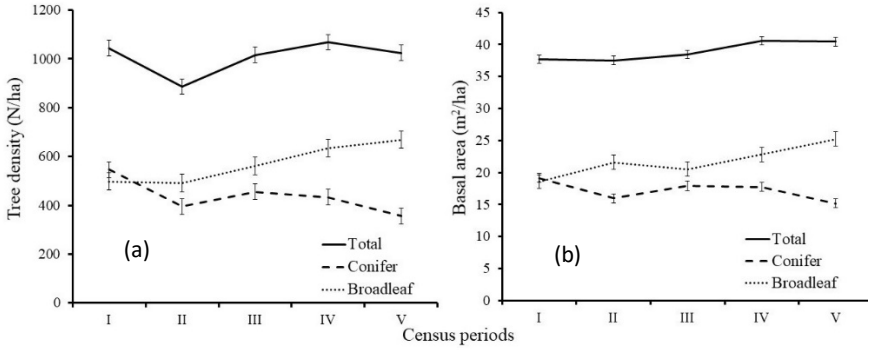


**Figure 4.3:** Development of stand level density (a), and basal area (b) of all species (mean (standard error)).

**Table 4.3:** The results of linear mixed-effect models showing the general temporal trend of stocking and demography of forest stand.

| Variable | Total | | Conifer | | Broadleaf | |
|---|---|---|---|---|---|---|
| | $a_0$ | $a_1$ | $a_0$ | $a_1$ | $a_0$ | $a_1$ |
| Tree density (N/ha) | −3114.45* | 2.07** | 6423.42*** | −3.01*** | −9561.88*** | 5.08*** |
| Basal area ($m^2$/ha) | −164.20*** | 0.10*** | 98.31*** | −0.04*** | −262.40*** | 0.14*** |
| Basal area increment ($m^2$/ha/year) | −4.48*** | 0.002*** | 2.58** | −0.001* | −7.09*** | 0.004*** |
| In-growth (N/ha) | $-1056.16^{ns}$ | $0.57^{ns}$ | $186.50^{ns}$ | $-0.08^{ns}$ | −1240.98* | 0.65* |
| Mortality (N/ha) | −1550.45** | 0.82** | $313.36^{ns}$ | $-0.14^{ns}$ | -1859.66*** | 0.95*** |
| Species proportion (%) | | | 664.93*** | −0.31*** | −564.93*** | 0.31*** |

Significant code: * $p < 0.05$, ** $p < 0.01$, *** $p < 0.001$. ns stands for non-significant. $a_0$ and $a_1$ are fixed-effect parameters of equation (4.1).

### 4.3.2 Changes in the demographic characteristics of high-value timber species

Changes in the demographic parameters of high-value timber species are shown in Table 4.4. The BAI of monarch birch in the last two census periods was significantly higher than the first three periods ($p < 0.001$). A significant higher BAI of Japanese oak ($p < 0.001$) was found in the last two measurement periods with the highest increment in the fourth census period. An increasing trend in the BAI of castor aralia was also observed. The mixed effect model also revealed a positive slope coefficient for the BAI of all species (Table 4.2). The Friedman test showed no statistically significant difference between census periods for N-mor (Table 4.4). However, a significant positive slope was observed for monarch birch and Japanese oak, meaning that the N-mor of monarch birch and Japanese oak may be likely to increase over time (Table 4.2). In all target species, an increased N-rec was observed in the second, third, and fourth census periods. However, a significant decline in the N-rec was observed in the last census period (Table 4.4), and no significant positive or negative slope coefficients were observed for any species in the results of the mixed effect model (Table 4.2).

**Table 4.4:** Demographic characteristics of high-value timber species (mean (standard deviation)).

| Census Period | Monarch Birch | | | Castor Aralia | | | Japanese Oak | | |
|---|---|---|---|---|---|---|---|---|---|
| | BAI | Mort-ality | In-growth | BAI | Mort-ality | In-growth | BAI | Mort-ality | In-growth |
| I | 0.0023 (0.004)[a] | 0.21 (0.92)[a] | 0.10 (0.65)[a] | 0.0053 (0.006)[a] | 1.56 (3.29)[a] | 0.93 (2.32)[a] | 0.0057 (0.009)[a] | 0.07 (0.45)[a] | 0.00[a] |
| II | 0.0021 (0.003)[a] | 0.39 (1.07)[a] | 0.13 (0.90)[a] | 0.0074 (0.007)[ab] | 2.37 (4.81)[a] | 3.19 (7.45)[b] | 0.0057 (0.010)[a] | 0.46 (1.48)[a] | 1.25 (4.39)[b] |
| III | 0.0027 (0.004)[a] | 0.16 (0.76)[a] | 1.81 (4.98)[b] | 0.0080 (0.008)[b] | 2.40 (4.14)[a] | 3.95 (6.94)[b] | 0.0062 (0.010)[a] | 0.15 (0.58)[a] | 1.77 (3.24)[b] |
| IV | 0.0058 (0.009)[b] | 0.39 (1.18)[a] | 2.86 (8.01)[b] | 0.0099 (0.007)[c] | 1.72 (3.34)[a] | 2.89 (5.75)[ab] | 0.0092 (0.012)[b] | 0.52 (1.60)[a] | 1.65 (2.64)[b] |
| V | 0.0069 (0.012)[b] | 0.96 (2.21)[a] | 0.28 (1.51)[a] | 0.0094 (0.008)[bc] | 2.47 (4.19)[a] | 0.94 (2.28)[a] | 0.0078 (0.012)[b] | 0.53 (1.03)[a] | 0.61 (1.82)[a] |

Note: Census periods with different letters show significant difference ($p < 0.05$).

Figure 4.4 shows changes in the BAI, N-mor and N-rec of all species. The total BAI of all species showed no statistically significant difference in the first three census periods. However, it was significantly higher in the last two periods than in the first three periods ($p < 0.05$). The total BAI of broadleaf species increased while the conifer BAI decreased in the last census period. These results are also confirmed by the results of the mixed effect model in which a significant negative slope was observed for conifer and a positive slope was observed for broadleaf. The broadleaf N-rec that entered into the 5.0 cm DBH was higher than that of the conifer N-rec. For both conifer and broadleaf species, the N-rec decreased from the third census period (Figure 4.4). The number of total N-mor significantly increased since third census period. When comparing the conifer and broadleaf N-mor, the broadleaf N-mor increased from the third census period. However, there was no significant increase or decrease in conifer N-mor after the third census period. The mixed effect model also revealed an increase in the total N-mor over time. In addition, the broadleaf N-mor also increased over time.

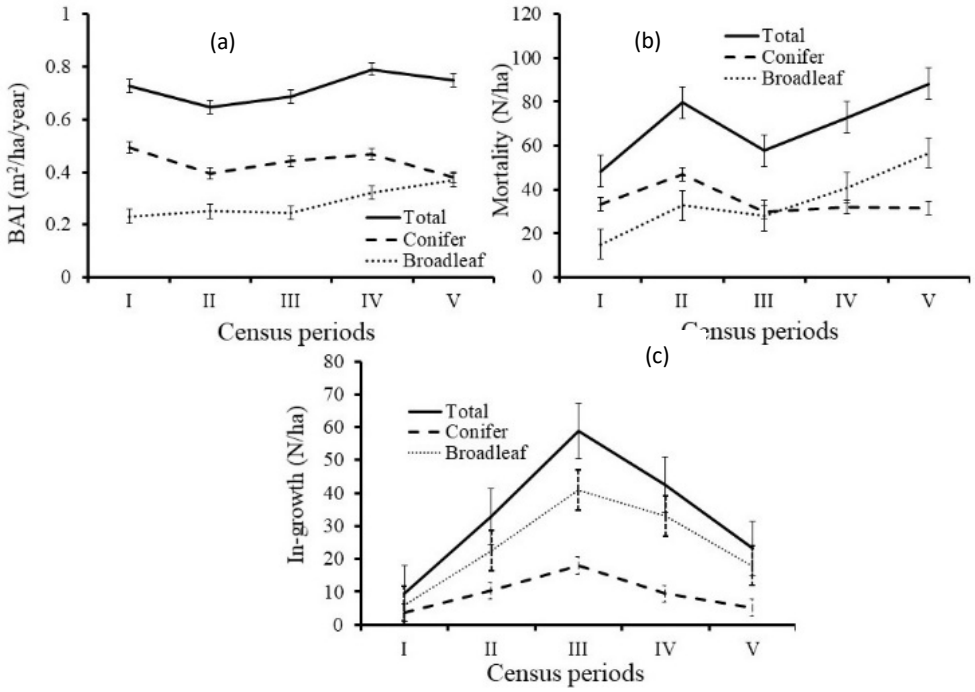


**Figure 4.4:** Development of demographic parameters of all species (mean (standard error)). (a) Basal area increment ($m^2$/ha/year), (b) Mortality (N/ha), and (c) In-growth (N/ha).

### 4.3.3 Changes in species proportion of high-value timber species

Table 4.5 shows the changes in species proportion of high-value timber species. Significant differences in the proportion of Japanese oak were observed ($p < 0.001$), while no significant differences were observed for monarch birch ($p < 0.22$) or castor aralia ($p < 0.31$) across census periods. However, a significant positive trend in the monarch birch proportion was observed over time (Table 4.2). Similarly, Table 4.2 shows a significant positive trend in the Japanese oak proportion. Table 4.5 also shows the changes in the proportion of conifer and broadleaf across census periods. The proportion of conifer declined after the first census period while that of broadleaf increased after the first period. These trends were also confirmed by the positive coefficients of mixed-effect models (Table 4.2).

**Table 4.5:** Changes in species proportion (%) of high-value timber species.

| Census Period | Monarch Birch | Castor Aralia | Japanese Oak | Conifer | Broadleaf |
|---|---|---|---|---|---|
| I | 0.37 (0.48) [a] | 1.87 (1.38) [a] | 1.01(1.43) [a] | 48.35(22.89) [a] | 51.65 (22.89) [a] |
| II | 0.41 (0.48) [a] | 2.37 (1.72) [a] | 1.25(1.64) [b] | 41.38(20.17) [a] | 58.62 (20.17) [ab] |
| III | 0.58 (0.82) [a] | 2.15 (1.30) [a] | 1.22(1.56) [ab] | 41.43(19.76) [b] | 58.56 (19.76) [bc] |
| IV | 1.13 (1.72) [a] | 2.24 (1.38) [a] | 1.46(1.44) [bc] | 38.13(18.69) [bc] | 61.84 (18.69) [cd] |
| V | 1.10 (1.79) [a] | 2.23 (1.39) [a] | 1.38(1.34) [c] | 33.01(14.30) [c] | 66.99 (14.30) [d] |

Note: Census periods with different letters show significant difference ($p < 0.05$).

### 4.3.4 Selection harvest

Table 4.6 shows the total N and BA harvest of high-value timber species. The small N and BA of high-value timber species were harvested during the 48-year period. Table 4.7 shows the total N and BA harvest of conifer and broadleaf across census periods. The number of broadleaf trees harvested in the first census period was higher than the number of conifer trees harvested. Starting from the second census period, more conifer trees than broadleaf trees were harvested. According to Table 4.6, the BA harvest for conifer was larger than the BA harvest for broadleaf in all periods. The BA harvest for broadleaf in the first census period was significantly higher than in the later four periods, with the lowest BA harvest occurring in the third period. The largest BA harvest for conifer occurred in the fourth census period.

**Table 4.6:** Harvest of high-value timber species (mean (standard deviation)).

| Census Periods | Monarch Birch | | Castor Aralia | | Japanese Oak | |
|---|---|---|---|---|---|---|
| | Number (N/ha) | BA ($m^2$/ha) | Number (N/ha) | BA ($m^2$/ha) | Number (N/ha) | BA ($m^2$/ha) |
| I | 0.50 (2.09) [a] | 0.04 (0.25) [a] | 2.20 (5.36) [a] | 0.02 (0.04) [a] | 0.47 (1.50) [a] | 0.03 (0.18) [a] |
| II | 0.04 (0.26) [a] | 0.01 (0.07) [a] | 0.28 (0.94) [b] | 0.007 (0.03) [ab] | 0.28 (1.16) [ab] | 0.09 (0.38) [ab] |
| III | 0.05 (0.37) [a] | 0.006 (0.05) [a] | 0.61 (3.17) [bc] | 0.012 (0.05) [ab] | 0.04 (0.32) [bc] | 0.0003 (0.002) [b] |
| IV | 0.06 (0.52) [a] | 0.003 (0.02) [a] | 0.04 (0.28) [c] | 0.002 (0.01) [b] | 0.04 (0.31) [bc] | 0.0001 (0.001) [b] |
| V | 0 [a] | 0 [a] | 0.31 (1.05) [bc] | 0.03 (0.11) [b] | 0.06 (0.45) [c] | 0.02 (0.15) [b] |

Note: Census periods with different letters show significant difference ($p < 0.05$).

**Table 4.7:** Harvest of conifer and broadleaf (mean (standard deviation)).

| Census Period | Conifer Harvest | | Broadleaf Harvest | |
|---|---|---|---|---|
| | Number (N/ha) | BA($m^2$/ha) | Number (N/ha) | BA($m^2$/ha) |
| I | 32.87 (51.11) [a] | 1.87 (2.60) [ab] | 55.25 (82.84) [a] | 1.31 (2.08) [a] |
| II | 11.07 (23.56) [bc] | 0.73 (1.43) [bc] | 10.33 (20.58) [ab] | 0.47 (0.96) [abc] |
| III | 14.16 (30.15) [c] | 1.10 (2.03) [c] | 7.98 (32.31) [c] | 0.26 (0.70) [c] |
| IV | 16.87 (26.22) [ab] | 2.02 (2.87) [a] | 4.58 (6.94) [bc] | 0.41 (0.73) [ab] |
| V | 9.92 (18.38) [bc] | 1.37 (2.40) [abc] | 4.72 (9.31) [bc] | 0.34 (0.78) [bc] |

Note: Census periods with different letters show significant difference ($p < 0.05$).

### 4.4 Discussion

In this Chapter, I investigated the long-term changes in stocking, demographic characteristics, and species proportion of high-value timber species as measures of sustainability. I used these parameters as criteria and indicators to evaluate the sustainability of high-value timber species as proposed by O'Hara et al. (2007). However, they used these criteria and indicators to evaluate the stand level sustainability of even-aged and uneven-aged

forest management. The changes or consistency of these parameters would be useful for establishing sustainable forest management by adjusting the tree marking for harvesting.

The main common characteristics of the targeted high-value timber species in this study were increases in N and BA. The increasing trend was also observed in the total N and total BA of forest stands. An increase in the N of forest stands managed under the selection system has occurred in the last few decades in other parts of the world with different environment and forest types. For example, Klopcic et al. (2011) found an increased total number of trees in their study in Slovenia. Compared with an unmanaged stand, a higher mean density and basal area in the managed stand was also reported by Young et al. (2017) in USA. Moreover, a decreasing tree density and basal area in an unmanaged stand was reported by Ediriweera et al. (2020) in their study in mixed-dipterocarp forests over a 40-year period.

One possible reason for increasing the N and BA of forest, including those of high-value timber species, would be due to some major disturbance, including natural (e.g., strong typhoon) and anthropogenic (e.g., selection harvest) factors (Noguchi and Yoshida, 2009). In the mixed conifer–broadleaf forest in northern Japan, a large typhoon occurred, causing widespread canopy opening (Yoshida and Noguchi, 2009) in some plots. Selection harvesting was carried out three to four times during the 48 years period. The increasing trend of both total N and BA of forest stand was greatly contributed by broadleaf species. These increasing trends in both N and BA are consistent with previous studies in mixed conifer–broadleaf forests in northern Japan such as that done by Yoshida et al. (2006). Those studies also highlighted the increasing trend of broadleaf tree density in mixed conifer–broadleaf forests managed under selection system.

Reversed J-shaped diameter distributions were observed for all target high-value timber species (Figure 4.2). Diameter distribution curves indicated an increasing number of smaller diameter class trees for all species across census periods. Owari et al. (2011) also reported a large number of smaller diameter class trees in northern Japanese mixed conifer–broadleaf forests. More fluctuation in size structure of monarch birch and Japanese oak were observed.

Similar to N and BA, the mean BAI of high-value timber increased over time. The increasing trend was also observed for the mean stand BAI even though it was not significantly different in the first three census periods. The results of regression modeling suggested temporal trends of BAI for high-value timber species and the total BAI of forest stands. In terms of the stand level BAI, a significant positive trend was observed. In northern mixed

conifer–broadleaf forests, similar results have been reported for the broadleaf species (Hiura et al., 2019; Yoshida et al., 2006).

The mean N-mor across census periods showed no significant difference for all high-value timber species. However, Japanese oak N-mor increased over time. Furthermore, no significant increasing or decreasing trends in N-rec were observed for high-value timber species across census periods in this study. These results are also consistent with previous studies by Hiura et al. (2019). For all target species, a significantly lower N-rec was observed in the first and last census periods, while a higher N-rec was observed in the second, third and fourth census periods. This trend can also be observed for the total N-rec of all species. This pattern may also be explained by a large disturbance caused by a large typhoon in 1981 (second census period) which created a canopy opening causing high light availability (Ishikawa and Ito, 1988) in some plots, favoring natural regeneration. As a result, higher N-rec in these plots would be expected following a large natural disturbance. This was also highlighted by previous studies in the mixed conifer–broadleaf forest in Northern Japan. Yoshida et al. (2006), for example, reported that a higher N-rec of castor aralia would be expected after a disturbance, and harvesting treatment in their study. In addition, Takahashi et al. (2003) reported that Japanese oak may tend to regenerate after a large disturbance before the establishment of other species.

The results in this Chapter also clearly show another important temporal trend of the forest stand. The forest composition and structure in the study area changed over time after the first census period (1968 to 1978). The proportion of conifer in the first census period was 48.35%, and it decreased to 33% in the last census period. An increasing broadleaf proportion might contribute to an increased N of high-value timber species (Table 4.2). Broadleaf N and BA exceeded those of conifer after the first census period, wherein the N and BA of conifer were larger than those of broadleaf. Even though there might be several reasons for this, one of the possible reasons for decreased conifer N and BA would be due to a bias in tree marking for harvesting. Table 4.6 showed that the total harvested basal area for conifer always exceeds that of broadleaf in all census periods. Owari et al. (2010) indicated that even though spatially unbiased tree marking was obtained, tree species that were marked for selection harvest in the study area was mostly conifer species. In addition, they observed that the trees marked for harvesting were larger than the unmarked trees.

In terms of BAI, conifer showed a decreasing trend over time (Table 4.3). Even though the mean BAI of conifer exceeded the mean BAI of broadleaf throughout the census periods,

both were almost similar in the last census period (0.379 $m^2$/ha for conifer and 0.369 $m^2$/ha for broadleaf). In addition, the mean BAI of conifer was significantly lower in the last census period than in the first four periods. Yoshida et al. (2006) reported that the growth of shade-intolerant broadleaf species was less than that of most common conifer species (i.e., *A. sachalinensis*), even after selection harvesting. However, this Chapter found that even though a larger mean BAI was observed for all conifer species, its BAI showed a decreasing trend while the total BAI of broadleaf species exhibited increasing trend. Harvesting of more conifer trees may contribute lower mean value in total BAI. The results are in line with a previous study by Hiura et al. (2019) in mixed conifer–broadleaf forest in northern Japan. According to this trend, the future forest composition of the study area would be more of a broadleaf-dominating type in terms of both N and BA. A similar decreasing trend in the conifer proportion has been reported in different regions (Klopcic and Boncina, 2011; Schuler, 2004).

The results of the sustainability measures revealed that there have been inconstancies in these measures over time. However, such inconsistencies could relate to a number of reasons. A recent study (Hiura et al., 2019) in mixed conifer–broadleaf forest with very little human disturbance in northern Japan revealed that changing climate conditions such as an increased temperature, precipitation, and decreased snowfall and snow cover period have led a to reduction in growth rate of conifer and an increasing in that of broadleaf species. Moreover, these inconsistencies in sustainability measures due to a changing climate have been widely reported in different regions (McMahon et al., 2010; Pretzsch et al., 2014). Similar to the results by O'Hara et al. (2007), the results of this Chapter indicate that a single-tree selection system is more of a dynamic entity.

The sustainability measures described in this Chapter would be useful for adjusting forest management activities, and various silvicultural activities, which could lead to consistency in sustainability measures in different forest types. Through the understanding of sustainability measures used in this Chapter, forest management can maintain the stocking of uneven-aged forest stand over time, BAI can be balanced by tree removals, and recruitment can be assessed whether it is sufficient. In addition, it would provide information for forest management operations such as stocking control, which is central to uneven-aged silviculture. Many stocking control approaches have been developed including reversed J-shape diameter distribution, selection system or plenter system, stand density index, and leaf area allocation, etc. (O'Hara and Gersonde, 2004). Sustainability measures can be achieved through these

stocking control approaches by removing those trees that surpass or maintain those of limited numbers in a certain diameter class.

## 4.5 Conclusions

In this Chapter, I examined the sustainability of high-value timber species in mixed conifer–broadleaf forest managed under selection system. Changes in the stocking, demographic characteristics, and species proportion of high-value timber species over a 48-year period have been used as measures of sustainability. These measures could provide useful information for their management in the long-run. In addition, I examined the general temporal trend of a selection forest stand. The main common characteristics of high-value timber species were increases in the tree density, basal area, and BAI across the census period. In terms of tree mortality, no significant differences were observed among census periods with no significant downward or upward trends. High fluctuation in the number of in-growth also occurred. Other important long-term characteristics of the forest stands are the changes in forest structure and composition to broadleaf forest in terms of the tree density and basal area. Even though some fluctuations in sustainability measures were observed, the results indicated that sustainability of high-value timber species was achieved under a single-tree selection system. The results of this Chapter would be useful for adapting silvicultural practices and harvesting practices such as single-tree selection, and also to maintain desired stocking of the forest stand. For example, attention should be paid to possible changes in species proportion and diameter distribution of remaining forest stand when marking trees for harvesting. The influence of natural and anthropogenic factors on long-term changes in stocking and demography of high-value timber species should be analyzed further.

# Chapter 5

# Predicting individual tree growth of high-value timber species

## 5.1 Introduction

Quantifying the tree growth of high-value timber species will provide useful information for single-tree management practice, since it will allow the estimation of time to reach desirable size, as well as the simulation of various silvicultural practices (Orellana et al. 2016). Individual tree growth models help explore the forest management alternatives, as they are flexible in predicting tree growth in stands with diverse structure, species composition and management history (Orellana et al. 2016). Tree growth models that use individual trees as the basic unit for modeling were also widely used in many different regions (Adame et al. 2008; Rohner et al. 2017; Schelhaas et al. 2018; Tenzin et al. 2017; Zhao et al. 2013). In mixed conifer-broadleaf forest in northern Japan, Tatsumi et al. (2016) quantified the neighborhood competition on the diameter growth of 38 tree species, including high-value timber species, using two times DBH measurement data. Using the tree ring data of 76 large-sized monarch birch trees, Shibano et al. (1995) examined the diameter growth of monarch birch trees in mixed conifer-broadleaf forest in northern Japan. Other studies, such as Noguchi and Yoshida (2009) and Fukuoka et al. (2013), examined the effects of selection cutting on individual tree growth and dynamics of Japanese oak. However, a simple and practically applicable tree growth model of high-value timber species was not widely studied, and data from long-term measurement plots in particular has not yet been used for the growth model development. In this Chapter, this issue will be addressed.

Forest trees, including high-value timber species, are slow growing and it may take several decades to detect their radial growth pattern (Pretzsch et al. 2019). In such case, long-term and repeated measurement data is indispensable offering robust empirical dataset to develop individual tree growth models for high-value timber species. Several studies derived individual tree growth information from tree ring data (Cunha et al. 2016; Shibano et al. 1995; Tenzin et al. 2017). However, growth measurement using tree ring data is relatively costly, and need extensive resources, time, and effort. Moreover, historical information of stands that are important in individual tree growth process may not be able to include in growth modeling using tree ring data. On the other hand, long-term and repeated measurement data provide information on the past stand conditions and management history (Pretzsch et al. 2019)

corresponding to tree growth process that are important for individual tree growth modeling (Noguchi and Yoshida 2009; Pretzsch et al. 2019). Therefore, the empirically derived data can provide valuable information for developing simple and practically applicable individual growth models for high-value timber species.

This Chapter aimed to develop practically useful growth models for three high-value timber species growing in northern Japan. The long-term data from forest measurement plots was used to predict the individual tree growth of high-value timber species and to determine the time required for high-value timber species to reach desirable size.

## 5.2 Materials and Methods

### 5.2.1 Study are and data

The study area and data used in this Chapter are same as the Chapter 4. Please refer to Chapter 4 for more detail (Sub-section 4.2.1).

### 5.2.2 Data preparation

The data analyses were based on the single-tree DBH data collected in the permanent plots. I used data from 168 monarch birch trees, 484 castor aralia trees, and 219 Japanese oak trees for model development. The frequency distribution of DBH among all observations is shown in Figure 5.1. The dependent variable was individual tree basal area increment (BAI; $cm^2$/year), which was calculated from the two consecutive DBH measurements on the same living tree, as verified using individual tree IDs. Some studies have indicated a preference for diameter increment models (Schelhaas et al. 2018); however, Vanclay (1994) reported that both are essentially the same because one can be derived from the other. Negative BAI values were excluded from the analysis as measurement error. Tree BA generally increases with an asymmetrical sigmoidal function through time with a slower rate in the younger trees, rapidly increasing at establishment, and then declining during senescence (Tomé et al. 2006). Theoretically, tree BAI can never reach zero because the creation of new tree rings is essential for water transport (Schelhaas et al. 2018); however, we included observations of zero BAI because they may represent to poor growth conditions due to environmental factors. BAI values > 100 $cm^2$/year were excluded from the analysis as outliers because BAI differences with BAI values > 20 $cm^2$/year represent < 0.01% of the total observations for all species.

In addition, variables normalized by area were derived, including total number of trees (T-tree; tree $ha^{-1}$), number of conifer trees (N-tree; tree $ha^{-1}$), number of broadleaf trees (L-tree; tree $ha^{-1}$), total stand BA (T-BA; $m^2$ $ha^{-1}$), conifer BA (N-BA; $m^2$ $ha^{-1}$), broadleaf BA (L-BA; $m^2$ $ha^{-1}$) and basal of trees larger than target trees (BAL; $m^2$ $ha^{-1}$). These variables were derived from the first measurement of the two consecutive DBH measurements of the permanent plots (e.g., when the DBH measurements were carried out in 2005 and 2010, the measurement data of 2005 was used to derive stand variables).

The study permanent plots are located in selection stands where selection harvests are carried out with cutting cycle of 15 to 20 years (10 to 20 years until 2005). Attention was paid to be spatially unbiassed when marking trees for selection harvest and larger trees are more likely to be marked than smaller ones while dominant species, i.e., *A. sachalinensis*, is more likely to be marked (Owari et al. 2010). In Chapter 4, the BA harvest of high-value timber species, conifer, and broadleaf species were analyzed. Chapter 4 found that small number of trees and BA of high-value timber species were harvested during the study period, and more conifer BA were harvested than broadleaf BA. The removal of trees by selection harvest may affect the growth of remaining trees. Therefore, basal area of harvested trees (BA-Har; $m^2$ $ha^{-1}$) was calculated that may positively affect the growth target trees.

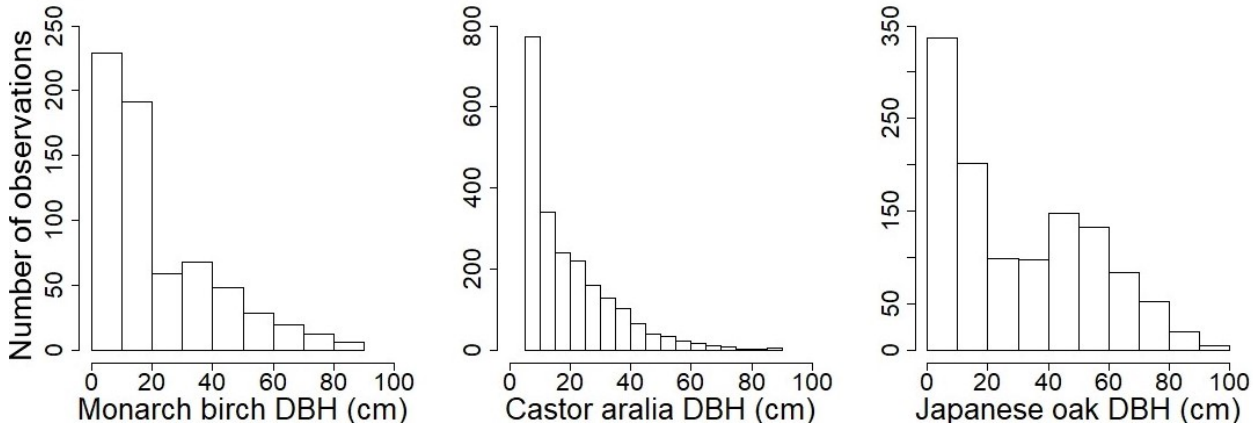


**Figure 5.1:** Frequency distribution of trees used for model development.

### 5.2.3 Individual tree BAI model

Individual tree BAI models were fitted separately for three target high-value timber species. The analysis used initial tree size, competition, and forest management variables as

independent variables. Tree size variables included initial DBH, square of initial DBH, and logarithm of initial DBH. Distance-dependent and distance-independent competition indices were generally used in individual tree growth modeling (Contreras et al. 2011; Cunha et al. 2016; Pokharel and Dech 2012; Rohner et al. 2017). Distance-dependent index accounts for spatial position of individual trees, while distance independent index does not require the spatial position of individual trees. Both indices may provide the comparable accuracy of growth prediction (Kahriman et al. 2018; Kuehne et al. 2019). On the other hand, distance-independent competition index can be derived easily from the long-term and repeated measurement data. Therefore, distance-independent competition index was considered in the model. Stand level variables, such as tree density and basal area, were generally considered to reflect stand scale competition (Kuehne et al. 2019; Wang et al. 2019). In this Chapter, stand-level variables, such as T-tree, N-tree, L-tree, T-BA, N-BA, L-BA and BAL were considered as competition variables. Further BA-Har was considered as the forest management variable.

### 5.2.4 Mixed-effects modeling

Repeated measurements of the same trees in long-term permanent plots result in a hierarchical data structure; such data lack independence among observations and are highly spatially and temporally correlated (Adame et al. 2008; Calama and Montero 2005). The mixed-effects approach has been widely used in individual tree growth modeling for repeated measurement data because it handles spatial and temporal correlation by incorporating variables as fixed, random or both effects in the model (Kiernan et al. 2008; Pokharel and Dech 2012; Uzoh and Oliver 2008; Wang et al. 2019). Using mixed-effects modeling approach, initial tree size, stand structure, and management variables were included as fixed effects, and plots, trees, and measurement years were included as random effects. Thus, the individual tree BAI model is as follow:

$$\ln(BAI_{ijk}+1) = \beta_0 + \beta_1 DBH_{ijk} + \beta_2 DBH^2_{ijk} + \beta_3 \log DBH_{ijk} + \beta_4 BAL_{ijk} + \beta_5 \text{T-tree}_{jk} + \beta_6 \text{N-tree}_{jk} + \beta_7 \text{L-tree}_{jk} + \beta_8 \text{T-BA}_{jk} + \beta_9 \text{N-BA}_{jk} + \beta_{10} \text{L-BA}_{jk} + \beta_{11} \text{BA-Har}_{jk} + \text{Tree}_i + \text{Plot}_j + \text{Measurement year}_k \quad \text{Equation (5.1)}$$

where $BAI_{ijk}$ is the basal area increment of the tree $i$ in plot $j$ in year $k$; $DBH_{ijk}$ is the initial DBH of the tree $i$ in plot $j$ measured in year $k$; $BAL_{ijk}$ is the total BAL of tree $i$ in plot $j$ in year $k$; T-tree$_{jk}$, N-tree$_{jk}$, L-tree$_{jk}$, T-BA$_{jk}$, N-BA$_{jk}$, and L-BA$_{jk}$ are the stand variables of the plot $j$ in year

$k$; and BA-Har$_{jk}$ is the selectively harvested BA of the plot $j$ in year $k$. Tree$_i$, Plot$_j$, and Measurement year$_k$ are random effects parameters for tree $i$ in the plot $j$ at year $k$. $\beta_0 - \beta_{11}$ are fixed effects parameters to be estimated.

### 5.2.5 Data analysis

Data analysis was carried out in R Software (R Core Team 2019) with "lme4" (Bates et al. 2020) and "lmerTest" (Kuznetsova et al. 2020) packages. The best models were selected using backward stepwise selection method based on Akaike's information criterion (AIC). However, variables with variance inflation factor (VIF) <5 were included in the models to avoid multicollinearity and overfitting of the models. Marginal and conditional $R^2$ was used to evaluate the goodness of fit of the selected models following Nakagawa and Schielzeth (2013). Because the dataset contained relatively few observations given the size distribution of individual trees (Figure 5.2), it was impractical to perform cross-validation by dividing the dataset into training and validation datasets, which would impose an uneven distribution of tree sizes in both datasets. Therefore, the leave-one-out cross validation approach was used, which allowed us to exclude one observation and fit the selected model to the remaining observations. Root mean square error (RMSE) and r values were calculated to compare observed BAI and predicted BAI.

From forest management perspectives, it is important to estimate the time required for a certain tree to reach target size. Based on the Equation (5.1), the number of years for a tree to reach a target size were predicted as follows (Cunha et al., 2016; Tenzin et al., 2017):

$$t = [\ln(BA_{i+n}) - \ln(BA_i)] / \ln(1+PBAI_i\%), \qquad \text{Equation (5.2)}$$

where t is the time (year), ln is the natural logarithm, $BA_i$ is the initial tree BA, $BA_{i+n}$ is the target tree BA. $PBAI_i\%$ is the BAI productivity potential for the $i$th tree, calculated as:

$$PBAI_i\ \% = (\text{Predicted } BAI_i / BA_i) * 100, \qquad \text{Equation (5.3)}$$

where predicted $BAI_i$ is the BAI of the $i$th individual tree predicted from Equation (5.1).

Equation (5.2) is based on compound interest law. Many natural phenomena follow the compound interest law (Han et al., 2014) and it was widely applied in forestry, e.g., estimation of growth period for a tree to reach a certain size (Cunha et al., 2016; Tenzin et al., 2017). It considered the interest rate, i.e., growth rate in this Chapter, to predict the value in the future,

i.e., DBH. The prediction of tree DBH in a given year is based on growth rate calculated from the final model of Equation (5.1). Even though the past forest stand conditions were considered in predicting the growth rate, the changes in future forest stand conditions could not be considered in the estimation of number of years for a tree to reach a certain DBH.

## 5.3 Results

### 5.3.1 Observed basal area increment (BAI)

The relationship between initial tree DBH and observed BAI is shown in Figure 5.2, and Table 5.1 shows the correlation between observed BAI and explanatory variables used in the model development. A significant positive correlation was found between initial tree DBH and observed BAI ($p < 0.001$), with correlation coefficients of 0.56, 0.77 and 0.72 for monarch birch, castor aralia and Japanese oak, respectively. As a pioneer species, monarch birch had a higher BAI at a smaller DBH size; as DBH increased, the growth decreased. Castor aralia and Japanese oak exhibited more stable BAI.

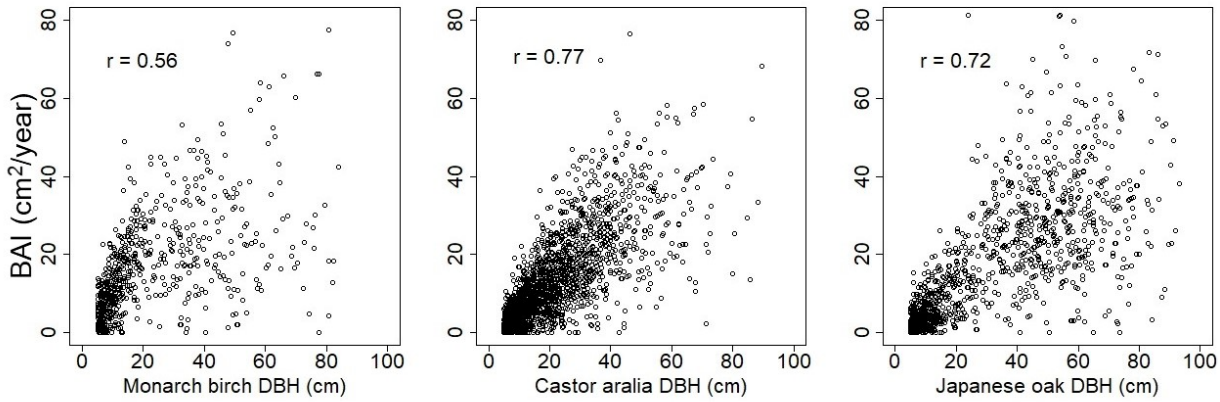


**Figure 5.2:** Relationships between initial tree diameter at breast height (cm) and observed basal area increment ($cm^2$/year).

**Table 5.1:** Correlation between observed basal area increment and explanatory variables.

| Variable | Monarch birch | Castor aralia | Japanese oak |
|---|---|---|---|
| DBH (cm) | 0.56*** | 0.77*** | 0.72*** |
| BAL ($m^2$ $ha^{-1}$) | -0.62*** | -0.65*** | -0.65*** |
| T-tree (tree $ha^{-1}$) | ns | -0.23*** | -0.10** |
| N-tree (tree $ha^{-1}$) | 0.08* | -0.24*** | ns |
| L-tree (tree $ha^{-1}$) | -0.15*** | -0.10*** | -0.16*** |
| T-BA ($m^2$ $ha^{-1}$) | 0.22*** | ns | ns |
| N-BA ($m^2$ $ha^{-1}$) | 0.15*** | -0.21*** | -0.15*** |
| L-BA ($m^2$ $ha^{-1}$) | ns | 0.21*** | 0.10** |
| BA-Har ($m^2$ $ha^{-1}$) | ns | ns | ns |

Significant code: *** $p < 0.000$, ** $p < 0.001$, * $p < 0.05$, ns represents not significant. DBH = diameter at breast height, BAL = basal area of trees larger than target trees, T-tree = total number of trees, N-tree = number of conifer trees, L-tree = number of broadleaf trees, T-BA=total basal area, N-BA=conifer basal area, L-BA = broadleaf basal area, and BA-Har = basal area of harvested trees.

### 5.3.2 Model fitting, parameter estimation and goodness of fit

The estimated parameters using the individual tree BAI model (Equation (5.1)) for each species are listed in Table 5.2. Variables selected in the final models were only included in the table. For each species, a mixed-effects model including individual trees, plots, and measurement year as random factors obtained lowest AIC values and was selected as the final model. High $R^2$ values of the selected models for fixed (marginal $R^2$) and random (conditional $R^2$) factors indicated an acceptable fit the data (Table 5.2). Negative coefficient value was observed for monarch birch DBH while significant positive coefficients were observed for castor aralia and Japanese oak DBH. For all species, significant negative coefficients of BAL were observed. Significant negative coefficient of conifer tree density was observed for castor aralia, and negative coefficients of broadleaf tree density were observed for monarch birch and castor aralia. Conifer basal area showed significant negative coefficient for Japanese oak.

**Table 5.2:** Estimated parameters of individual tree BAI models for three high-value timber species.

| Variable | | Monarch birch | Castor aralia | Japanese oak |
|---|---|---|---|---|
| Intercept | $\beta_0$ | 4.00*** | 2.92*** | 2.82*** |
| DBH (cm) | $\beta_1$ | -0.01 | 0.02*** | 0.02*** |
| BAL ($m^2$ $ha^{-1}$) | $\beta_4$ | -0.07 *** | -0.04*** | -0.04*** |
| N-tree (tree $ha^{-1}$) | $\beta_6$ | -2.1e-05 | -3.7e-04* | - |
| L-tree (tree $ha^{-1}$) | $\beta_7$ | -5.7e-04** | -3.8e-04*** | -1.7e-04 |
| N-BA ($m^2$ $ha^{-1}$) | $\beta_9$ | - | - | - 0.02** |
| BA-Har ($m^2$ $ha^{-1}$) | $\beta_{11}$ | 0.007 | 0.01 | 0.07* |
| AIC | | 1231.3 | 3742.9 | 2087.8 |
| $R^2$ – marginal | | 0.39 | 0.51 | 0.61 |
| $R^2$ – conditional | | 0.77 | 0.80 | 0.85 |

Significant code: *** $p < 0.000$, ** $p < 0.001$, * $p < 0.05$. DBH = diameter at breast height, BAL = basal area of trees larger than target trees, N-tree = number of conifer trees, L-tree = number of broadleaf trees, N-BA = conifer basal area, BA-Har = basal area of harvested trees, AIC = Akaike's information criterion.

### 5.3.3 Model prediction for BAI and years to reach target DBH

Figure 5.3 shows the relationship between observed and predicted BAI for three high-value timber species. Model prediction produced BAI RMSE of 10.44, 7.91, and 11.62 $cm^2$/year; significant positive correlations were detected between observed and predicted BAI, with r values of 0.62, 0.73 and 0.70 for monarch birch, castor aralia, and Japanese oak respectively ($p < 0.001$ for all species).

The derived models of Equation (5.1) were used to predict the time required for a tree of a given initial DBH to reach an expected target DBH using Equation (5.2). The Equation (5.1) was predicted based on the best model described in Table 5.2 for all species. It can be assumed that variables related to initial tree size, stand, and management were included for the prediction of time using Equation (5.2). As an example, the time for a given tree with DBH =30 cm to reach DBH = 50 cm and 70 cm was estimated. The predicted durations for a tree with DBH = 30 cm to reach DBH =50 cm were 29, 28, 48 years in average and 48, 46, and 80 years in average to reach DBH = 70 cm for monarch birch, castor aralia and Japanese oak respectively (Table 5.3 and Figure 5.4).

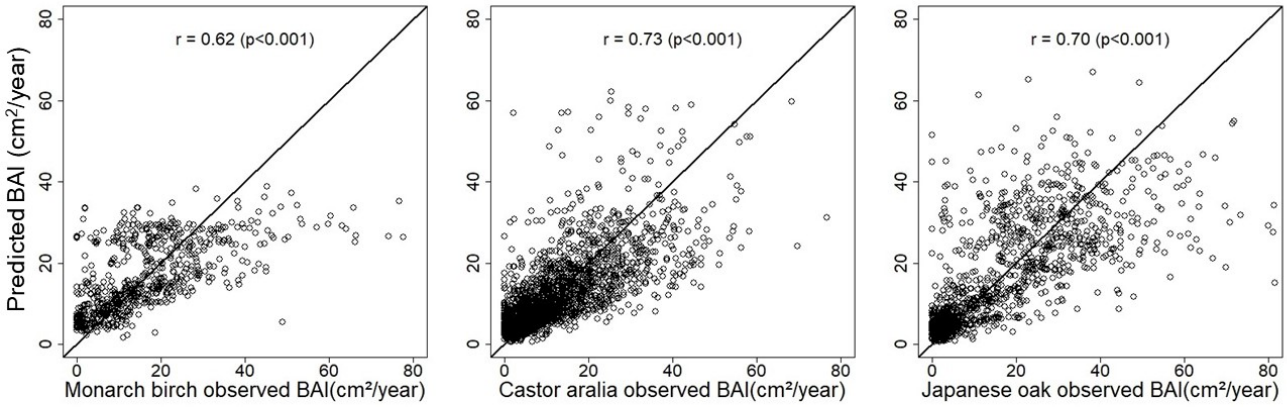


**Figure 5.3:** Observed and predicted basal area increment ($cm^2$/year) for three high-value timber species.

**Table 5.3:** The predicted number of years for a tree with 30 cm of initial DBH to reach target DBH of 50 cm and 70 cm.

| Species | Average years (SD) | |
|---|---|---|
| | 50 cm DBH | 70 cm DBH |
| Monarch birch (n = 168) | 29(40) | 48(65) |
| Castor aralia (n = 484) | 28(20) | 46(32) |
| Japanese oak (n = 219) | 48(37) | 80(61) |

SD stands for standard deviation.

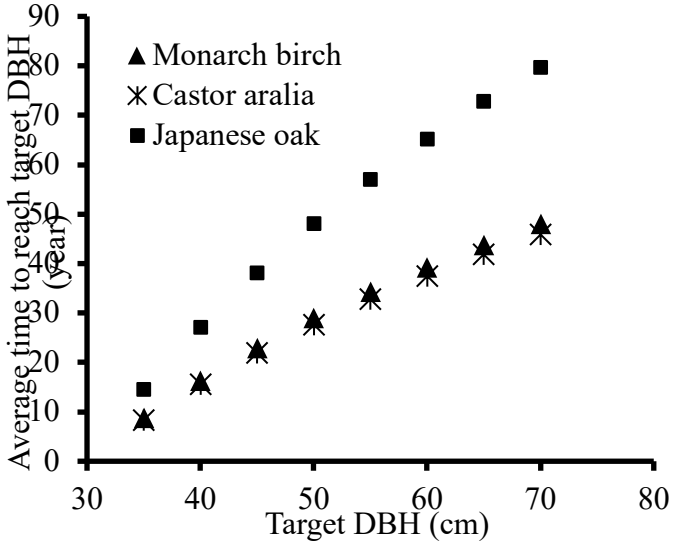


**Figure 5.4:** The predicted years for a tree with 30 cm of initial DBH to reach target DBH. Each marker represents the average time (years) to reach the target DBH.

## 5.4. Discussion

I used a linear mixed-effects model including fixed effects and random effects parameters to predict individual tree growth using a long-term repeated measurements dataset. The individual tree growth models developed in this study exhibited acceptable predictive accuracy (Table 5.2). Explanatory variables were selected in consideration of statistical fitting and biological importance to individual tree growth.

BAI of monarch birch followed a sigmoidal relationship with initial tree DBH, whereas those of castor aralia and Japanese oak increased steadily as DBH increased. The effect of DBH on BAI was positive and significant in all species except for monarch birch (Table 5.2). Negative coefficient of DBH was observed for monarch birch, even though it was not significant, meaning that the BAI of monarch birch decreased with increasing DBH. This pattern could be explained by Figure 5.2, showing that the BAI of monarch birch became larger in the smaller DBH and then declined after reaching certain DBH size. Even though BAI for monarch birch was underestimated in larger DBH, the $R^2$ and RMSE values indicated the acceptable prediction power.

Stand variables related to tree density and basal area were included as competition variables in the individual tree growth models. Negative relationships between BAI and stand variables, i.e., broadleaf tree density, conifer tree density and conifer basal area, were observed suggesting that trees in dense stands exhibit slower growth than those in sparsely populated stands. Using the long-term thinning experiments data, Lhotka (2017) also reported the negative effect of tree density on the growth of individual trees. From the practical forest management perspective, these stand variables could be manipulated for improved growth of target trees through the use of various silvicultural interventions.

In the selected models (Table 5.2), stand variables related to tree density (i.e., N-tree and L-tree) were selected more often than variables related to BA. However, BAL, a stand-level variable related to BA, were selected in the final models for all species. The inclusion of BAL in the all selected models indicated that individual tree BAI could be explained better by BAL than by BA. Significant negative relationships between BAL and BAI were observed for all three targeted high-value timber species (Table 5.2). As BAL increases, individual tree BAI decreases. These results are biologically meaningful, since BAL accounts for a subject tree's social ranking and the stand density simultaneously (Schröder and Gadow 1999). When there are higher numbers of trees that are larger than subject tree in an area, the BAI of subject trees will be lower. Similar results have been obtained in recent previous studies in different forest

types using different growth modelling approaches (Contreras et al. 2011; Rohner et al. 2017; Ruslandi et al. 2017; Schelhaas et al. 2018).

General expectation of selection harvest include increased growth of remaining trees (Yoshida et al. 2006). Previous studies indicated that the canopy gaps created by selection harvest improved the growth of remaining trees especially that of smaller trees (Amaral et al. 2019; Yoshida et al. 2006; Yoshida and Kamitani 1998). Positive coefficients of BA-Har for all high-value tree species was observed, although the coefficients were not significant (Table 5.2). The result of no significant coefficient of BA-Har can be explained by the fact that BA-Har is a stand scale variable and the gap created by selection harvest may not represent the intensity of canopy gap around the target individual trees that included in the model development.

The models developed in this study would be useful tools for prediction of the growth of high-value individual trees and have potential to be applied in forest management. Shibano et al. (1990) examined the relationship between the DBH and wood quality of monarch birch and suggested to harvest trees with DBH > 60 cm, when the heartwood ratio is expected to be greater than 60%. According to Owari et al. (2016), DBH threshold to register as superior tree has been set to 50 cm under single-tree management system. From a practical forest management perspective, key question is the length of time a tree of certain size requires to reach such desirable DBH. As shown in Table 5.3 and Figure 5.4, the BAI model allows predicting the time to reach a target DBH. As an example, the time of a tree with 30 cm DBH to reach 50 cm DBH and 70 cm DBH for all species were estimated (Table 5.3) using derived BAI models (Equation (5.1) and Table 5.2). Japanese oak is predicted to take longer time than the other two species to reach the target DBH. Since, such information was scarce, BAI models developed in this study can be used for this purpose, and it allows planning for harvest and sustainable production of high-value timber species. In models developed in this Chapter, it implicitly assumed that stand-structure variables (e.g., BAL, T-tree) are not subject to change over time. As a given tree grows higher, it will overtop the surrounding trees. Consequently, it will most likely become less affected by the competition which might positively affect its growth. It should be careful when interpreting the results, since the assumption may have caused the overestimation of years to reach target DBH. It could be useful for short term prediction of the growth of individual trees because there would be variation in growth rates of trees depending on the size of the target trees.

The individual tree growth models developed in this Chapter will provide useful information for forestry practitioner. The variables used for model development can be derived simply and easily from long-term and repeated measurements data. Further, variables used in this Chapter do not require the data of tree coordinates and distance between trees. Similar models can be developed for the other species because the long-term plot data included every tree species within the UTHF permanent plots with DBH ≥ 5 cm.

## 5.4 Conclusion

This Chapter demonstrated the use of long-term UTHF measurement dataset for predicting individual tree growth useful for forest management purpose. Individual tree BAIs were predicted from a long-term plot measurement dataset using a linear mixed-effects modeling approach. Initial tree size, competition, and management variables were considered in the models; the results showed reasonable predictive accuracy. However, the model was unable to include some important factors affecting tree growth such as natural disturbance, soil, elevation, slope, slope direction, and climatic data. Therefore, it should be generalized carefully in other regions considering possible change in species composition and stand conditions, which might alter ecosystem functions of the forests.

# Chapter 6

# General discussion and conclusion

## 6.1 General discussion

This study aims to examine the potential use of UAV and LiDAR data combined with resource assessment technique for single- tree management system. Several research attempts have been made on the use of RS data, i.e. UAV and LiDAR data, in the estimation of forest resource (Dalponte et al., 2019; Dalponte and Coomes, 2016; Goodbody et al., 2019; Hyyppä et al., 2012; Iglhaut et al., 2019; Sibona et al., 2016; Takagi et al., 2015; Wulder et al., 2014, 2013) at both individual tree level and forest stand level. However, their applicability for management of high-value timber species remains uncertain and, needs more detailed study. In addition, resource assessment techniques that support the single-tree management of high-value timber species still require detailed analysis for the reliable application of the system. My study addressed these issues. Further, this study will support forest managers with the information of tree locations, stem size estimation method, sustainability assessment method, and individual tree growth information that can be applied simply and practically in management planning of high-value timber species.

### 6.1.1 General consideration of RS and resource assessment techniques for the single-tree management of high-value timber species

#### 6.1.1.1 RS technique

Since large-size trees with high commercial value were the target species under single-tree management system, how RS data could be applied reliably for individual tree height measurement of these species remains uncertain. Due to the problems related to automatic tree detection (Kaartinen et al., 2012; Nuijten et al., 2019; Vauhkonen et al., 2012), the accuracy of tree height measurement using RS data for large-size tree with heterogeneous crowns were not widely assessed and reported. In particular, I evaluated the similarity of three height data sources to assess the reliable application of RS data in the individual tree height measurement of high-value timber species.

Chapter 2 confirmed the applicability of RS data for tree height measurement of large-size high-value timber species. However, the results indicated that the accuracy of individual tree height measurement could vary with species and tree height classes. In addition to statistical comparison, I evaluated the reliability of three tree height sources using tree-height diameter models since tree height and DBH are highly correlated (Hulshof et al., 2015; Jucker et al., 2017; Mehtätalo et al., 2015). The results indicated that LiDAR derived tree height was strongly

correlated with individual tree DBH compared to field and UAV derived tree height. UAV derived tree height showed comparable level of accuracy to field and LiDAR data. This result indicated the important implications of UAV in practical forest measurement purpose. I assumed that this result is meaningful since the target trees species were large-size in terms of DBH and crown area. Large tree crown with limited visibility to the tree top could contribute to the accuracy of tree height measurement in the field (Hunter et al., 2013; Larjavaara and Muller-Landau, 2013; Stereńczak et al., 2019). UAV and LiDAR data can overcome this problem, and therefore produce more accurate tree height compared to field measurement. However, there were not existing literature, to the best of my knowledge, on the performance of different tree height measurement methods on the height-diameter models. Tree height data derived from UAV and LiDAR could improve the height-diameter allometric models.

In Chapter 3, I demonstrated the applicability of RS data to predict the individual tree spatial position and their stem size of high-value timber species. To estimate the tree spatial positions, I first classified the forest canopy into three high-value timber species, other broadleaf and conifer classes. The results of classification were used to estimate the individual tree spatial position of high-value timber species.

Even though the classification results in Chapter 3 were lower than other studies using multispectral or hyperspectral data (Dalponte et al., 2019; Franklin and Ahmed, 2018; Matsuki et al., 2015; Michez et al., 2016), I assumed the results were reasonable given at fewer spectral bands, and the UAV data were taken at only one time. The result of classification accuracy could be improved through determining of best season and timing of UAV-DAP data acquisition to identify the high-value timber species and their locations since the target species were deciduous broadleaf species with significant changes in leaf phenology especially in the autumn. In addition, further inclusion of more spectral bands, such as near infrared, etc., could improve the accuracy of classification results. Further research attempts should be emphasized on these issues.

As indicated by the results of tree crown segmentation in Chapter 3, one of the major problems of DBH estimation of high-value timber species was the accuracy of automatic tree crown delineation. The lower accuracy in tree crown delineation could lead to significant errors in the estimation of DBH of individual trees since estimation of DBH relied on the crown area and tree height (Hulshof et al., 2015; Jucker et al., 2017). Several previous studies reported the same problem (Dalponte et al., 2019; Kaartinen et al., 2012; Nuijten et al., 2019) and it is an active area of research. However, I assumed that with the estimated tree locations, visual interpretation of tree crown on UAV-DAP orthophotograph would help to determine the tree crown area that can be used for the estimation of tree size. The availability of tree location map could help reduce the

effort and time of tree searching within large area of forests. The DBH estimation could be also possibilities through the use of other data collection techniques such as under-canopy UAV laser scanning (Hyyppä et al., 2020), mobile laser scanning, and personal laser scanning techniques (Bauwens et al., 2016; Chen et al., 2019). However, given the trade-off between costs, time and resolution, the methods presented in Chapter 3 could be an alternative source of data acquiring individual tree information of sparsely distributed high-value timber species in mixed-wood forests.

#### 6.1.1.2 Resource assessment techniques

I demonstrated the assessment of sustainability and the prediction of individual tree growth in Chapter 4 and Chapter 5 that can be applied in single-tree management system. Assessing the resource sustainability of forest under a certain forest management system play a critical role since the achievement of sustainability is a central precept in forestry. I applied commonly used stocking and demographic parameters to assess the resource sustainability. These variables were mainly used for assessing the dynamics of a forest stand (Amaral et al., 2019; Pretzsch et al., 2014; Yoshida et al., 2006; Yoshida and Noguchi, 2010; Young et al., 2017). Through the use of long-term forest measurement data, these variables could be used to assess sustainability of forest resources under a certain forest management system.

The results of the Chapter 4 indicated that the current forest management system employed in the study area ensured the sustainability of high-value timber species. The results of this Chapter would be useful for adapting silvicultural practices and harvesting practices such as single-tree selection, and also to maintain stocking and demography of the forest stand through various forest management and silvicultural operations. Even though overharvesting and illegal harvesting are not common in the study area, the methods used in this Chapter could be used for the monitoring of high-value timber species as well as other tree species. For example, I found the significant variation in the in-growth of all species with significantly low number in the last census interval. In such case, further studies should be emphasized on the influences of natural and anthropogenic factors on the in-growth of high-value timber species. The results of Chapter 4 contributed to the existing knowledge of forest dynamics of high-value timber species as well as the methods to assess the sustainability of forest resources. In addition, the importance of long-term forest measurement data was highlighted.

Taking advantage of long-term forest management dataset, I developed simple and practically applicable individual tree growth models for high-value timber species in Chapter 5. I demonstrated the use of developed models to predict the time for a certain tree to reach desirable

size. Individual tree growth models play a critical role in forestry since they can be used in the simulation of silvicultural and forest management options. With the tree location and size data derived from Chapter 3, the growth models developed in this Chapter would be a powerful tool for single-tree management planning. Further simulation study combining remote sensing data and individual tree growth model in a forest management compartment level or larger area would contribute to sustainable utilization and management of high-value timber species.

## 6.2 Conclusion

### 6.2.1 Summary of the results

*Chapter 2: The applicability of UAV-DAP for tree height estimation: comparison with airborne LiDAR and field survey*

The results of this Chapter highlighted applicability of UAV-DAP data for individual tree height measurement of high-value broadleaf trees. However, lower tree height values for higher trees and higher values for lower trees may occur in UAV-DAP derived tree height in comparison with field-based measurement. It is likely to observe higher tree height values for higher trees and lower tree height values for lower trees in UAV-DAP derived tree height when comparing with LiDAR derived tree height. Height-diameter models revealed that tree height derived from UAV-DAP can be explained by tree DBH with comparable accuracy to LiDAR and field measured tree height. This results confirmed the practical application of UAV-DAP for measuring tree height of large size high-value timber species in northern Japanese mixed-wood forests.

*Chapter 3: Estimation of spatial positions and DBH of high-value timber species*

The applicability of UAV-DAP and LiDAR for the estimation of individual tree spatial position and individual tree DBH was demonstrated in this Chapter. The estimation of individual tree spatial positions was carried out though forest canopy classification. The results indicated that the classification of forest canopy into three high-value timber species, other broadleaf, and conifer classes produced overall accuracy of 73 % in sub-compartment 36B and 63% in sub-compartment 59A. Since target species in this study included only large-size high-value timber species with highly heterogenous crown, the multiresolution segmentation revealed low accuracy of individual tree crown segmentation. When estimating DBH, UAV-DAP could produce high-prediction accuracy comparable to field and LiDAR data. The results of this Chapter contribute to single tree management of high-value timber species by providing useful information for searching of high-value timber trees and their estimated tree size in large area of mixed-wood forests.

*Chapter 4: Resource assessment of high-value timber species*

In this Chapter, the sustainability of high-value timber species in mixed conifer–broadleaf forest managed under selection system. The main common characteristics of high-value timber species were increases in the tree density, basal area, and BAI over nearly 50 years period. In terms of tree mortality, no significant differences were observed among census periods with no significant downward or upward trends. High fluctuation in the number of in-growth also occurred. Through the understanding of sustainability measures used in this study, forest management can maintain the stocking of uneven-aged forest stand over time, BAI can be balanced by tree removals, and recruitment can be assessed whether it is sufficient. Since commonly used forest variables were used for the purpose of sustainability assessment, the method could be generalized to other tree species and regions.

*Chapter 5: Predicting individual tree growth of high-value timber species*

In this Chapter, individual tree BAI were predicted from a long-term plot measurement dataset using a linear mixed-effects modeling approach. Initial tree size, distance independent competition index, stand structure, and management variables were considered in the models; the results showed reasonable predictive accuracy. In addition, the developed model in this Chapter could be used for prediction of time for a tree to reach a certain diameter. The results were comparable prediction accuracy comparing with previous studies. Since variables used in this Chapter are simple and easy to derive from forest measurement data, the models can be easily adapted to other species.

### 6.2.2 Main Conclusion

This study demonstrated the potential use of UAV-DAP data and LiDAR data in the single-tree management of high-value timber species. In addition, this thesis examined the resource assessment techniques that can be applied in the monitoring and future resource estimation of high-value timber species. These two techniques could provide useful information for single-tree management of high-value timber species. The results of Chapter 2 and Chapter 3 could be applied in operational measurement of individual tree parameters, i.e. DBH and tree height, of target high-value timber species. Further, Chapter 3 could contribute to the estimation of individual tree spatial positions that play one of the crucial roles in single-tree management. Chapter 4 could help to examine the recourse conditions of target species under a selection system. Prediction of future resource conditions could be facilitated by the growth models developed in Chapter 5. The

application of RS technique and resource assessment techniques, as a whole, contribute to necessary information that is important for the single-tree management of high-value timber species in northern Japanese mixed-wood forest.

### 6.3 Limitations and future direction

UAV-DAP derived CHMs were mainly used in Chapter 3 and Chapter 4. However, these CHMs were normalized using the accurate DTM derived from LiDAR data. When the LiDAR data were not available, the applicability of UAV-DAP data could be limited. In addition, to derive species specific information, such as species classification, the use of RGB information only may limit the classification accuracy. Since the time and weather conditions at the time of UAV data acquisition might greatly influence spectral response of forest canopy, the method followed in this study needs to be generalized carefully to other sites. In addition, the phenology of forest tree species varied from time to time, through for the spring, summer, autumn, and winter, the repeated flight missions of UAV might improve spectral separability between canopy species. Since the target species were deciduous broadleaf species with significant changes in leaf phenology especially in the autumn, the result of classification could be improved through searching of the best timing of UAV flights.

Even though the results revealed that LiDAR and UAV-DAP derived height metrics were more important than intensity metrics for individual tree DBH estimation, the calculation of LiDAR intensity metrics for each specific return (1$^{st}$ to last) would improve the DBH estimation accuracy especially for high-intensity LiDAR data. The use of under-canopy laser scanning (Hyyppä et al., 2020), mobile laser scanning and personal laser scanning techniques (Bauwens et al., 2016; Chen et al., 2019) could be alternative DBH estimation techniques.

I analyzed the resource conditions of high-value timber species under selection management stands. However, analysis on the influence of natural and anthropogenic factors affecting the growth, regeneration, and mortality of high-value timber species be analyzed further.

The growth model developed in this study used the long-term forest measurement data set. Even though estimation of number of years for a certain diameter tree to reach a target diameter was carried out, the results need to be validated with more accurate growth data such as dendrochronological study with the use of tree-ring data. In addition, the model was also unable to include some important factors affecting tree growth such as natural disturbance, soil, elevation, slope, slope direction, and climatic data. Therefore, it should be generalized carefully in other regions considering possible change in species composition and stand conditions, which might alter ecosystem functions of the forests. The individual tree growth models developed in this study

could be improved by the incorporation of LiDAR and UAV-DAP derived crown metrics. For example, Ma et al. (2018) examined the growth and competition at individual tree level with the use of bi-temporal LiDAR data. Using similar approach with low cost UAV data, it would be one of the potentials to improved growth prediction of target species. Further studies focusing on the use of multi-temporal UAV-DAP for quantifying individual tree crown competition would be analyzed further.

## References


Abetz, P., Klädtke, J., 2002. The target tree management system. Forstw. Cbl. 121, 73–82. https://doi.org/10.1046/j.1439-0337.2002.00073.x

Adame, P., Hynynen, J., Cañellas, I., del Río, M., 2008. Individual-tree diameter growth model for rebollo oak (*Quercus pyrenaica* Willd.) coppices. For. Ecol. Manage. 255, 1011–1022. https://doi.org/10.1016/j.foreco.2007.10.019

Agisoft., 2018. Agisoft PhotoScan user manual: professional edition, Version 1.4. Agisoft. St. Petersburg, Russia.

Akaike, H., 1973. Information theory and an extension of the maximum likelihood principle, in: Proceedings of the 2nd International Symposium on Information Theory, B.N.Petrov and F. Caski, Eds. pp. 267–281, Akademiai Kiado, Budapest, Hungary.

Alexander, C., Deák, B., Kania, A., Mücke, W., Heilmeier, H., 2015. Classification of vegetation in an open landscape using full-waveform airborne laser scanner data. Int. J. Appl. Earth Obs. Geoinf. 41, 76–87. https://doi.org/10.1016/j.jag.2015.04.014

Alonzo, M., Andersen, H.E., Morton, D.C., Cook, B.D., 2018. Quantifying boreal forest structure and composition using UAV structure from motion. Forests 9, 119. https://doi.org/10.3390/f9030119

Alonzo, M., Morton, D.C., Cook, B.D., Andersen, H.E., Babcock, C., Pattison, R., 2017. Patterns of canopy and surface layer consumption in a boreal forest fire from repeat airborne lidar. Environ. Res. Lett. 12, 065004. https://doi.org/10.1088/1748-9326/aa6ade

Amaral, M.R.M., Lima, A.J.N., Higuchi, F.G., dos Santos, J., Higuchi, N., 2019. Dynamics of tropical forest twenty-five years after experimental logging in central amazon mature forest. Forests 10, 89. https://doi.org/10.3390/f10020089

Andersen, H.E., Reutebuch, S.E., McGaughey, R.J., 2006. A rigorous assessment of tree height measurements obtained using airborne lidar and conventional field methods. Can. J. Remote Sens. 32, 355–366. https://doi.org/10.5589/m06-030

Anderson, K., Gaston, K.J., 2013. Lightweight unmanned aerial vehicles will revolutionize spatial ecology. Front. Ecol. Environ. 11, 138–146. https://doi.org/10.1890/120150

Apostol, B., Petrila, M., Lorenţ, A., Ciceu, A., Gancz, V., Badea, O., 2020. Species discrimination and individual tree detection for predicting main dendrometric characteristics in mixed temperate forests by use of airborne laser scanning and ultra-high-resolution imagery. Sci. Total Environ. 698, 134074. https://doi.org/10.1016/j.scitotenv.2019.134074

Baena, S., Moat, J., Whaley, O., Boyd, D.S., 2017. Identifying species from the air : UAVs and the very high resolution challenge for plant conservation. PLoS One 12, e0188714. https://doi.org/10.1371/journal.pone.0188714

Bates, D., Maechler, M., Bolker, B., Walker, S., Christensen, R.H.B., Singmann, H., Dai, B., Scheipl, F., Grothendieck, G., Green, P., Fox, J., 2020. Linear mixed-effects model using "Eigen" and S4, R Package Version 1.1- 23, https://github.com/lme4/lme4/.

Bauwens, S., Bartholomeus, H., Calders, K., Lejeune, P., 2016. Forest inventory with terrestrial LiDAR: A comparison of static and hand-held mobile laser scanning. Forests 7, 127. https://doi.org/10.3390/f7060127

Belgiu, M., Drăgu, L., 2016. Random forest in remote sensing: a review of applications and future directions. ISPRS J. Photogramm. Remote Sens. 114, 24–31. https://doi.org/10.1016/j.isprsjprs.2016.01.011

Blaschke, T., 2010. Object based image analysis for remote sensing. ISPRS J. Photogramm. Remote Sens. 65, 2–16. https://doi.org/10.1016/j.isprsjprs.2009.06.004

Bohlin, J., Wallerman, J., Fransson, J.E.S., 2012. Forest variable estimation using photogrammetric matching of digital aerial images in combination with a high-resolution DEM. Scand. J. For. Res. 27, 692–699. https://doi.org/10.1080/02827581.2012.686625

Bourland, N., Kouadio, Y.L., Lejeune, P., Sonké, B., Philippart, J., Daïnou, K., Fétéké, F., Doucet, J.-L., 2012. Ecology of *Pericopsis elata* (Fabaceae), an endangered timber species in southeastern Cameroon. Biotropica 44, 840–847.

Bragg, D.C., 2014. Accurately measuring the height of (real) forest trees. J. For. 112, 51–54. https://doi.org/10.5849/jof.13-065

Calama, R., Montero, G., 2005. Multilevel linear mixed model for tree diameter increment in Stone Pine (*Pinus pinea*): a calibrating approach. Silva Fenn. 39, 37–54.

Cao, L., Coops, N.C., Innes, J.L., Dai, J., Ruan, H., She, G., 2016. Tree species classification in subtropical forests using small-footprint full-waveform LiDAR data. Int. J. Appl. Earth Obs. Geoinf. 49, 39–51. https://doi.org/10.1016/j.jag.2016.01.007

Cao, L., Liu, H., Fu, X., Zhang, Z., Shen, X., Ruan, H., 2019. Comparison of UAV LiDAR and digital aerial photogrammetry point clouds for estimating forest structural attributes in subtropical planted forests. Forests 10, 145. https://doi.org/10.3390/f10020145

Chen, Q., Gong, P., Baldocchi, D., Tian, Y.Q., 2007. Estimating basal area and stem volume for individual trees from LiDAR data. Photogramm. Eng. Remote Sens. 73, 1355–1365. https://doi.org/10.14358/pers.73.12.1355

Chen, S., Liu, H., Feng, Z., Shen, C., Chen, P., 2019. Applicability of personal laser scanning in forestry inventory. PLoS One 14, e0211392. https://doi.org/10.1371/journal.pone.0211392

Colomina, I., Molina, P., 2014. Unmanned aerial systems for photogrammetry and remote sensing: a review. ISPRS J. Photogramm. Remote Sens. 92, 79–97. https://doi.org/10.1016/j.isprsjprs.2014.02.013

Contreras, M.A., Affleck, D., Chung, W., 2011. Evaluating tree competition indices as predictors of basal area increment in western Montana forests. For. Ecol. Manage. 262, 1939–1949. https://doi.org/10.1016/j.foreco.2011.08.031

Cunha, T.A. da, Finger, C.A.G., Hasenauer, H., 2016. Tree basal area increment models for *Cedrela*, *Amburana*, *Copaifera* and *Swietenia* growing in the Amazon rain forests. For. Ecol. Manage. 365, 174–183. https://doi.org/10.1016/j.foreco.2015.12.031

Dalponte, M., Bruzzone, L., Gianelle, D., 2012a. Tree species classification in the Southern Alps based on the fusion of very high geometrical resolution multispectral/hyperspectral images and LiDAR data. Remote Sens. Environ. 123, 258–270. https://doi.org/10.1016/j.rse.2012.03.013

Dalponte, M., Bruzzone, L., Gianelle, D., 2011. A system for the estimation of single-tree stem diameter and volume using multireturn LIDAR data. IEEE Trans. Geosci. Remote Sens. 49, 2479–2490.

Dalponte, M., Coomes, D.A., 2016. Tree-centric mapping of forest carbon density from airborne laser scanning and hyperspectral data. Methods Ecol. Evol. 7, 1236–1245. https://doi.org/10.1111/2041-210X.12575

Dalponte, M., Coops, N.C., Bruzzone, L., Gianelle, D., 2009. Analysis on the use of multiple returns LiDAR data for the estimation of tree stems volume. IEEE J. Sel. Top. Appl. Earth Obs. Remote Sens. 2, 310–318. https://doi.org/10.1109/JSTARS.2009.2037523

Dalponte, M., Frizzera, L., Gianelle, D., 2019. Individual tree crown delineation and tree species classification with hyperspectral and LiDAR data. PeerJ 6:e6227. https://doi.org/10.7717/peerj.6227

Dalponte, M., Frizzera, L., Ørka, H.O., Gobakken, T., Næsset, E., Gianelle, D., 2017. Predicting stem diameters and aboveground biomass of individual trees using remote sensing data. Ecol. Indic. 85, 367–376. https://doi.org/10.1016/j.ecolind.2017.10.066

Dalponte, M., Ørka, H.O., Gobakken, T., Gianelle, D., Næsset, E., 2012b. Tree species classification in boreal forests with hyperspectral data. IEEE Trans. Geosci. Remote Sens. 51, 2632–2645. https://doi.org/10.1109/tgrs.2012.2216272

Dieler, J., Uhl, E., Biber, P., Müller, J., Rötzer, T., Pretzsch, H., 2017. Effect of forest stand management on species composition, structural diversity, and productivity in the temperate zone of Europe. Eur. J. For. Res. 136, 739–766. https://doi.org/10.1007/s10342-017-1056-1

Ding, Y., Zang, R., Lu, X., Huang, J., 2017. The impacts of selective logging and clear-cutting on woody plant diversity after 40 years of natural recovery in a tropical montane rain. Sci. Total Environ. 579, 1683–1691. https://doi.org/10.1016/j.scitotenv.2016.11.185

Ediriweera, S., Bandara, C., Woodbury, D.J., Mi, X., Gunatilleke, I.A.U.N., Gunatilleke, C.V.S., Ashton, M.S., 2020. Changes in tree structure, composition, and diversity of a mixed-dipterocarp rainforest over a 40-year period. For. Ecol. Manage. 458, 117764. https://doi.org/10.1016/j.foreco.2019.117764

Fassnacht, F.E., Latifi, H., Stereńczak, K., Modzelewska, A., Lefsky, M., Waser, L.T., Straub, C., Ghosh, A., Fassnacht, F.E., Waser, L.T., Latifi, H., Straub, C., Stereńczak, K., Lefsky, M., 2016. Review of studies on tree species classification from remotely sensed data. Remote Sens. Environ. 186, 64–87. https://doi.org/10.1016/j.rse.2016.08.013

Feldpausch, T.R., Banin, L., Phillips1, O.L., Baker, T.R., Lewis, S.L., Quesada, C.A., Affum-Baffoe, K., Arets, E.J.M.M., Berry, N.J., Bird, M., Brondizio, E.S., Camargo, P. de, Chave, J., Djagbletey, G., Domingues, T.F., Drescher, M., Fearnside, P.M., Franc¸a, M.B., Fyllas, N.M., Lopez-Gonzalez, G., Hladik, A., Higuchi, N., Hunter, M.O., Iida, Y., Salim, K.A., Kassim, A.R., Keller, M., Kemp, J.,

King, D.A., Lovett, J.C., Marimon, B.S., Marimon-Junior, B.H., Lenza, E., Marshall, A.R., Metcalfe, D.J., Mitchard, E.T.A., Moran, E.F., Nelson, B.W., Nilus, R., Nogueira, E.M., Palace, M., Patiˇno, S., K. S.-H. Peh, Raventos, M.T., Reitsma, J.M., Saiz, G., Schrodt, F., Sonk´e, B., Taedoumg, H.E., Tan, S., White, L., W¨oll, H., Lloyd, J., 2011. Height-diameter allometry of tropical forest trees. Biogeosciences 8, 1081–1106. https://doi.org/10.5194/bg-8-1081-2011

Franklin, S.E., Ahmed, O.S., 2018. Deciduous tree species classification using object-based analysis and machine learning with unmanned aerial vehicle multispectral data. Int. J. Remote Sens. 39, 5236–5245. https://doi.org/10.1080/01431161.2017.1363442

Fridman, J., Holm, S., Nilsson, M., Nilsson, P., Ringvall, A.H., Ståhl, G., 2014. Adapting national forest inventories to changing requirements - the case of the Swedish National Forest Inventory at the turn of the 20th century. Silva Fenn. 48, 1095. https://doi.org/10.14214/sf.1095

Fukuoka, S., Oikawa, N., Tokuni, M., Isozaki, Y., Goto, S., 2013. Effects of selection cutting on population dynamics, *Quercus crispula* in a conifer-hardwood mixed forest in the University of Tokyo Hokkaido Forest. Bull. Univ. Tokyo For. 129, 1-14 (in Japanese with English summary).

Ganz, S., Käber, Y., Adler, P., 2019. Measuring tree height with remote sensing - a comparison of photogrammetric and LiDAR data with different field measurements. Forests 10, 694. https://doi.org/doi:10.3390/f10080694

Giuliarelli, D., Mingarelli, E., Corona, P., Pelleri, F., Alivernini, A., Chianucci, F., 2016. Tree-oriented silviculture for valuable timber production in mixed Turkey oak (*Quercus cerris* L.) coppices in Italy. Ann. Silvic. Res. 40, 148–154. https://doi.org/10.12899/asr-1198

González-Ferreiro, E., Diéguez-Aranda, U., Fernández, L.B.-, Buján, S., Barbosa, M., Suárez, J.C., Bye, I.J., Miranda, D., 2013. A mixed pixel- and region-based approach for using airborne laser scanning data for individual tree crown delineation in Pinus radiata D. Don plantations. Int. J. Remote Sens. 34, 7671–7690. https://doi.org/10.1080/01431161.2013.823523

Goodbody, T.R.H., Coops, N.C., White, J.C., 2019. Digital aerial photogrammetry for updating area-based forest inventories: a review of opportunities, challenges, and future directions. Curr. For. Reports 5, 55–75. https://doi.org/10.1007/s40725-019-00087-2

Guerra-Hernández, J., Cosenza, D.N., Rodriguez, L.C.E., Silva, M., Tomé, M., Díaz-Varela, R.A., González-Ferreiro, E., 2018. Comparison of ALS- and UAV(SfM)-derived high-density point clouds for individual tree detection in Eucalyptus plantations. Int. J. Remote Sens. 39, 5211–5235. https://doi.org/10.1080/01431161.2018.1486519

Han, Z.Q., Liu, T., Sun, Q.M., Li, R., Xie, J.B., Li, B.L., 2014. Application of compound interest laws in biology: Reunification of existing models to develop seed bank dynamics model of annual plants. Ecol. Modell. 278, 67–73. https://doi.org/10.1016/j.ecolmodel.2014.01.024

Heinzel, J.N., Weinacker, H., Koch, B., 2008. Full automatic detection of tree species based on delineated single tree crowns - a data fusion approach for airborne laser scanning data and aerial photographs. Silvilaser 2008 Proc. 76–85.

Hemery, G., Spiecker, H., Aldinger, E., Kerr, G., Collet, C., Bell, S., 2008. COST Action E42: growing valuable broadleaved tree species 40 pp. Available at http://www.valbro.uni-freiburg.

Hemery, G.E., Clark, J.R., Aldinger, E., Claessens, H., Malvolti, M.E., O'connor, E., Raftoyannis, Y., Savill, P.S., Brus, R., 2010. Growing scattered broadleaved tree species in Europe in a changing climate: a review of risks and opportunities. Forestry 83, 65–81. https://doi.org/10.1093/forestry/cpp034

Hirata, Y., 2004. The effects of footprint size and sampling density in airborne laser scanning to extract individual trees in mountainous terrain. Int. Arch. Photogramm. Remote Sens. Spat. Inf. Sci. 36, 102–107.

Hiura, T., Go, S., Iijima, H., 2019. Long-term forest dynamics in response to climate change in northern mixed forests in Japan: a 38-year individual-based approach. For. Ecol. Manage. 449, 117469. https://doi.org/10.1016/j.foreco.2019.117469

Hoover, C.M., Bush, R., Palmer, M., Treasure, E., 2020. Using forest inventory and analysis data to support national forest management: regional case studies. J. For. 1–11. https://doi.org/10.1093/jofore/fvz073

Hovi, A., Korhonen, L., Vauhkonen, J., Korpela, I., 2016. LiDAR waveform features for tree species classification and their sensitivity to tree- and acquisition related parameters. Remote Sens. Environ. 173, 224–237. https://doi.org/10.1016/j.rse.2015.08.019

Huang, H., He, S., Chen, C., 2019. Leaf abundance affects tree height estimation derived from UAV images. Forests 10, 931. https://doi.org/10.3390/f10100931

Hulshof, C.M., Swenson, N.G., Weiser, M.D., 2015. Tree height-diameter allometry across the United States. Ecol. Evol. 5, 1193–1204. https://doi.org/10.1002/ece3.1328
Hunter, M.O., Keller, M., Victoria, D., Morton, D.C., 2013. Tree height and tropical forest biomass estimation. Biogeosciences 10, 8385–8399. https://doi.org/10.5194/bg-10-8385-2013
Husch, B., Beers, T.W., Kershaw, J.A., 2003. Forest mensuration, 4th ed. John Wiley & Sons, New York.
Hyyppä, E., Hyyppä, J., Hakala, T., Kukko, A., Wulder, M.A., White, J.C., Pyörälä, J., Yu, X., Wang, Y., Virtanen, J.P., Pohjavirta, O., Liang, X., Holopainen, M., Kaartinen, H., 2020. Under-canopy UAV laser scanning for accurate forest field measurements. ISPRS J. Photogramm. Remote Sens. 164, 41–60. https://doi.org/10.1016/j.isprsjprs.2020.03.021
Hyyppä, J., Yu, X., Hyyppä, H., Vastaranta, M., Holopainen, M., Kukko, A., Kaartinen, H., Jaakkola, A., Vaaja, M., Koskinen, J., Alho, P., 2012. Advances in forest inventory using airborne laser scanning. Remote Sens. 4, 1190–1207. https://doi.org/10.3390/rs4051190
Iglhaut, J., Cabo, C., Puliti, S., Piermattei, L., O'Connor, J., Rosette, J., 2019. Structure from motion photogrammetry in forestry: a review. Curr. For. Reports 5, 155–168. https://doi.org/10.1007/s40725-019-00094-3
Iizuka, K., Yonehara, T., Itoh, M., Kosugi, Y., 2018. Estimating tree height and diameter at breast height (DBH) from digital surface models and orthophotos obtained with an unmanned aerial system for a Japanese Cypress (*Chamaecyparis obtusa*) Forest. Remote Sens. 10, 13. https://doi.org/10.3390/rs10010013
Imai, Y., Setojima, M., Yamagishi, Y., Fujiwara, N., Greenery, U., Development, T., Management, I., 2004. Tree-height measuring characteristics of urban forests by LiDAR data different in resolution. Int. Soc. Photogramm. Remote Sensing, Florida, USA, 1–4.
Imani, G., Boyemba, F., Lewis, S., Nabahungu, N.L., Calders, K., Zapfack, L., Riera, B., Balegamire, C., Cuni-Sanchez, A., 2017. Height-diameter allometry and above ground biomass in tropical montane forests: insights from the Albertine Rift in Africa. PLoS One 12, e0179653. https://doi.org/10.1371/journal.pone.0179653
Immitzer, M., Atzberger, C., Koukal, T., 2012. Tree species classification with Random Forest using very high spatial resolution 8-band WorldView-2 satellite data. Remote Sens. 4, 2661–2693. https://doi.org/10.3390/rs4092661
Ishibashi, S., Hirokawa, T., 1986. An analysis of data on selection forest in the Tokyo University Forest in Hokkaido. Trans. Annu. Meet. Kanto Branch, Jpn. For. Soc. 37, 15-18 (in Japanese).
Ishikawa, Y., Ito, K., 1988. The regeneration process in a mixed forest in central Hokkaido, Japan. Vegetatio 79, 75–84. https://doi.org/10.1007/BF00044850
Jayathunga, S., Owari, T., Tsuyuki, S., 2018a. The use of fixed–wing UAV photogrammetry with LiDAR DTM to estimate merchantable volume and carbon stock in living biomass over a mixed conifer–broadleaf forest. Int. J. Appl. Earth Obs. Geoinf. 73, 767–777. https://doi.org/10.1016/j.jag.2018.08.017
Jayathunga, S., Owari, T., Tsuyuki, S., 2018b. Evaluating the performance of photogrammetric products using fixed-wing UAV imagery over a mixed conifer-broadleaf forest: comparison with airborne laser scanning. Remote Sens. 10, 187. https://doi.org/10.3390/rs10020187
Jayathunga, S., Owari, T., Tsuyuki, S., Hirata, Y., 2020. Potential of UAV photogrammetry for characterization of forest canopy structure in uneven-aged mixed conifer–broadleaf forests. Int. J. Remote Sens. 41, 53–73. https://doi.org/10.1080/01431161.2019.1648900
Jucker, T., Caspersen, J.J., Chave, J., Antin, C., Barbier, N., Bongers, F., Dalponte, M., Ewijk, K.Y. Van, Forrester, D.I., Haeni, M., I.Higgins, S., Holdaway, R.J., Iida, Y., Lorimer, C., Marshall, P.L., Momo, S., Moncrieff, G.R., Ploton, P., Poorter, L., Rahman, K.A., Schlund, M., Sonké, B., Sterck, F.J., Trugman, A.T., Usoltsev, V.A., Vanderwel, M.C., Waldner, P., Wedeux, B.M.M., Wirth, C., Wöll, H., Woods, M., Xiang, W., Zimmermann, N.E., Coomes, D.A., 2017. Allometric equations for integrating remote sensing imagery into forest monitoring programmes. Glob. Chang. Biol. 23, 177–190. https://doi.org/10.1111/gcb.13388
Kaartinen, H., Hyyppä, J., Yu, X., Vastaranta, M., Hyyppä, H., Kukko, A., Holopainen, M., Heipke, C., Hirschmugl, M., Morsdorf, F., Næsset, E., Pitkänen, J., Popescu, S., Solberg, S., Wolf, B.M., Wu, J.-C., 2012. An international comparison of individual tree detection and extraction using airborne laser scanning. Remote Sens. 4, 950–974. https://doi.org/10.3390/rs4040950
Kahriman, A., Ahin, A.S., Sönmez, T., Yavuz, M., 2018. A novel approach to selecting a competition index: the effect of competition on individual-tree diameter growth of Calabrian pine. Can. J. For. Res. 48, 1217– 1226. https://doi.org/10.1139/x98-199

Kane, V.R., McGaughey, R.J., Bakker, J.D., Gersonde, R.F., Lutz, J.A., Franklin, J.F., 2010. Comparisons between field- and LiDAR-based measures of stand structural complexity. Can. J. For. Res. 40, 761–773. https://doi.org/10.1139/x10-024

Kangas, A., Astrup, R., Breidenbach, J., Fridman, J., Gobakken, T., Korhonen, K.T., Maltamo, M., Nilsson, M., Nord-Larsen, T., Næsset, E., Olsson, H., 2018. Remote sensing and forest inventories in Nordic countries–roadmap for the future. Scand. J. For. Res. 33, 397–412. https://doi.org/10.1080/02827581.2017.1416666

Kangas, A., Räty, M., Korhonen, K.T., Vauhkonen, J., Packalen, T., 2019. Catering information needs from global to local scales-potential and challenges with national forest inventories. Forests 10, 800. https://doi.org/10.3390/f10090800

Kerr, G., 1996. The effect of heavy or "free growth" thinning on oak (*Quercus petraea* and *Q. robur*). Forestry 69, 303–317. https://doi.org/10.1093/forestry/69.4.303

Khai, T.C., Mizoueb, N., Kajisa, T., Ota, T., Yoshida, S., 2016. Stand structure, composition and illegal logging in selectively logged production forests of Myanmar: comparison of two compartments subject to different cutting frequency. Glob. Ecol. Conserv. 7, 132–140. https://doi.org/10.1016/j.gecco.2016.06.001

Khosravipour, A., Skidmore, A.K., Wang, T., Isenburg, M., Khoshelham, K., 2015. Effect of slope on treetop detection using a LiDAR Canopy Height Model. ISPRS J. Photogramm. Remote Sens. 104, 44–52. https://doi.org/10.1016/j.isprsjprs.2015.02.013

Kiernan, D.H., Bevilacqua, E., Nyland, R.D., 2008. Individual-tree diameter growth model for sugar maple trees in uneven-aged northern hardwood stands under selection system. For. Ecol. Manage. 256, 1579–1586. https://doi.org/10.1016/j.foreco.2008.06.015

King, D.A., 2005. Linking tree form, allocation and growth with an allometrically explicit model. Ecol. Modell. 185, 77–91. https://doi.org/10.1016/j.ecolmodel.2004.11.017

Kitahara, F., Mizoue, N., Yoshida, S., 2010. Effects of training for inexperienced surveyors on data quality of tree diameter and height measurements. Silva Fenn. 44, 657–667.

Klopcic, M., Boncina, A., 2011. Stand dynamics of silver fir (Abies alba Mill.)-European beech (*Fagus sylvatica* L.) forests during the past century: A decline of silver fir? Forestry 84, 259–271. https://doi.org/10.1093/forestry/cpr011

Kock, N., Lynn, G.S., 2012. Lateral collinearity and misleading results in variance-based SEM: An illustration and recommendations. J. Assoc. Inf. Syst. 13, 546–580. https://doi.org/10.17705/1jais.00302

Kuehne, C., Weiskittel, A.R., Waskiewicz, J., 2019. Comparing performance of contrasting distance-independent and distance-dependent competition metrics in predicting individual tree diameter increment and survival within structurally-heterogeneous, mixed-species forests of Northeastern United States. For. Ecol. Manage. 433, 205–216. https://doi.org/10.1016/j.foreco.2018.11.002

Kukunda, C.B., Duque-Lazo, J., González-Ferreiro, E., Thaden, H., Kleinn, C., 2018. Ensemble classification of individual Pinus crowns from multispectral satellite imagery and airborne LiDAR. Int. J. Appl. Earth Obs. Geoinf. 65, 12–23. https://doi.org/10.1016/j.jag.2017.09.016

Kuuluvainen, T., 2002. Natural variability of forests as a reference for restoring and managing biological diversity in boreal Fennoscandia. Silva Fenn. 36, 97–125.

Kuuluvainen, T., Tahvonen, O., Aakala, T., 2012. Even-aged and uneven-aged forest management in boreal fennoscandia: a review. Ambio 41, 720–737. https://doi.org/10.1007/s13280-012-0289-y

Kuznetsova, A., Brockhoff, P.B., Christensen, R.H.B., Jensen, S.P., 2020. "lmerTest": Tests in Linear Mixed Effects Models, R Package Version 3.1-2, https://github.com/runehaubo/lmerTestR.

Laiho, O., Lähde, E., Pukkala, T., 2011. Uneven-vs even-aged management in Finnish boreal forests. Forestry 84, 547–556. https://doi.org/10.1093/forestry/cpr032

Larjavaara, M., Muller-Landau, H.C., 2013. Measuring tree height: a quantitative comparison of two common field methods in a moist tropical forest. Methods Ecol. Evol. 4, 793–801. https://doi.org/10.1111/2041-210X.12071

Laurin, G.V., Ding, J., Disney, M., Bartholomeus, H., Herold, M., Papale, D., Valentini, R., 2019. Tree height in tropical forest as measured by different ground, proximal, and remote sensing instruments, and impacts on above ground biomass estimates. Int. J. Appl. Earth Obs. Geoinf. 82, 101899. https://doi.org/10.1016/j.jag.2019.101899

Lhotka, J.M., 2017. Examining growth relationships in *Quercus stands*: an application of individual-tree models developed from long-term thinning experiments. For. Ecol. Manage. 385, 65–77. https://doi.org/10.1016/j.foreco.2016.11.029

Lim, K., Treitz, P., Wulder, M., St-Ongé, B., Flood, M., 2003. LiDAR remote sensing of forest structure. Prog. Phys. Geogr. 27, 88–106. https://doi.org/10.1191/0309133303pp360ra
Lindenmayer, D.B., Laurance, W.F., Franklin, J.F., Likens, G.E., Banks, S.C., Blanchard, W., Gibbons, P., Ikin, K., Blair, D., McBurney, L., Manning, A.D., JohnA.R.Stein, 2013. New policies for old trees: averting a global crisis in a keystone ecological structure. Conserv. Lett. 7, 61–69. https://doi.org/10.1111/conl.12013
Lisein, J., Michez, A., Claessens, H., Lejeune, P., 2015. Discrimination of deciduous tree species from time series of unmanned aerial system imagery. PLoS One 10, e0141006. https://doi.org/10.1371/journal.pone.0141006
Lisein, J., Pierrot-Deseilligny, M., Bonnet, S., Lejeune, P., 2013. A photogrammetric workflow for the creation of a forest canopy height model from small unmanned aerial system imagery. Forests 4, 922–944. https://doi.org/10.3390/f4040922
Liu, K., Wang, S., Li, X., Li, Y., Zhang, B., Zhai, R., 2019. The assessment of different vegetation indices for spatial disaggregating of thermal imagery over the humid agricultural region. Int. J. Remote Sens. 00, 1–20. https://doi.org/10.1080/01431161.2019.1677969
Löf, M., Brunet, J., Filyushkina, A., Lindbladh, M., Skovsgaard, J.P., Felton, A., 2016. Management of oak forests: striking a balance between timber production, biodiversity and cultural services. Int. J. Biodivers. Sci. Ecosyst. Serv. Manag. 12, 59–73. https://doi.org/10.1080/21513732.2015.1120780
Luoma, V., Saarinen, N., Wulder, M.A., White, J.C., Vastaranta, M., Holopainen, M., Hyyppä, J., 2017. Assessing precision in conventional field measurements of individual tree attributes. Forests 8, 1–16. https://doi.org/10.3390/f8020038
Ma, L., Cheng, L., Li, M., Liu, Y., Ma, X., 2015. Training set size, scale, and features in Geographic Object-Based Image Analysis of very high resolution unmanned aerial vehicle imagery. ISPRS J. Photogramm. Remote Sens. 102, 14–27. https://doi.org/10.1016/j.isprsjprs.2014.12.026
Ma, Q., Su, Y., Tao, S., Guo, Q., 2018. Quantifying individual tree growth and tree competition using bi-temporal airborne laser scanning data: a case study in the Sierra Nevada Mountains, California. Int. J. Digit. Earth 11, 485–503. https://doi.org/10.1080/17538947.2017.1336578
MacDicken, K.G., Sola, P., Hall, J.E., Sabogal, C., Tadoum, M., Wasseige, C. de, 2015. Global progress toward sustainable forest management. For. Ecol. Manage. 352, 47–56. https://doi.org/10.1016/j.foreco.2015.02.005
Manetti, M.C., Becagli, C., Sansone, D., Pelleri, F., 2016. Tree-oriented silviculture: a new approach for coppice stands. IForest 9, 791–800. https://doi.org/10.3832/ifor1827-009
Marselis, S.M., Tang, H., Armston, J.D., Calders, K., Labrière, N., Dubayah, R., 2018. Distinguishing vegetation types with airborne waveform LiDAR data in a tropical forest-savanna mosaic: a case study in Lopé National Park, Gabon. Remote Sens. Environ. 216, 626–634. https://doi.org/10.1016/j.rse.2018.07.023
Matsuki, T., Yokoya, N., Iwasaki, A., 2015. Hyperspectral tree species classification of Japanese complex mixed forest with an aid of LiDAR data. IEEE J. Sel. Top. Appl. Earth Obs. Remote Sens. 8, 2177–2187. https://doi.org/10.1109/WHISPERS.2014.8077510
McGaughey, R.J., 2018. FUSION/LDV: Software for LiDAR data analysis and visualization. USDA Forest Service Pacific Northwest Research Station: Seattle, WA, USA.
McMahon, S.M., Parker, G.G., Miller, D.R., 2010. Evidence for a recent increase in forest growth. Proc. Natl. Acad. Sci. U. S. A. 107, 3611–3615. https://doi.org/10.1073/pnas.0912376107
McRoberts, R.E., Tomppo, E.O., Næsset, E., 2010. Advances and emerging issues in national forest inventories. Scand. J. For. Res. 25, 368–381. https://doi.org/10.1080/02827581.2010.496739
Mehtätalo, L., De-Miguel, S., Gregoire, T.G., 2015. Modeling height-diameter curves for prediction. Can. J. For. Res. 45, 826–837. https://doi.org/10.1139/cjfr-2015-0054
Michez, A., Piégay, H., Lisein, J., Claessens, H., Lejeune, P., 2016. Classification of riparian forest species and health condition using multi-temporal and hyperspatial imagery from unmanned aerial system. Environ. Monit. Assess. 188, 1–19. https://doi.org/10.1007/s10661-015-4996-2
Mielcarek, M., Stereńczak, K., Khosravipour, A., 2018. Testing and evaluating different LiDAR-derived canopy height model generation methods for tree height estimation. Int. J. Appl. Earth Obs. Geoinf. 71, 132–143. https://doi.org/10.1016/j.jag.2018.05.002
Miya, H., Yoshida, T., Noguchi, M., Nakamura, F., 2009. Individual growing conditions that affect diameter increment of tree saplings after selection harvesting in a mixed forest in northern Japan. J. For. Res. 14, 302–310. https://doi.org/10.1007/s10310-009-0136-6
Miyamoto, Y., Oakmura, K., Okamuru, K., 2010. A study of Oak (*Quercus crispula* Blume) working

group. Trans. Meet. Hokkaido Branch Jpn. For. Soc. 58, 107-109 (in Japanese).
Müller, S., Ammer, C., Nüsslein, S., 2000. Analyses of stand structure as a tool for silvicultural decisions - a case study in a *Quercus petraea* - Sorbus torminalis stand. Forstw Cbl 119, 32–42. https://doi.org/10.1007/BF02769124
Næsset, E., 2004. Practical large-scale forest stand inventory using a small-footprint airborne scanning laser. Scand. J. For. Res. 19, 164–179. https://doi.org/10.1080/02827580310019257
Nakagawa, S., Schielzeth, H., 2013. A general and simple method for obtaining R2 from generalized linear mixed-effects models. Methods Ecol. Evol. 4, 133–142. https://doi.org/10.1111/j.2041-210x.2012.00261.x
Nex, F., Remondino, F., 2014. UAV for 3D mapping applications: a review. Appl. Geomatics 6, 1–15. https://doi.org/10.1007/s12518-013-0120-x
Nguyen, H.M., Demir, B., Dalponte, M., 2019. A weighted SVM-based approach to tree species classification at individual tree crown level using LiDAR data. Remote Sens. 11, 2948. https://doi.org/10.3390/rs11242948
Noguchi, M., Yoshida, T., 2009. Individual-scale responses of five dominant tree species to single-tree selection harvesting in a mixed forest in Hokkaido, northern Japan. J. For. Res. 14, 311–320. https://doi.org/10.1007/s10310-009-0137-5
Noordermeer, L., Bollandsås, O.M., Ørka, H.O., Næsset, E., Gobakken, T., 2019. Comparing the accuracies of forest attributes predicted from airborne laser scanning and digital aerial photogrammetry in operational forest inventories. Remote Sens. Environ. 226, 26–37. https://doi.org/10.1016/J.RSE.2019.03.027
Nuijten, R.J.G., Coops, N.C., Goodbody, T.R.H., Pelletier, G., 2019. Examining consistency of individual tree segmentation on deciduous stands using digital aerial photogrammetry (DAP) and unmanned aerial systems (UAS). Remote Sens. 11, 739. https://doi.org/10.3390/rs11070739
O'Hara, K.L., 2016. What is close-to-nature silviculture in a changing world? Forestry 89, 1–6. https://doi.org/10.1093/forestry/cpv043
O'Hara, K.L., Gersonde, R.F., 2004. Stocking control concepts in uneven-aged silviculture. Forestry 77, 131–143. https://doi.org/10.1093/forestry/77.2.131
O'Hara, K.L., Hasenauer, H., Kindermann, G., 2007. Sustainability in multi-aged stands: an analysis of long-term plenter systems. Forestry 80, 163–181. https://doi.org/10.1093/forestry/cpl051
Oosterbaan, A., Hochbichler, E., Nicolescu, V.N., Spiecker, H., 2009. Silvicultural principles, goals and measures in growing valuable broadleaved tree species. Die Bodenkultur 60, 45–51.
Orellana, E., Filho, A.F., Netto, S.P., Vanclay, J.K., 2016. A distance-independent individual-tree growth model to simulate management regimes in native Araucaria forests. J. For. Res. 22, 30–35. https://doi.org/10.1080/13416979.2016.1258961
Ota, T., Ogawa, M., Shimizu, K., Kajisa, T., Mizoue, N., Yoshida, S., Takao, G., Hirata, Y., Furuya, N., Sano, T., Sokh, H., Ma, V., Ito, E., Toriyama, J., Monda, Y., Saito, H., Kiyono, Y., Chann, S., Ket, N., 2015. Aboveground biomass estimation using structure from motion approach with aerial photographs in a seasonal tropical forest. Forests 6, 3882–3898. https://doi.org/10.3390/f6113882
Owari, T., 2013. Sustainable and adaptive forest management and data infrastructure under the stand-based silvicultural system. Proc. Inst. Stat. Math. 61, 201-216 (in Japanese).
Owari, T., Inukai, H., Koike, Y., Minowa, Y., Nakajima, T., 2010. Single-tree selection techniques in the stand-based forest management system. Trans. Meet. Hokkaido Branch Jpn. For. Soc. 58, 101-104 (in Japanee).
Owari, T., Matsui, M., Inukai, H., Kaji, M., 2011. Stand structure and geographic conditions of natural selection forests in central Hokkaido, northern Japan. J. For. Plan. 16, 207–214. https://doi.org/10.20659/jfp.16.Special_Issue_207
Owari, T., Okamura, K., Fukushi, K., Kasahara, H., Tatsumi, S., 2016. Single-tree management for high-value timber species in a cool-temperate mixed forest in northern Japan. Int. J. Biodivers. Sci. Ecosyst. Serv. Manag. 12, 74–82. https://doi.org/10.1080/21513732.2016.1163734
Panagiotidis, D., Abdollahnejad, A., Surový, P., Chiteculo, V., 2017. Determining tree height and crown diameter from high-resolution UAV imagery. Int. J. Remote Sens. 38, 2392–2410. https://doi.org/10.1080/01431161.2016.1264028
Pokharel, B., Dech, J.P., 2012. Mixed-effects basal area increment models for tree species in the boreal forest of Ontario, Canada using an ecological land classification approach to incorporate site effects. Forestry 85, 255–270. https://doi.org/10.1093/forestry/cpr070
Poudyal, B.H., Maraseni, T., Cockfield, G., 2019. Impacts of forest management on tree species richness

and composition: assessment of forest management regimes in Tarai landscape Nepal. Appl. Geogr. 111, 102078. https://doi.org/10.1016/j.apgeog.2019.102078
Prates-Clark, C.D.C., Saatchi, S.S., Agosti, D., 2008. Predicting geographical distribution models of high-value timber trees in the Amazon Basin using remotely sensed data. Ecol. Modell. 211, 309–323. https://doi.org/10.1016/j.ecolmodel.2007.09.024
Pretzsch, H., Biber, P., Schütze, G., Uhl, E., Rötzer, T., 2014. Forest stand growth dynamics in Central Europe have accelerated since 1870. Nat. Commun. 5, 4967. https://doi.org/10.1038/ncomms5967
Pretzsch, H., del Río, M., Biber, P., Arcangeli, C., Bielak, K., Brang, P., Dudzinska, M., Forrester, D.I., Klädtke, J., Kohnle, U., Ledermann, T., Matthews, R., Nagel, J., Nagel, R., Nilsson, U., Ningre, F., Nord-Larsen, T., Wernsdörfer, H., Sycheva, E., 2019. Maintenance of long-term experiments for unique insights into forest growth dynamics and trends: review and perspectives. Eur. J. For. Res. 138, 165–185. https://doi.org/10.1007/s10342-018-1151-y
Puettmann, K.J., Wilson, S.M., Baker, S.C., Donoso, P.J., Drössler, L., Amente, G., Harvey, B.D., Knoke, T., Lu, Y., Nocentini, S., Putz, F.E., Yoshida, T., Bauhus, J., 2015. Silvicultural alternatives to conventional even-aged forest management - what limits global adoption? For. Ecosyst. 2:8, 1–16. https://doi.org/10.1186/s40663-015-0031-x
Pukkala, T., Lähde, E., Laiho, O., Salo, K., Hotanen, J.-P., 2011. A multifunctional comparison of even-aged and uneven-aged forest management in a boreal region. Can. J. For. Res. 41, 851–862. https://doi.org/10.1139/x11-009
Puliti, S., Ørka, H.O., Gobakken, T., Næsset, E., 2015. Inventory of small forest areas using an unmanned aerial system. Remote Sens. 7, 9632–9654. https://doi.org/10.3390/rs70809632
R Core Team, 2019. R: The R Project for Statistical Computing, R Foundation for Statistical Computing, Vienna, Austria.
RColorBrewer, S., Liaw, M.A., 2018. Package "randomForest", University of California, Berkeley: Berkeley, CA, USA. https://doi.org/10.1023/A
Reutebuch, S.E., Andersen, H.E., McGaughey, R.J., 2005. Light detection and ranging (LiDAR): An emerging tool for multiple resource inventory. J. For. 103, 286–292. https://doi.org/10.1093/jof/103.6.286
Rodriguez-Galiano, V.F., Ghimire, B., Rogan, J., Chica-Olmo, M., Rigol-Sanchez, J.P., 2012. An assessment of the effectiveness of a random forest classifier for land-cover classification. ISPRS J. Photogramm. Remote Sens. 67, 93–104. https://doi.org/10.1016/j.isprsjprs.2011.11.002
Rohner, B., Waldner, P., Lischke, H., Ferretti, M., Thürig, E., 2017. Predicting individual-tree growth of central European tree species as a function of site, stand, management, nutrient, and climate effects. Eur. J. For. Res. 137, 29–44. https://doi.org/10.1007/s10342-017-1087-7
Ruslandi, Cropper, W.P., Putz, F.E., 2017. Tree diameter increments following silvicultural treatments in a dipterocarp forest in Kalimantan, Indonesia: a mixed-effects modelling approach. For. Ecol. Manage. 396, 195–206. https://doi.org/10.1016/j.foreco.2017.04.025
Schall, P., Schulze, E.D., Fischer, M., Ayasse, M., Ammer, C., 2018. Relations between forest management, stand structure and productivity across different types of Central European forests. Basic Appl. Ecol. 32, 39–52. https://doi.org/10.1016/j.baae.2018.02.007
Schelhaas, M., Hengeveld, G.M., Heidema, N., Thürig, E., Rohner, B., Vacchiano, G., 2018. Species-specific, pan-European diameter increment models based on data of 2.3 million trees. For. Ecosyst. 5:21.
Schröder, J., Gadow, K. Von, 1999. Testing a new competition index for Maritime pine in northwestern Spain. Can. J. For. Res. 29, 280–283. https://doi.org/10.1139/x98-199
Schuler, T.M., 2004. Fifty years of partial harvesting in a mixed mesophytic forest: composition and productivity. Can. J. For. Res. 34, 985–997. https://doi.org/10.1139/x03-262
Schulze, M., Grogan, J., Landis, R.M., Vidal, E., 2008. How rare is too rare to harvest? Management challenges posed by timber species occurring at low densities in the Brazilian Amazon. For. Ecol. Manage. 256, 1443–1457. https://doi.org/10.1016/j.foreco.2008.02.051
Schütz, J.P., Saniga, M., Diaci, J., Vrška, T., 2016. Comparing close-to-nature silviculture with processes in pristine forests: lessons from Central Europe. Ann. For. Sci. 73, 911–921. https://doi.org/10.1007/s13595-016-0579-9
Sharma, A., Bohn, K., Jose, S., Dwivedi, P., 2016. Even-aged vs. uneven-aged silviculture: implications for multifunctional management of southern Pine ecosystems. Forests 7, 86. https://doi.org/10.3390/f7040086
Shi, Y., Wang, T., Skidmore, A.K., Heurich, M., 2020. Improving LiDAR-based tree species mapping in

Central European mixed forests using multi-temporal digital aerial colour-infrared photographs. Int. J. Appl. Earth Obs. Geoinf. 84, 101970. https://doi.org/10.1016/j.jag.2019.101970
Shibano, S., Iguchi, K., Kimura, N., Watanabe, S., 1990. Hartwood rate trunk of large *Betula maximowicziana* timbers. Trans. Meet. Hokkaido Branch Jpn. For. Soc. 38, 203-205 (in Japanese).
Shibano, S., Kasahara, H., Kimura, N., Fukushi, K., Iguchi, K., Oakmura, K., Takahashi, Y., 1995. Processes of diameter growth for large trees of *Betula maximowicziana*: growth declining and dead trees at the Tokyo University Forest in Hokkaido. Trans. Meet. Hokkaido Branch Jpn. For. Soc. 106, 263-264 (in Japanese).
Sibona, E., Vitali, A., Meloni, F., Caffo, L., Dotta, A., Lingua, E., Motta, R., Garbarino, M., 2016. Direct measurement of tree height provides different results on the assessment of LiDAR accuracy. Forests 8, 7. https://doi.org/10.3390/f8010007
Singh, M., Evans, D., Tan, B.S., Nin, C.S., 2015. Mapping and characterizing selected canopy tree species at the Angkor world heritage site in Cambodia using aerial data. PLoS One 10, e0121558. https://doi.org/10.1371/journal.pone.0121558
Stereńczak, K., Mielcarek, M., Wertz, B., Bronisz, K., Zajączkowski, G., Jagodziński, A.M., Ochał, W., Skorupski, M., 2019. Factors influencing the accuracy of ground-based tree-height measurements for major European tree species. J. Environ. Manage. 231, 1284–1292. https://doi.org/10.1016/j.jenvman.2018.09.100
Surový, P., Almeida Ribeiro, N., Panagiotidis, D., 2018. Estimation of positions and heights from UAV-sensed imagery in tree plantations in agrosilvopastoral systems. Int. J. Remote Sens. 39, 4786–4800. https://doi.org/10.1080/01431161.2018.1434329
Takagi, K., Yone, Y., Takahashi, H., Sakai, R., Hojyo, H., Kamiura, T., Nomura, M., Liang, N., Fukazawa, T., Miya, H., Yoshida, T., Sasa, K., Fujinuma, Y., Murayama, T., Oguma, H., 2015. Forest biomass and volume estimation using airborne LiDAR in a cool-temperate forest of northern Hokkaido, Japan. Ecol. Inform. 26, 54–60. https://doi.org/10.1016/j.ecoinf.2015.01.005
Takahashi, K., Mitsuishi, D., Uemura, S., Suzuki, J.I., Hara, T., 2003. Stand structure and dynamics during a 16-year period in a sub-boreal conifer-hardwood mixed forest, northern Japan. For. Ecol. Manage. 174, 39–50. https://doi.org/10.1016/S0378-1127(02)00018-X
Tatsumi, S., Owari, T., Kasahara, H., Nakagawa, Y., 2014. Individual-level analysis of damage to residual trees after single-tree selection harvesting in northern Japanese mixedwood stands. J. For. Res. 19, 369–378. https://doi.org/10.1007/s10310-013-0418-x
Tatsumi, S., Owari, T., Mori, A.S., 2016. Estimating competition coefficients in tree communities: a hierarchical Bayesian approach to neighborhood analysis. Ecosphere 7, e01273. https://doi.org/10.1002/ecs2.1273
Tenzin, J., Tenzin, K., Hasenauer, H., 2017. Individual tree basal area increment models for broadleaved forests in Bhutan. Forestry 90, 367–380. https://doi.org/10.1093/forestry/cpw065
Tomé, J., Tomé, M., Barreiro, S., Paulo, J.A., 2006. Age-independent difference equations for modelling tree and stand growth. Can. J. For. Res. 36, 1621–1630. https://doi.org/10.1139/X06-065
Torresan, C., Berton, A., Carotenuto, F., Gennaro, S.F. Di, Gioli, B., Matese, A., Miglietta, F., Vagnoli, C., Zaldei, A., Wallace, L., 2018. Forestry applications of UAVs in Europe: a review. Int. J. Remote Sens. 38, 2427–2447. https://doi.org/10.1080/01431161.2016.1252477
Tsuda, Y., Ide, Y., 2005. Wide-range analysis of genetic structure of *Betula maximowicziana*, a long-lived pioneer tree species and noble hardwood in the cool temperate zone of Japan. Mol. Ecol. 14, 3929–3941. https://doi.org/10.1111/j.1365-294X.2005.02715.x
Tsuda, Y., Sawada, H., Ohsawa, T., Nakao, K., Nishikawa, H., Ide, Y., 2010. Landscape genetic structure of *Betula maximowicziana* in the Chichibu mountain range, central Japan. Tree Genet. Genomes 6, 377–387. https://doi.org/10.1007/s11295-009-0256-3
Uzoh, F.C.C., Oliver, W.W., 2008. Individual tree diameter increment model for managed even-aged stands of ponderosa pine throughout the western United States using a multilevel linear mixed effects model. For. Ecol. Manage. 256, 438–445. https://doi.org/10.1016/j.foreco.2008.04.046
Vanclay, J., 1994. Modelling forest growth and yield: Applications to mixed tropical forests, CAB International, Wallingford UK.
Vandekerkhovea, K., Vanhellemont, M., Vrška, T., Meyer, P., Tabaku, V., Thomaes, A., Leyman, A., Keersmaeker, L. De, Verheyen, K., 2018. Very large trees in a lowland old-growth beech (*Fagus sylvatica* L.) forest: density, size, growth and spatial patterns in comparison to reference sites in Europe. For. Ecol. Manage. 417, 1–17. https://doi.org/10.1016/j.foreco.2018.02.033
Vastaranta, M., Wulder, M.A., White, J.C., Pekkarinen, A., Tuominen, S., Ginzler, C., Kankare, V.,

Holopainen, M., Hyyppä, J., Hyyppä, H., Wulder, M.A., White, J.C., Ginzler, C., Kankare, V., Vastaranta, M., Pekkarinen, A., Tuominen, S., Hyyppä, J., Wulder, M.A., White, J.C., Pekkarinen, A., Tuominen, S., Ginzler, C., Kankare, V., Holopainen, M., Hyyppä, J., Hyyppä, H., 2013. Airborne laser scanning and digital stereo imagery measures of forest structure: comparative results and implications to forest mapping and inventory update. Can. J. Remote Sens. 39, 382–395. https://doi.org/10.5589/m13-046

Vauhkonen, J., Ene, L., Gupta, S., Heinzel, J., Holmgren, J., Pitkänen, J., Solberg, S., Wang, Y., Weinacker, H., Hauglin, K.M., Lien, V., Packalén, P., Gobakken, T., Koch, B., Næsset, E., Tokola, T., Maltamo, M., 2012. Comparative testing of single-tree detection algorithms under different types of forest. Forestry 85, 27–40. https://doi.org/10.1093/forestry/cpr051

Verhoeven, G., Doneus, M., Briese, C., Vermeulen, F., 2012. Mapping by matching: a computer vision-based approach to fast and accurate georeferencing of archaeological aerial photographs. J. Archaeol. Sci. 39, 2060–2070. https://doi.org/10.1016/j.jas.2012.02.022

Verma, N.K., Lamb, D.W., Reid, N., Wilson, B., 2014. An allometric model for estimating DBH of isolated and clustered Eucalyptus trees from measurements of crown projection area. For. Ecol. Manage. 326, 125–132. https://doi.org/10.1016/j.foreco.2014.04.003

Wallace, L., Lucieer, A., Malenovskỳ, Z., Turner, D., Vopěnka, P., 2016. Assessment of forest structure using two UAV techniques: a comparison of airborne laser scanning and structure from motion (SfM) point clouds. Forests 7, 62. https://doi.org/10.3390/f7030062

Wang, L., Gong, P., Biging, G.S., 2004. Individual tree-crown delineation and treetop detection in high-spatial-resolution aerial imagery. Photogramm. Eng. Remote Sens. 70, 351–357. https://doi.org/10.14358/pers.70.3.351

Wang, W., Chen, X., Zeng, W., Wang, J., Meng, J., 2019. Development of a mixed-effects individual-tree basal area increment model for oaks (*Quercus* spp.) considering forest structural diversity. Forests 10, 474.

Wang, Y., Hyyppa, J., Liang, X., Kaartinen, H., Yu, X., Lindberg, E., Holmgren, J., Qin, Y., Mallet, C., Ferraz, A., Torabzadeh, H., Morsdorf, F., Zhu, L., Liu, J., Alho, P., 2016. International benchmarking of the individual tree detection methods for modeling 3-D canopy structure for silviculture and forest ecology using airborne laser scanning. IEEE Trans. Geosci. Remote Sens. 54, 5011–5027. https://doi.org/10.1109/TGRS.2016.2543225

Wang, Y., Lehtomäkia, M., Lianga, X., Pyörälä, J., Kukko, A., Jaakkola, A., Liu, J., Feng, Z., Chend, R., Hyyppäa, J., 2019. Is field-measured tree height as reliable as believed - a comparison study of tree height estimates from field measurement, airborne laser scanning and terrestrial laser scanning in a boreal forest. ISPRS J. Photogramm. Remote Sens. 147, 132–145. https://doi.org/10.1016/j.isprsjprs.2018.11.008

White, J.C., Coops, N.C., Wulder, M.A., Vastaranta, M., Hilker, T., Tompalski, P., 2016. Remote sensing technologies for enhancing forest inventories: a review. Can. J. Remote Sens. 42, 619–641. https://doi.org/10.1080/07038992.2016.1207484

White, J.C., Wulder, M.A., Vastaranta, M., Coops, N.C., Pitt, D., Woods, M., 2013. The utility of image-based point clouds for forest inventory: a comparison with airborne laser scanning. Forests 4, 518–536. https://doi.org/10.3390/f4030518

Winfield, K., Scott, M., Grayson, C., 2016. Global status of *Dalbergia* and *Pterocarpus* rosewood producing species in trade, Convention on international trade in endangered species, 17th conference of the parties - Johannesburg.

Wulder, M.A., Coops, N.C., Hudak, A.T., Morsdorf, F., Nelson, R., Newnham, G., Vastaranta, M., 2013. Status and prospects for LiDAR remote sensing of forested ecosystems. Can. J. Remote Sens. 39, S1–S5. https://doi.org/10.5589/m13-051

Wulder, M.A., Hilker, T., Bater, C.W., White, J.C., Coops, N.C., 2014. The role of LiDAR in sustainable forest management. For. Chron. 84, 807–826. https://doi.org/10.5558/tfc84807-6

Wulder, M.A., White, J.C., Nelson, R.F., Næsset, E., Ørka, H.O., Coops, N.C., Hilker, T., Bater, C.W., Gobakken, T., 2012. Lidar sampling for large-area forest characterization: a review. Remote Sens. Environ. 121, 196–209. https://doi.org/10.1016/j.rse.2012.02.001

Xie, Y., Sha, Z., Yu, M., 2008. Remote sensing imagery in vegetation mapping: a review. J. Plant Ecol. 1, 9–23. https://doi.org/10.1093/jpe/rtm005

Yamamoto, H., Nagumo, H., Watanabe, S., 1989. The selection cutting system of high valued natural hardwoods: a new method of managing natural forests. J. Jpn. For. Soc. 17, 1-9 (in Japanese with English summary).

Yao, W., Krzystek, P., Heurich, M., 2012. Tree species classification and estimation of stem volume and DBH based on single tree extraction by exploiting airborne full-waveform LiDAR data. Remote Sens. Environ. 123, 368–380. https://doi.org/10.1016/j.rse.2012.03.027

Yasuda, A., Yoshida, T., Miya, H., Harvey, B.D., 2013. An alternative management regime of selection cutting for sustaining stand structure of mixed forests of northern Japan: a simulation study. J. For. Res. 18, 398–406. https://doi.org/10.1007/s10310-012-0362-1

Yoshida, T., Kamitani, T., 1998. Effects of crown release on basal area growth rates of some broad-leaved tree species with different shade-tolerance. J. For. Res. 3, 181–184. https://doi.org/10.1007/bf02762141

Yoshida, T., Noguchi, M., 2010. Growth and survival of *Abies sachalinensis* seedlings for three years after selection harvesting in northern Hokkaido, Japan. Landsc. Ecol. Eng. 6, 37–42. https://doi.org/10.1007/s11355-009-0080-9

Yoshida, T., Noguchi, M., 2009. Vulnerability to strong winds for major tree species in a northern Japanese mixed forest: analyses of historical data. Ecol. Res. 24, 909–919. https://doi.org/10.1007/s11284-008-0566-1

Yoshida, T., Noguchi, M., Akibayashi, Y., Noda, M., Kadomatsu, M., Sasa, K., 2006. Twenty years of community dynamics in a mixed conifer-broad-leaved forest under a selection system in northern Japan. Can. J. For. Res. 36, 1363–1375. https://doi.org/10.1139/x06-041

Young, B.D., D'Amato, A.W., Kern, C.C., Kastendick, D.N., Palik, B.J., 2017. Seven decades of change in forest structure and composition in *Pinus resinosa* forests in northern Minnesota, USA: comparing managed and unmanaged conditions. For. Ecol. Manage. 395, 92–103. https://doi.org/10.1016/j.foreco.2017.04.003

Yu, X., Hyyppä, J., Vastaranta, M., Holopainen, M., Viitala, R., 2011. Predicting individual tree attributes from airborne laser point clouds based on the random forests technique. ISPRS J. Photogramm. Remote Sens. 66, 28–37. https://doi.org/10.1016/j.isprsjprs.2010.08.003

Zarco-Tejada, P.J., Diaz-Varela, R., Angileri, V., Loudjani, P., 2014. Tree height quantification using very high resolution imagery acquired from an unmanned aerial vehicle (UAV) and automatic 3D photo-reconstruction methods. Eur. J. Agron. 55, 89–99. https://doi.org/10.1016/j.eja.2014.01.004

Zhao, L., Li, C., Tang, S., 2013. Individual-tree diameter growth model for fir plantations based on multi-level linear mixed effects models across southeast China. J. For. Res. 18, 305–315. https://doi.org/10.1007/s10310-012-0352-3